行政院國家科學委員會專題研究計畫 成果報告

重組燃料燃燒之實驗與數值研究--加氫對混合燃料火焰穩定性、化學動力、火焰結構及污染排放之影響(第 3 年)
研究成果報告(完整版)

計 畫 類 別 ：個別型
計 畫 編 號 ：NSC 96-2221-E-216-016-MY3
執 行 期 間 ：98 年 08 月 01 日至 99 年 08 月 31 日
執 行 單 位 ：中華大學機械與航太工程研究所

計 畫 主 持 人：鄭藏勝
共 同 主 持 人：趙怡欽
計畫參與人員：碩士班研究生-兼任助理人員：柳文祥
博士班研究生-兼任助理人員：蘇佑翔

報 告 附 件 ：出席國際會議研究心得報告及發表論文

處 理 方 式 ：本計畫可公開查詢

中 華 民 國 99 年 11 月 07 日

行政院國家科學委員會補助專題研究計畫成果報告

重組燃料燃燒之實驗與數值研究—加氫對混合燃料火焰穩定性、化學動力、火焰結構及污染排放之影響

Experimental and Numerical Investigations of Reforming Fuel Combustion: Effect of H_2 Addition on Flame Stability, Chemical Kinetics, Flame Structure, and Pollutant Emission of Blended Fuels

計畫類別：■個別型計畫　□整合型計畫
計畫編號：NSC 96-2221-E-216-016-MY3
執行期間：96 年 08 月 01 日至 98 年 08 月 31 日

計畫主持人：鄭藏勝 教授
共同主持人：趙怡欽 教授
計畫參與人員：吳志勇、李約亨、陳志鵬、林河川、侯俊慶、蘇佑翔、張彥丞、柳文祥、鄭雅云、蘆韋廷

成果報告類型(依經費核定清單規定繳交)：□精簡報告■完整報告

本成果報告包括以下應繳交之附件：
□赴國外出差或研習心得報告
□赴大陸地區出差或研習心得報告
■出席國際學術會議心得報告
□國際合作研究計畫國外研究報告

處理方式：除產學合作研究計畫、提升產業技術及人才培育研究計畫、列管計畫及下列情形者外，得立即公開查詢
□涉及專利或其他智慧財產權，□一年□二年後可公開查詢

中　華　民　國　99　年　11　月　30　日

中文摘要

本研究計畫之主要目的是以發展應用替代能源（如氫能、生質能）而達成溫室氣體減量為最終目標，由於目前正在使用之工業燃燒爐、渦輪引擎燃燒室、內燃機引擎等燃燒器之設計皆以燃燒石化碳氫燃料為主，尚無法完全燃燒純氫氣體，因此使用氣化生質燃料或煤氣短期不但可達到降低二氧化碳及氮氧化物的目標，長期而言亦可作為將來無碳能源燃燒系統之轉換策略。惟因氣化生質燃料或煤氣之主要含量為氫氣、一氧化碳及甲烷，而三種主要氣體之含量比例不一，且熱值較低，容易造成燃燒不穩定現象。因此探討三種主要氣體在不同混合比例下，其對火焰燃燒速度、燃燒穩定性、化學動力及火焰結構等核心機制之影響，以瞭解重組(混合)燃料之關鍵特性、建立替代能源燃燒特性資料庫及作為將來設計無碳燃燒系統之參考，是一值得研究的主題。

本計畫係以實驗與數值方法，先探討甲烷/一氧化碳/空氣當量混合時，改變混合燃料中一氧化碳或甲烷之體積分率，瞭解混合燃料比例改變對火焰燃燒速度、火焰結構、及化學動力之影響。之後再探討氫氣/甲烷/一氧化碳/空氣當量混合時，改變混合燃料中氫氣之體積分率，以瞭解加氫對混合燃料之火焰燃燒速度、火焰結構、及化學動力之影響。實驗方法是利用直接火焰照相、火焰自然螢光技術量測OH*分佈及雷射誘發螢光技術量測OH分佈來決定火焰前端位置；利用熱電偶來量測火焰溫度；利用粒子影像測速儀來量測流場速度。數值方法則是利用CHEMKIN Collection 3.5之PREMIX程式來計算層流燃燒速度;利用OPPDIF軟體結合GRI-Mech 3.0化學反應機構及完整的傳輸性質來計算火焰結構及化學動力結構。

甲烷/一氧化碳/空氣當量混合時之研究結果顯示，實驗量測之火焰前端位置、溫度分佈及速度分佈與數值模擬之結果相當吻合。詳細分析計算之化學動力結構顯示，當混合燃料之一氧化碳含量由0%增加至80%時，一氧化碳氧化反應(R99)顯著增加，且貢獻大量的熱釋放率。當混合燃料之一氧化碳含量為80%時，層流燃燒速度達到最大值(57.5 cm/s)，當一氧化碳含量80%超過時，一氧化碳消耗反應移至乾式反應機制。經比較計算所得之層流燃燒速度、火焰溫度、一氧化碳消耗率及靈敏度分析之後，得到一氧化碳含量對當量甲烷/一氧化碳/空氣火焰層流燃燒速度之影響，其主要因素是由於主宰化學反應之反應機構路徑轉換的關係。

氫氣/甲烷/一氧化碳/空氣當量混合時之研究結果顯示，當氫氣加入總燃料的比例增加時，除了整體燃燒速度提升之外，最大火焰速度也會隨著一氧化碳與甲烷比例的不同而改變。預混對衝噴流火焰的實驗與計算結果亦證實了此特性，當氫氣佔總燃料比例分別為 10%與 20%時，最大火焰速度分別發生在 90%一氧化碳與 10%甲烷及 94%一氧化碳與 6%甲烷。而從火焰結構的分析結果也證實了氫氣的加入對火焰速度變化的影響一樣是來自主要化學機構路徑的轉變所造成。雖然最大火焰速度發生時的一氧化碳與甲烷比例因氫氣的加入有所改變，但在各自火焰速度最大發生的比例下，一氧化碳快速氧化反應式（R99）的反應速率依然會達到最高，並提供了主要且大量的熱釋率。然而較不同的是，氫氣氧化反應式（R84）的反應發生位置、反應速率及熱釋率都會因氫氣的增加而超越甲烷的氧化反應式（R98）。靈敏度分析結果則顯示氫氣的加入並不影響反應

步驟上重要性的改變過程，其最為重要的反應步驟皆在 80%一氧化碳時由鏈鎖反應（R38）轉變為一氧化碳快速氧化反應（R99）。污染物排放量測顯示加氫可降低一氧化碳排放，但加氫也會提升火焰溫度，因此提高氮氧化物排放。此外對當量氫氣/甲烷/一氧化碳/空氣火焰而言，加氫並無法降低二氧化碳排放。

關鍵詞：重組燃料、層流燃燒速度、火焰結構、化學動力、對衝噴流火焰、數值模擬

ABSTRACT

The objective of this research is to study the key combustion characteristics of reforming fuels that could be used as a short term solution to the immediate need for CO_2 and NO_x reductions, and provides a transitional strategy to a carbon free energy system in the future. The goal is to replace fossil fuel usage as much as possible with environmentally friendly, clean and renewable energy sources (pure hydrogen or biomass fuels) for greenhouse gas reduction. Unfortunately, the use of pure hydrogen or gasified biomass fuels in industrial combustors remains difficulties due to production, storage, cost, and safety concerns. Therefore, the use of hydrogen addition with traditional fossil fuels is an alternative toward pollutant emission reductions. Nonetheless, the applications of reforming fuels to practical combustion systems rely on fundamental understanding of the characteristics of multi-component fuels.

The main focus of the present study is to thoroughly investigate the detailed laminar burning velocity, flame stability limits, flame structures, and chemical kinetics mechanisms of blended fuels (H_2/CH_4/CO) through experimental measurements and numerical simulations. Direct photograph of the flame, chemiluminescence emission of OH*, and laser-induced predissociative fluorescence (LIPF) of OH techniques are employed to determined the flame front position. Flame temperatures are measured by thermocouple. Particle imaging velocity (PIV) technique is used to measure the flowfield velocity. While the PREMIX and OPPDIF codes from CHEMKIN Collection 3.5 in conjunction with GRI-Mech 3.0 chemical kinetic mechanisms as well as detailed transport properties are used for laminar burning velocity, flame structure and chemical kinetic structure calculations.

Experimental measurements and numerical simulations of the flame front position, temperature, and velocity are performed in the *stoichiometric* CH_4/CO/air opposed-jet flames with various CO contents in the fuel. The measured flame front position, temperature, and velocity of the stoichiometric CH_4/CO/air flames are closely predicted by the numerical calculations. Detailed analysis of the calculated chemical kinetic structures reveals that as the CO content in the fuel is increased from 0% to 80%, CO oxidation (R99) increases significantly and contributes to a significant level of heat-release rate. It is also shown that the laminar burning velocity reaches a maximum value (57.5 cm/s) at the condition of 80% of CO in the fuel. Based on the results of sensitivity analysis, the chemistry of CO consumption shifts to the dry oxidation kinetics when CO content is further increased over 80%. Comparison between the results of computed laminar burning velocity, flame temperature, CO consumption rate, and sensitivity analysis reveals that the effect of CO addition on the laminar burning velocity of the stoichiometric CH_4/CO/air flames is due mostly to the transition of the dominant chemical kinetic steps.

Experimental and numerical studies of the the *stoichiometric* H_2/CH_4/CO/air

opposed-jet flames reveal that the addition of H_2 to the reforming fuel not only increases the laminar burning velocity, but also the ratio of CH_4/CO at which the maximum laminar burning velocity occurred is changed. When 10% and 20% of H_2 are used in the H_2/CH_4/CO fuel, the maximum burning velocity occurs at the CH_4/CO fuel ratio of 10% CH_4–90% CO and 6% CH_4–94% CO, respectively. The analysis of flame structures indicates that the effect of H_2 addition on the laminar burning velocity is primary due to the transition of dominant chemical reaction steps. Although the ratio of CH_4/CO at which the maximum laminar burning velocity occurred is varied with H_2 addition, the CO oxidation reaction (R99) is still the dominant and major contributor to the heat-release rate. The major difference is that with H_2 addition the reaction location, reaction rate, and heat-release rate of H_2 reaction (R84) exceed those of CH_4 reaction (R98). Sensitivity analysis shows that the variation of important reaction steps is not affected by H_2 addition, and the most important reaction step is changed from the chain-branching reaction (R38) to the reaction of CO fast oxidation (R99) when CO in the CH_4/CO fuel mixture is increased over 80%. Pollutant emission measurements indicate that the addition of H_2 to the fuel mixture reduces CO emission, but increases NO_x emission due to increased flame temperature. In addition, the addition of H_2 (up to 30%) to the fuel mixture does not reduce CO_2 emission for stoichiometric H_2/CH_4/CO/air flames.

Keywords: Reforming fuel, Laminar burning velocity, Flame structure, Chenical kinetic, Oppsed-jet flame, Numerical simulation.

CONTENTS

LIST OF TABLES

LIST OF FIGURES

CHAPTER I
INTRODUCTION

1-1 Background

According to the energy consumption report [1], the amount of energy (11,769 KLOE) consumed by the industrial and transportation sectors was 65.37% of the total annual energy consumption in Taiwan during the year of 2008. In these two sectors, about 90% of energy sources (fossil fuels) were used to generate power, process heat, and electricity through combustion. Extensive fossil fuel consumptions have resulted in rapid fuel depletion over the world as well as atmospheric and environmental pollutions. Consequently, the terminologies such as global warming, greenhouse effect, climate change, ozone layer depletion and acid rain have appeared in our daily life quite frequently. It has been understood scientifically that these pollutions are closely related to fossil fuel uses because they emit greenhouse gases, the dominant contributor being carbon dioxide (CO_2) which hinder the long wavelength terrestrial radiation to escape into space, and consequently, the earth troposphere becomes warmer. In order to reduce further impacts of these phenomena, public awareness and legislation have led to a policy of reduction of greenhouse gas emissions in most economically developed countries, with the regulations partially driven by international initiative such as Kyoto protocol and the Intergovernmental Panel on Climate Change [2]. Taiwan, although is not a member of the United Nations, has taken serious measures and set forth the first National Energy Conference in 1998 to cope with the challenges and impacts of the stringent regulations.

In view of CO_2 reductions, there are two alternatives that are either to improve the combustion efficiency with considerable reductions in the pollutant emissions into the atmosphere or more significantly to replace fossil fuel usage as much as possible with environmentally friendly, clean and renewable energy sources. These two alternatives were the major topics discussed in the 2005-National Energy Conference [3]. And the goal has been set to reduce CO_2 production by an amount of 17,000 million metric-tons compared to the BAU (Business as Usual) level in 2000 and to increase the energy supply from renewable energy sources (1.2% in 2004) up to 7.1% of the total energy supply by the end of 2025. The main renewable energy sources include biomass, hydropower, geothermal, solar, wind, and wave tidal in which biomass shares 62.1% of total renewable energy sources of the world in 1995 and it is increasing continuously [4].

Among the renewable energy sources, hydrogen and biomass are two of the attractive fuels because combustion of hydrogen fuel produces completely no greenhouse gases and biomass is readily available worldwide [5]. Hydrogen has been used in aerospace propulsion systems for a long time because of its short ignition delay time, its high energy per unit weight, and its better cooling ability. Nowadays, it becomes not only the National Energy Security of the U.S. but also the key to a cleaner energy future [6, 7]. The U.S. government has committed US$1.2 billion (since FY 2003) over five years for the research,

development, and demonstration of hydrogen and fuel cell technologies. Their goal is to make practical and cost-effective fuel-cell vehicles widely available in auto showroom by 2020. Since hydrogen can be produced from many domestic sources of energy, including fossil fuels, such as natural gas and coal; renewable energy sources, such as solar radiation, wind, and biomass; and nuclear energy, the diversity of hydrogen sources would make the widespread use of hydrogen for transportation and stationary power that is an important step in protecting the future energy security. Although hydrogen is a vision of future energy, the cost-effective of hydrogen production, delivery, storage, manufacturing, safety, and fuel cell conversion, etc is a significant challenge. Hydrogen is not a fuel that exists in nature in a readily usable form, such as oil or coal. It more closely resembles electricity-an energy carrier that must be generated from another fuel source. Therefore, researches on hydrogen related technologies are underway all over the world and Taiwan, as a Nation of energy shortage, should keep upon the research trend of the world.

In addition to hydrogen, biomass is another attractive renewable fuel. The use of biomass fuels provides substantial benefits as far as the environment is concerned. Biomass absorbs CO_2 during growth, and emits it during combustion. Therefore, biomass helps the atmospheric CO_2 recycling and does not contribute to the greenhouse effect. Biomass consumes about the same amount of CO_2 from atmosphere during growth as is released during combustion. The average majority of biomass energy is produced from wood and wood waste (64%), followed by solid waste (24%), agricultural waste (5%) and landfill gases (5%) [8]. There are three ways to use biomass. It can be burned to produce heat and electricity directly, gasified to gas-like fuels with composition of hydrogen (H_2), methane (CH_4), and carbon monoxide (CO) or changed to a liquid fuel. Liquid fuels, also called bio-fuels, include ethanol (C_2H_5OH) and methanol (CH_3OH). The most commonly used bio-fuel is ethanol, which is produced from sugarcane, corn and other grains. The use of gasoline and ethanol blended fuel for cars has been very popular in Brazil. Although the use of biomass energy possesses many unique advantages, the combustion of biomass remains some technological problems. For instance, the compositions of biomass among fuel types are considerable variable. Direct combustion of biomass fuel in furnaces and power boilers may result in the critical problems of fouling and slagging. Therefore, the use of gasified biomass that contains a mixture of carbon monoxide, hydrogen and methane, together with carbon dioxide and nitrogen, is more versatile than the original solid biomass. However, it should be noticed that in comparison with solid fossil fuels, biomass contains much less carbon and more oxygen and has a low heating value. Thereby, it becomes essential to develop combustion techniques that can burn the gasified biomass or low-grade syngas effectively.

In Taiwan, a lot of efforts have been devoted to seeking the way for CO_2 reduction. Among these efforts, the research and development of fuel cell related technology is one of the examples. Indeed, the use of fuel cell that utilizes hydrogen as a fuel not only produces

no greenhouse gases but also reduces fossil fuel usages. However, the application of fuel cell is mainly limited to transportation and residential sectors. It should be noted that in Taiwan, more than 90% of total CO_2 is produced from the industrial sector through combustion for generating power, process heat, and electricity. The effective way to reduce CO_2 production from industrial sector is either to further improve the combustion efficiency of existing combustors or to replace fossil fuels with hydrogen or biomass or blended fuels in the future. We believe that the later choice could be more effective and better than the former. Unfortunately, the use of pure hydrogen or biomass fuels in industrial combustors remains difficulties due to production, storage, cost, and safety concerns. Therefore, the use of hydrogen addition with traditional fossil fuels not only yields a short term solution to the immediate need for CO_2 and NO_x reductions, but also provides a transitional strategy to a carbon free energy system in the future.

Various types of turbulent flames, premixed, nonpremixed, or partially premixed, are employed in industrial boilers, process heating burners, internal combustion engines, hazardous waste incinerators, and both aircraft and land-based gas turbine engine combustors, etc. The control the turbulent combustion [9, 10] for reducing pollutant emission [11-13], increasing combustion efficiency [14], and obtaining stable flame holding [15-17] have been extensively studied. However, all of studies have concentrated on the single-component fuels. Since the combustion characteristics of biomass or blended fuels may differ substantially from those of single-component fuels, the applications of blended fuels to practical combustion systems rely on fundamental understanding of the characteristics of multi-component fuels. Therefore, the detailed investigations of chemical kinetics, flame stability limits, flame structures, and pollutant formation mechanism of blended fuels are of vital importance.

The investigations of hydrogen blended fuels in both practical combustors and fundamental jet flames are underway. Tests on a Ford F-150 pickup truck using 15 to 50 vol% blends of hydrogen with compressed natural gas (CNG) showed a reduction of 7.5% on hydrocarbon, 83% on CO, 53% on NO_x, and 30% on CO_2 emissions [18]. Experimental testing [19] and numerical analysis [20] on gas turbine combustors using hydrogenated fuels also showed the feasibility of 20-90% CO_2 reduction with control of NO_x emissions to below 10 ppmvd at 15% oxygen. Experiments in a lean premixed combustor were conducted to obtain data on flame stability/blowout and on emissions of CO and NO_x using hydrogen-enriched methane or natural gas [21]. An experimental and numerical investigation of flame structure and intermediate radical (OH, O, H, CH) concentrations was carried out in hydrogen-natural gas hybrid fuel diffusion flames to study the effects of hydrogen addition on jet flame structure [22]. Recently, the influence of hydrogen injection on CO, HC, and CO_2 emissions in hydrocarbon fuelled gas turbine combustor was investigated and the reduction of these emissions was attributed to hydrocarbon fuel substitution and chemical kinetics [23]. The above mentioned studies mainly concentrated

on the effects of hydrogen addition on the global performance of gas turbine combustors or jet flames and the resultant pollutant emissions. None of the studies has focused on the effect of chemical kinetic of blended fuels on flame stability and pollutant emissions.

1-2 Motivation

In order to understand the effect of chemical kinetics of hydrogen blended fuels on flame stability and pollutant emissions, laminar jet flames or counterflow (opposed) flames were frequently employed for such a study [24], due to its experimental simplicity and exclusion of complex turbulence-chemistry interactions. The effect of hydrogen and methane addition on the propagation and extinction of atmospheric CO/air flames was investigated experimentally and numerically [25]. Effects of pressure and dilution on the extinction of nonpremixed hydrogen-air were also experimentally and computationally studied [26]. Both studies have used counterflow, twin-flame and laser-Doppler velocimetry (LDV) techniques for the determination of laminar flame speeds and extinction strain rates. The simulations were conducted by using the one-dimensional flame code with detailed transport model and C_2 chemistry. Further experimental and numerical study of the strain-rate effects on hydrogen-enhanced lean premixed methane/air flames was reported [27]. Again, LDV and 1-D flame code were respectively employed for strain rate measurements and for numerical predictions, while sampling quartz microprobe was used for major species concentration measurements. Computational studies using a modified version of OPPDIF code [28] and using direct numerical simulation [29] were performed to investigate the effects of hydrogen addition on flame stability and pollutant formation of stretched methane/air premixed flames. The influence of hydrogen addition on the response of lean premixed methane flames to high strained flows was also experimentally and numerically investigated using LDV and 1-D flame code, respectively [30]. Experimental and numerical studies on the extinction limits of counterflow premixed and nonpremixed methanol and ethanol flames were reported recently [31].

Literature survey indicates that previous studies mainly concentrated on the characteristics of H_2/CH_4/air combustion. Little attention has been paid to the combustion characteristics of reforming fuels such as H_2/CH_4/CO/air, which are the major constituents of biomass fuels. In addition, experimental studies were focused on the velocity derived laminar flame speed and strain rate measurements. A few of temperature and species concentration measurements [22, 30] has been made. Thereby, comparisons of experimental results with numerical predictions were limited to the effect of hydrogen addition on the flame stability. No detailed comparison of measured thermochemical flame structures with model predictions has been reported to elucidate the effect of hydrogen addition on chemical kinetics, laminar burning velocity, and flame structures of reforming fuels and to valid the combustion models for future applications. This motivates the needs to thoroughly investigate these issues.

1-3 Objective

The objective of this research is to study the key combustion characteristics of reforming fuels that could be used as a short term solution to the immediate need for CO_2 and NO_x reductions, and provides a transitional strategy to a carbon free energy system in the future. The main focus of the present study is to thoroughly investigate the detailed laminar burning velocity, flame stability limits, flame structures, and chemical kinetics mechanisms of blended fuels (H_2/CH_4/CO) through experimental measurements and numerical simulations. Direct photograph of the flame, chemiluminescence emission of OH*, and laser-induced predissociative fluorescence (LIPF) of OH techniques are employed to determined the flame front position. Flame temperatures are measured by thermocouple. Particle imaging velocity (PIV) technique is used to measure the flowfield velocity. While the PREMIX and OPPDIF codes from CHEMKIN Collection 3.5 in conjunction with GRI-Mech 3.0 chemical kinetic mechanisms as well as detailed transport properties are used for laminar burning velocity, flame structure, and chemical kinetic structure calculations.

CHAPTER II
METHODOLOGY

2-1 Experimental Methods

The experimental setup is schematically shown in Fig. 1. The opposed-jet burner consists of two water cold, well-contoured circular nozzles (i.d. = 2 cm) with slow coaxial shielding flows (Fig. 1a). Two premixed CH_4/CO/air jets are directed towards each other to form two symmetrical, planar flames. Both premixed flames are operated at the fixed stoichiometric condition while the volumetric concentration of CO is varied from 0 to 100% in the blended fuel. The separation distance between two nozzles is 2 cm and the bulk velocity at each jet exit is maintained at 1 m/s for the present study. Research-grade fuels and compressed air are metered by electronic mass flowmeters and mixed in a mixing chamber prior to the opposed-jet burner. The compressed air is filtered and dried by using a refrigeration dryer, and the dew point can be reduced to -20°C. The flame is shielded from ambient air by a nitrogen coaxial flow with low velocity, which is controlled using a rotameter. The uncertainties of the rotameter for coaxial nitrogen stream and mass flowmeters for methane and carbon monoxide are ±2.5% and ±1.0% of full scale, respectively. The experimental conditions and corresponding net heating values of mixtures and adiabatic flame temperatures of the premixed stoichiometric CH_4/CO/air opposed-jet flames are listed in Table 1. Note that the adiabatic flame temperature is calculated under the unstrained condition and it increases with the CO content in the fuel mixture. Moreover, in order to clarify the effect of molecular diffusion of in the stretched flame with different molecular weights, the Lewis numbers, which are defined as the ratio of thermal diffusivity and mass diffusivity for the mixture of methane, carbon monoxide and oxygen, are also shown in Table 1. In experiments, the non-intrusive particle image velocimetry (PIV) and qualitative laser-induced predissociative fluorescence (LIPF) of OH imaging are applied to measure the flow velocity and flame front position, respectively. The visible flame features are obtained using a high sensitivity 3-chip color CCD camera (Sony DXC-9000) and digitized by the frame grabber for further digital image processing to identify the flame front position. An R-type (Pt/Pt–13Rh) thermocouple with 25 μm wire diameter is used to measure the flame temperature. BeO and 10–15% Y_2O_3 coating is applied to eliminate catalytic reactions induced by platinum in the flame [32]. The measured temperature in the flame is corrected for radiation heat loss by assuming a spherical thermocouple bead [33, 34].

The PIV system including two Nd:YAG lasers and optics is shown in Fig. 1b. The laser beams from the two lasers are aligned with the optics through two polarizers and a wave plate. The resulting beam is then expanded by three cylindrical lenses into a thin sheet of approximately 0.7 mm thickness, which is actually measured on the projection screen. The time interval of the PIV system is controlled by a pulse signal/delay generator. The fuel and air streams are seeded with sieved fine Al_2O_3 particles of sizes less than 10 μm. A

high-resolution, high-sensitivity, and low dark current camera (SharpVision 1300DE) is used for image recording. This CCD, which is equipped with a progressive scan interline CCD sensor, is especially suitable for PIV measurements. The image array has 1300 × 1030 pixels but is limited to 1280 × 1024 pixels in practical use, and the pixel size is 6.7 μm × 6.7 μm. With the current optical arrangement the spatial resolution is 12.5 μm/pixel. All images are captured, digitized through a 16-bit digitizer, and recorded on the hard disk for further analysis.

In order to control the exposure quality for flame measurements, an additional mechanical shutter is added to the PIV system. The triggering sequence of the CCD, two Nd:YAG lasers, and mechanical shutter is shown in Fig. 2. The delay time between two laser pulses is 50 μs. For data processing, it is impractical to trace every particle displacement between two sequential images; therefore, a statistical cross-correlation method is applied to a group of particles in the interrogation window. An interrogation window with 32 × 32 matrix is used to achieve a spatial resolution of 0.47 mm with fine quality in the resultant velocity vector plots. In addition to direct photograph of flame features, laser-induced predissociative fluorescence (LIPF) imaging of OH [35] is also employed to determine the flame front position. A schematic diagram of LIPF imaging system is shown in Fig. 1c. A narrowband tunable KrF excimer laser is used to excite the P2(8) rotational line of the A–X (3, 0) transition at λ = 248.46 nm. The laser beam is formed to a thin sheet of 34 mm height and 0.2 mm thickness by a single cylindrical lens (f = 1000 mm); the sheet intersects vertically through the burner axis. Only the 20 mm central portion of the laser sheet, where the laser intensity is high and uniform, is used for the imaging. The OH fluorescence signal is imaged onto an intensified CCD camera (576 × 384 pixels) with an UV camera lens (Nikkor, f = 105 mm, f/4.5). A 10-mm thick butyl acetate liquid–filter and a narrow band-pass filter (296.7 ± 12 nm) are placed in front of the camera to reject the Rayleigh light and other scattering signals, respectively. The applications of the LIPF-OH imaging technique to hydrocarbon and hydrogen jet flames have been reported previously [36, 37].

2-2 Numerical Methods

The adiabatic, unstrained, free propagation velocities of the laminar premixed CH_4/CO/air flames are calculated using the PREMIX code of Chemkin collection 3.5. On the other hand, the flame structures of the premixed stoichiometric CH4/CO/air opposed-jet flames are simulated using the OPPDIF package with the GRI-Mech 3.0 chemical kinetic mechanisms [38] and detailed transport properties. For the opposed-jet flame calculations, the computation domain and input parameters for each flame condition are in accordance with experiments. The mixture temperature at the jet exit is set as 300 K. In flowfield computation, the flow is reduced mathematically to one dimension by assuming that the radial velocity varies linearly in the radial direction, which leads to a simplified form in which the flowfield

properties are functions of the axial distance only. The adaptive regridding method is applied to solve the flame structure, and the grid independence of the solutions is achieved by tuning the GRAD and CURV parameters in the package. The number of grid lines is set to more than 400 for each case. The minimum grid dimension is approximately 0.1 μm, which is sufficient to resolve the flame thickness and the steep temperature gradient.

CHAPTER III
RESULTS AND DISCUSSION

The discussion of the results is divided into two parts: the first part is for CH_4/CO/air flames and the second part is for the H_2/CH_4/CO/air flames.

Premixed Stoichiometric CH4/CO/air Flames

3-1 Laminar Burning Velocity

The computed laminar burning velocities of the premixed CH_4/CO/air flames under various CH_4/CO fuel compositions and equivalence ratios are shown in Fig. 3. Note that the laminar burning velocity is calculated based on the "dry" oxidation condition, i.e., no water vapor is present in the air. Fig. 3 shows that for a fixed fuel composition the maximum burning velocity occurs on the rich side of stoichiometry. The maximum burning velocity increases with increasing CO concentration in the fuel mixture, and it reaches its highest value (77.43 cm/s) at φ = 1.9 of flame 11 (6% CH_4–94% CO in the fuel mixture). It then decreases as CO is further increased. For pure CO combustion, the calculated laminar burning velocities are much less than those of the flames with CH_4 content in the fuel, and the maximum burning velocity
(0.68 cm/s) occurs at $\varphi \approx 1.2$. The calculated results are in good agreement with those predicted using the asymptotic model and simple reaction mechanisms for dry CO–air flames at p = 1 atm and T_0 = 300 K [39]. It is noted that for dry CO–air flames, convergent solutions are not obtainable for $\varphi < 0.8$ and $\varphi > 2.2$ and the cause of the decrease of burning velocity for φ = 1.6–1.8 is not clear.

Comparison of the computed maximum burning velocities for different CO contents in fuel is depicted in Fig. 4. The computed maximum laminar burning velocity increases monotonically with increasing CO content in the CH_4–air mixtures, and it reaches to a maximum value (77 cm/s) at the condition of 94% of CO in fuel and then decreases rapidly as CO is further increased. It can be seen that the calculated maximum burning velocities have the same tendency with those measured by Scholte and Vaags [44].

In order to investigate the effect of fuel variations on the characteristics of blended fuel combustion, the attention is focused on *stoichiometric* flames. The numerically calculated laminar burning velocities are compared with results from the mixing rule of Spalding [41], Payman and Wheeler [42], and the flame-temperature-based predictions proposed by Hirasawa et al. [40]. Fig. 5 shows that for the stoichiometric flames the computed laminar burning velocity increases monotonically with increasing CO content in the CH_4–air mixtures, and it reaches a maximum value (57.5 cm/s) at the condition of 80% of CO in fuel and then decreases rapidly as CO is further increased. The laminar burning velocity of 20% CH_4–80% CO stoichiometric flame is about a factor of 1.5 higher than that of for the pure methane flame. This fact suggests that the addition of an appropriate amount of CO to CH_4–air

mixtures could increase the flame propagation and influence the chemistry and structure of premixed CH_4/CO/air flames. The results of mixing-rule methods, which are calculated based on Spalding's method [41], of Payman and Wheeler's method [42], and flame-temperature-based methods [40] show different trends from those of the numerical simulations. Mixing rules predict a monotonic decrease of the burning velocities with increasing CO content in the blended fuel, which contradicts the present numerical simulation and previous experimental studies [44] as it reaches a maximum when CO is increased to 80% in the fuel mixture. Recall that the adiabatic flame temperature increases with an increase in CO vol% in the fuel, from 2264 K at 10% CO to 2385 K at 96% CO (see Table 1). The increase in flame temperature should, in principle, increase the burning velocity. Therefore, it is clear that the mixing rule is not valid for laminar burning velocity predictions in CH_4/CO/air flames. The effect of CO variations on the laminar burning velocity will be further discussed in Section 3.4.

3-2 Flame Appearance and Flame Front Position

Photographs of the premixed stoichiometric CH_4/CO/air opposed-jet flames with different CO volumetric contents in the CH_4–air mixtures are shown in Fig. 6. Fig. 6a shows that for 100% of CH_4 in fuel, two symmetrical, planar flames exist and the flames are blue in color. When 10% of CO is added to the fuel, the postflame zone (region between two planar flames) immediately becomes orange in color (Fig. 6b). The flame emission becomes bright as the CO concentration is increased to 70% in volume (Fig. 6h). For the pure CO premixed flame, the flame becomes silver-white in color around the center and blue near the edge of the flame as shown in Fig. 6m. It is also noted that the separation distance between the two symmetrical flames increases with increasing CO concentration. The separation distance reaches a maximum value for flame 9 (Fig. 6i) and then decreases as the CO concentration is further increased. For the pure CO flame (Fig. 6m), the two symmetrical, planar flames almost merge into a single flame. Fig. 6 indicates that the addition of CO to the CH_4–air mixtures changes the flame front position. The radiation from the post flame especially for the cases with higher CO composition is induced from decomposition of metal carbonyls [46]. CO stored in high pressure cylinder results in contamination from iron pentacarbonyl as the CO reacts with the iron content in the cylinder wall. According to prior papers, addition of CO pentacarbonyl may affect studies on flame ignition and extinction phenomena. 50 ppm iron pentacarbonyl addition may reduce laminar burning velocity of stoichiometric methane–air flames by 20% [47]. In general, averaged concentration of iron pentacarbonyl in CO from steel cylinder is about 869 ppb [48]. For experiments, semiconductor-grade CO which has been filtered and stored in alumina cylinder is suggested to apply in further study in the future. Fortunately, the contamination of iron pentacarbonyl does not seem to severely affect flame stabilization locations of stretched flame.

In order to determine the flame front position, direct photograph and single-shot

LIPF-OH imaging measurements are performed in premixed stoichiometric CH_4/CO/air opposed-jet flames. Fig. 7 shows the typical results for flame 4 using both techniques. The flame front position (the distance from the nozzle exit) is defined at the location along the jet axis where maximum flame luminosity or maximum OH intensity occurs. Comparison of the measured and predicted flame front positions is shown in Fig. 8 to examine the effects of CO contents on the flame structure and to validate the numerical predictions. For the opposed-jet flames, the calculated flame front position is defined at the axial location of maximum temperature gradient. Fig. 8 shows the good agreements between the measured and the predicted results. It can be seen that the flame front position decreases with increasing CO concentration, and it reaches to a minimum value at 80% of CO in the fuel and then increases as CO is further increased. It is interesting to note that the profile of the variation of flame front position with CO contents in the CH_4–air mixtures (Fig. 8) looks like an inversion of the laminar flame velocity profile (Fig. 5). Comparison of Figs. 5 and 8 indicates that flame 9 (20% CH_4–80% CO) has the maximum laminar burning velocity and produces the shortest distance from the nozzle to the flame front position as compared to the other flames studied. The effects of CO variations on the flame speed and flame front position is closely related to the chemical kinetics of the blended fuels. Therefore, four characteristic conditions identified in Fig. 8 are selected to elucidate the effects of CO variations on the chemical kinetic structures of the flames.

3-3 Temperature and Velocity Measurements

In addition to measurements of the flame front position for premixed stoichiometric CH_4/CO/air opposed-jet flames, temperature and velocity measurements are also performed. Typical results for flame 2 (90% CH_4–10% CO) and flame 10 (10% CH_4–90% CO) coupled with numerical predictions of temperature and velocity are shown in Figs. 9 and 10, respectively. For temperature measurements, due to the limitation of the R-type thermocouple (~2040 K) only the preheated and partial oxidation zones are measured. Fig. 9 shows that both flames result in a similar temperature gradient, but the preheat zone for the higher CO concentration in the fuel (flame 10) shifts closer to the nozzle exit and leads to a slightly higher calculated flame temperature. The predicted flame temperatures are in good agreement with the measured data for both flames.

Comparison of the measured and calculated axial velocities for flames 2 and 10 is shown in Fig. 10. It can be seen that the PIV system is only capable of measuring the region from the jet exit to the beginning of preheat zone, similar to that reported by Huang et al. [45]. In the reaction zone, due to high temperature, the gas density decreases by nearly a factor of 7 leading to significant decrease of density and scattering cross-section of the seeding particles in the PIV images [49]. Fig. 10 shows that the axial velocity decreases flame. In addition, the model fairly predicts the measured data for both flames. Comparisons of the predicted flame front position, temperature, and velocity with the measured data indicate that the numerical

model can accurately predict the general flame characteristics. This, in turn, validates the correct settings of the boundary conditions in the model and also shows the capability of the combustion model and mechanism used for the current CH_4/CO/air flame calculations. This fact suggests that the model can be used for further analysis of the flame chemical structures as the composition of the blended fuel is varied.

3-4 Chemical Kinetic Structures

In order to further understand the effect of the variation of blended fuel composition on flame characteristics, detailed flame structures of four characteristic flames selected, as indicated in Fig. 8, are examined. The profiles of the temperature, species mole fraction, production rate, net reaction rate, and heat-release rate of the major elementary steps along the jet axis are plotted in Figs. 11, 12, 13, and 14 for flames 1, 5, 9, and 12, respectively. In the figures the dashed line indicates the axial location of the peak temperature gradient which separates the preheat zone and the oxidation zone. Figs. 11a and 11b show that the distributions of temperature, species mole fraction, and production rate are typical of premixed stoichiometric methane flame. The production of CO is primarily from the oxidation of CH_4 and the CO oxidation starts after the CH_4 has been consumed to a large extent. Figs. 11c and 11d show the net reaction rate and the heat-release rate of major elementary steps. The most significant reaction is the chain-branching reaction

$$H + O_2 \leftrightarrow OH + O \quad \text{(R38)}$$

followed by the OH attack on H2 through reaction

$$OH + H_2 \leftrightarrow H + H_2O \quad \text{(R84)}$$

to form the product H_2O and to further build up the H radical pool. Both the reactions

$$OH + CH_4 \leftrightarrow CH_3 + H_2O \quad \text{(R98)}$$

and

$$H + CH_4 \leftrightarrow CH_3 + H_2 \quad \text{(R53)}$$

play an equivalent role in the dehydrogenation of methane in this premixed CH4/air flame, but the reaction (R98) occurs slightly prior to the reaction (R53). The production of the intermediate CO is mainly from the reactions

$$O + CH_3 \rightarrow H + H_2 + CO \quad \text{(R284)}$$

and

$$O_2 + HCO \leftrightarrow HO_2 + CO \quad \text{(R168)}$$

The oxidation of CO is mainly through reaction

$$OH + CO \leftrightarrow H + CO_2 \quad \text{(R99)}$$

and its rate is slow until the CH_4 has been consumed through (R98) and (R53) to a large extent. Fig. 11d indicates that the major contributions to the positive heat release are the reactions, including

$O + CH_3 \leftrightarrow H + CH_2O$ (R10)

$O + CH_3 \rightarrow H + H_2 + CO$ (R284)

$OH + H_2 \leftrightarrow H + H_2O$ (R84)

$OH + CH_4 \leftrightarrow CH_3 + H_2O$ (R98)

$OH + CO \leftrightarrow H + CO_2$ (R99)

$O_2 + HCO \leftrightarrow HO_2 + CO$ (R168)

$OH + CH_2O \leftrightarrow HCO + H_2O$ (R101)

$H + CH_2O \leftrightarrow H_2 + HCO$ (R58)

$HO_2 + H \leftrightarrow OH + OH$ (R46)

The major negative contributors are (R38), (R166), and (R167). The major reaction steps discussed in this paper are summarized in Table 2.

Fig. 12 shows the axial variations of calculated variables for flame 5 (60% CH_4–40% CO). As 40% of CO is added to the fuel mixture, several noticeable features are observed. The oxidation of the additive CO does not occur during the methane oxidation stage in which intermediate CO is also produced. The CO mole fraction keeps increasing up to the point where the OH pool reaches approximately a maximum, and a gradual consumption starts. This result is also in agreement with the finding of Ref. [25]. In addition, Fig. 12c indicates that the intermediate CO is mainly produced through reactions

$O + CH_3 \rightarrow H + H_2 + CO$ (R284)

and

$O_2 + HCO \leftrightarrow HO_2 + CO$ (R168)

which follow the CH_4 dehydrogenation reactions (R98) and (R53). Finally, the rate of CO oxidation (R99) not only increases significantly but also contributes to a significant amount of heat-release (Fig. 11d) as compared to the premixed pure methane flame (flame 1).

Fig. 13 shows similar axial variations of calculated variables for flame 9 (20% CH_4–80% CO). As the volume fraction of CO increases to 80% in the fuel mixture, the CH_4 mole fraction drops sharply across the maximum temperature gradient, but the CO is decreasing gradually due to the accompanied production of the intermediate CO from methane oxidation. However, the dominant chemistry of this flame, unlike that of flames 1 and 5, shifts toward

the CO kinetics. It can be seen from Fig. 13c that in the preheat zone, the rate of reaction

$HO_2 + H \leftrightarrow OH + OH$ (R46)

for OH production and the rate of reaction (R99) for CO oxidation exceed that of reactions (R98) and (R53) for the dehydrogenation of methane. Therefore, in the preheat zone, the OH radicals react with CO through a faster reaction rate compared to that of methane oxidation and hence, results in a faster CO consumption rate (Fig. 13b). In the oxidation zone, the large amount of OH produced from reaction (R38) is mainly for CO oxidation reaction, though the dehydrogenation of methane through reaction (R98) is still very active. Thus the reaction (R99) almost dominates the overall reaction rate (Fig. 13c) and contributes most of the positive heat-release in the preheated and oxidation zones (Fig. 13d).

As the concentration of CO is further increased to 96%, the calculated axial distribution of variables is shown in Fig. 14 for flame 12 (4% CH_4–96% CO). For such a large amount of additive CO in the fuel mixture, the CH4 chemistry plays only a minor role in the overall reaction as evident by the consumption rates of CH_4 and CO (Fig. 14b). Fig. 14c also shows that the rate of methane dehydrogenation reactions (R98) and (R53) is much less than the rate of OH production reactions (R38) and (R46). The produced OH radicals accelerate the CO oxidation through reaction (R99) which contributes to the overall heat release of this flame.

Comparison of the computed chemical kinetic structures reveals that for a fixed stoichiometry of the CH_4/CO/air flame, the flame temperature and the reaction rate of reaction (R99) increase with increasing CO content in the fuel mixture; and they reach a maximum value at 80% of CO in the fuel and then decrease beyond this fuel mixture. Moreover, the overlap of heat release rate distributions of reaction (R10), reaction (R284), and reaction (R99) in Fig. 13d imply that higher heat release density is found at reaction zone when 80% of CO is added in the fuel. These facts suggest that the reactions which have high heat release rate and CO consumption rate (R99) play an important role in affecting the heat release behavior and the laminar burning velocity as the CO content in the fuel is varied. Sung et al. [24] reported that the increase in the laminar flame speed with CO addition to n-C_4H_{10}/air flames results from changes in the adiabatic flame temperature (thermal effect) and from an increase in active radicals during combustion (chemical effect). They found that the laminar flame speed increases linearly with the amount of CO addition and the thermal effect on the laminar flame speed is more significant than the chemical effect with CO addition for rich and lean mixtures. They also explained that the effect of CO addition is thermal in nature which is based on the findings of Vagelopoulos and Egolfopoulos [25] that the added CO will not react until most of the hydrocarbon species have been consumed.

3-5 Sensitivity Analysis

To interpret the influence of chemical reaction effect on the flame phenomena of CH_4/CO/air premixed flame, the first-order sensitivity coefficients of selected reactions with

respect to the reaction rate constants for CH_4 and CO are calculated and shown respectively in Fig. 15. It can be seen that the sensitivities of (R53) and (R98) become lower as the concentration of CO is increased. For CO, the oxidation of CO is mainly through (R12) (dry oxidation step) and (R99) (H atom assisted step). The sensitivities of (R12) and (R99) become higher and lower respectively as the concentration of CO is increased in fuel mixture. In addition, the oxidation of CO is dominated by (R12) as the concentration of CO is higher than 80% in fuel mixture. The reactions (R166) and (R167), which are the main reaction process of CO production in CH_4 oxidation, become less important when CO concentration is increased. According to the results shown in Figs. 12–15, the laminar burning velocity is depends on heat release rate of (R10), (R284) and (R99) and their spatial distribution. When concentration of CO is increased, heat release rate contributed from (R99) is increased and becomes comparable to that from (R10) and (R284) in Fig. 13d when the laminar burning velocity reaches a maximum. As the concentration of CO is higher than 80%, due to insufficient H atom in flame, the oxidation of CO is dominated by dry oxidation step (R12) which has a lower heat release rate and leads to a slower reaction. This suggests that the insufficient amount of H atom, due to the limited amount of CH_4 in the fuel, decelerates the reaction of (R99), generates less heat release and hence results in a significantly decrease of laminar burning velocity. Reviewing the adiabatic flame temperatures and net heating value listed in Table 1 and results shown in Fig. 5, it becomes clear that the variations of laminar burning velocity for such kind of blended fuels can not be determined solely based on adiabatic flame temperature. This fact suggests that the concept of pure thermal effect [50] on the laminar burning velocity is not applicable for blended stoichiometric CH_4/CO/air flames. This finding seems contradictory to the conclusion made by Sung et al. [50] that the effect of CO addition on the laminar burning velocity is thermal in nature. However, a detailed examination of the results of Sung et al. [50] reveals that the thermal effect is more significant for rich and lean *n*-C_4H_{10}/CO/air flames, whereas the chemical effect is more significant for stoichiometric flame at atmospheric pressure condition. On the other hand, the Lewis numbers of methane, carbon monoxide, and oxygen almost remain constant for different cases in this study. Hence, it also suggests that the effect of Lewis number on the temperature and laminar burning velocity of stretched flame in the present study could be minor. In summary, we find that the effect of CO addition on the laminar burning velocity of the stoichiometric CH_4/CO/air flames is most likely dominated by the chemical effect of the transition of dominant reaction steps. This, in part, explains the failure in prediction of laminar burning velocity using the flame-temperature-based mixing rules.

Premixed Stoichiometric $H_2/CH_4/CO$/air Flames

3-6 Adiabatic Flame Temperature

For premixed stoichiometric $H_2/CH_4/CO$/air flames, the experimental conditions are shown in Table 3. The effect of H_2 addition on the adiabatic flame temperatures of premixed stoichiometric $H_2/CH_4/CO$/air flames is shown in Fig. 16. The adiabatic flame temperatures are calculated using the STANJAN code [51]. It can be seen that the adiabatic flame temperature increases with increasing H_2 concentration in the $H_2/CH_4/CO$ fuel mixture. For a fixed H_2 concentration the adiabatic flame temperature increases with increasing CO content in the CH_4/CO fuel ratio and it reaches to a maximum value when CO is increased to 100%. However, the maximum adiabatic flame temperature does not increase significantly with increasing H_2 concentration when the fuel is a purely stoichiometric H_2/CO mixture. This fact suggests that at stoichiometric condition the effect of H_2 addition on the adiabatic flame temperature is lager for the H_2/CH_4 flames than for the H_2/CO flames.

3-7 Laminar Burning Velocity

The computed laminar burning velocities of the premixed stoichiometric $H_2/CH_4/CO$/air flames under various $H_2/CH_4/CO$ fuel compositions are shown in Fig. 17. Note that the laminar burning velocity is also calculated based on the "dry" oxidation condition, i.e., no water vapor is present in the air. Fig. 17 shows that with 0% of H_2 in the fuel mixture, the laminar burning velicity increases with increasing CO content in the CH_4-air mixture, and it reaches to a maximum value (55 cm/s) at the condition of 80% of CO in fuel and decreases rapidly as CO is further increased.

When 10% of H_2 is added to the fuel mixture, the laminar burning velocity is increased, especially for the condition of 100% of CO in the CH_4/CO mixture. Note that the burning velocity has increased from near zero for the pure CO flame to a value of 46 cm/s for the 10% H_2–(100% CO+0% CH_4) flame. In addition, the increase of H_2 content in the blended fuel not only increases the burning velocity, but also shifts the maximum burning velocity form that occurred at the condition of 10% H_2–(85% CO+15% CH_4) to 50% H_2–(100% CO+0% CH_4). Comparison of Figs. 16 and 17 indicates that the adiabatic flame temperature and laminar burning velocity are not only infuenced by the content of H_2, but also by the CO concentration in the fuel mixture. This fact suggests that further investigations of the flame and chemical kinetic structures of the premixed stoichiometric $H_2/CH_4/CO$/air flames are needed.

3-8 Flame Appearance and Flame Front Position

Photographs of the premixed stoichiometric $H_2/CH_4/CO$/air opposed-jet flames with 0%, 10% and 20% of H_2 and various CO contents in the fuel mixture are shown in Fig. 18. Fig. 18 shows that for 0% of H_2 in fuel, the flame appearences are similar to those previously shown in Fig. 6. When 10% and 20% of H_2 are added to the fuel mixture, the overall flame appearences are similar to those of pure CH_4/CO/air flames except for the case of 100% CO in fuel. At low CO concentrations (≤ 10%), two symmetrical, plannar flames exist and the flames are blue in color. As the CO concentration is increased, the postflame zone (region between two plannar flames) immediately becomes orange in color and extends in lateral direction. It is noted that the separation distance between two symmetrical flames increases with increasing CO concentration. The separation distance reaches to a maximum value at the conditions of 90% CO–10% CH_4 and 94% CO–6% CH_4 for 10% and 20% of H_2 additions, respectively. Fig. 18 also indicates that the increase of H_2 addition to the CH_4/CO/air mixtures increases the separation distance and changes the flame front position.

In order to determine the flame front position, direct photographs of the premixed stoichiometric $H_2/CH_4/CO$/air opposed-jet flames are performed. The flame front position (the distance from the nozzle exit) is determined at the location along the jet axis where maximum flame luminosity occurs. Comparison of the measured and predicted flame front positions is shown in Fig. 19 to examine the effects of H_2 and CO contents on the flame structure and to validate the numerical predictions. For the opposed-jet flames, the calculated flame front position is defined at the axial location of maximum temperature gradient. Fig. 19 shows the good agreements between the measured and the predicted results. It can be seen that for 0%, 10%, and 20% of H_2 additions the flame front position decreases with increasing CO concentration, and it reaches to a minimum value at 80%, 90% and 94% of CO in the CH_4–CO fuel and then increases as CO is further increased. It is interesting to note that the profile of the variation of flame front position with CO contents in the $H_2/CH_4/CO$/air mixtures (Fig. 19) looks like an inversion of the laminar flame velocity profile (Fig. 17). Comparison of Figs. 17 and 19 indicates that 0% H_2–20% CH_4–80% CO, 10% H_2–9% CH_4–81% CO, and 20% H_2–4.8% CH_4–75.2% CO flames have the maximum laminar burning velocity and produce the shortest distance from the nozzle to the flame front position as compared to the other flames studied. The effects of H_2 and CO variations on the flame speed and flame front position are closely related to the chemical kinetics of the blended fuels.

3-9 Temperature Measurements

In addition to measurements of the flame front position for premixed stoichiometric $H_2/CH_4/CO$/air opposed-jet flames, temperature measurements are also performed. Typical results for 0%, 10%, and 20% of H_2 additions with various CO and CH_4 contents coupled with numerical predictions of temperature are shown in Fig. 20. For temperature

measurements, due to the limitation of the R-type thermocouple (~2040 K) only the preheated and partial oxidation zones are measured. Fig. 20 shows that for 0% of H_2 addition, four flames result in a similar temperature gradient, but the preheat zone for the 80% CO–20% CH_4 flame shifts closest to the nozzle exit and leads to a slightly higher calculated flame temperature. When 10% and 20% of H_2 are added to the fuel mixture, the preheated zone closest to the nozzle exit occurs at the condition of 90% CO–10% CH_4 and 94% CO–6% CH_4, respectively. The predicted flame temperatures are in good agreement with the measured data for all the flames measured.

3-10 Chemical Kinetic Structures

In order to understand the effect of H_2 addition and the variation of CH_4 and CO fuel compositions on flame characteristics, detailed flame structures for the premixed stoichiometric $H_2/CH_4/CO$/air flames are examined. The chemical kinetic structures of CH_4/CO/air flames with various CO contents in fuel have been presented in previous section and shown in Ref. [51]. Here we only present the calculated results for 10% H_2 with 10% CO–90% CH_4, 50% CO–50% CH_4, 80% CO–20% CH_4, 90% CO–10% CH_4, and 98% CO–2% CH_4 in CH_4/CO fuel and 20% H_2 with 10% CO–90% CH_4, 50% CO–50% CH_4, 80% CO–20% CH_4, 94% CO–6% CH_4, and 98% CO–2% CH_4 in CH_4/CO fuel. The profiles of the temperature, species mole fraction, production rate, net reaction rate, and heat-release rate of the major elementary steps along the jet axis are plotted in Figs. 21–25 and 26–30 for 10% and 20% H_2, respectively. In the figures the dashed line indicates the axial location of the peak temperature gradient which separates the preheat zone and the oxidation zone. It can be seen form Figs. 21a, 22a, 26a and 27a that when the CO concentration in fuel is low (10% and 50%) the production of H_2 and CO is primarily from the oxidation of CH_4 and the H_2 and CO oxidations start after the CH_4 has been consumed to a large extent. The production of H_2O is prior to that of CO_2. As the volume fraction of CO increases to 80% in the fuel mixture (Figs. 23a and 28a), the oxidation of H_2 starts slightly earilier than that of CH_4 and CO. The CH_4 mole fraction drops sharply across the maximum temperature gradient, but the CO is decreasing gradually due to the accompanied production of the intermediate CO from methane oxidation. However, the dominant chemistry of these flames, unlike the 10% and 50% CO flames, shifts toward the CO kinetics. When the concentration of CO is increased to 90% (Fig. 24a) and 94% (Fig. 29a), the oxidation of CH_4 and CO occurs almost at the same time. Similar behavior is observed for the production of H_2O and CO_2. The CH_4 chemistry plays only a minor role in the overall reaction as evident by the consumption rates of CH_4 and CO (Figs. 24c and 29c). As the concentration of CO is further increased to 98%, the dry oxidation of CO becomes the dominant reaction in the flame.

Computed net reaction rates indicate that with H_2 addition, the reaction (R38) dominates the overall reaction for the CO volume fraction less than 90%. The maximum reaction rate of

R38 occurs at 20% H_2 and 80% CO. When the CO is increased to 90% and higher, the reaction rate of R99 exceeds that of R38. The maximum reaction rate of R99 appears at the condition where the maximum laminar burning velocity occurs, i.e. at 10% H_2–90% CO–10% CH_4 and 20% H_2–94% CO–6% CH_4. The reaction rate of R84 is always higher than that of R53 and R98, but its reaction location occurs later than R53 and R98 for CH_4/CO/air flames. When H_2 is added to the fuel, the reaction location of R84 shifts closer to that of R98. The reactions (R84) and (R98) occur at the same location when the maximum burning velocity also occurs. As the CO is increased to 98%, the reaction (R84) occurs before the reaction (R98). When 20% of H_2 is added to the fuel, the reaction location of R84 is different from that with 10% H_2 addition. The reactions (R84) and (R98) occur at the same location at 80% CO. As the CO is increased to 94%, the reaction (R84) occurs before the reaction (R98) and its rate is also higher in the preheated zone. It is noted that the addition of H_2 increases the overall reaction rate, especially for the reactions (R38) and (R84).

Computed heat-release rates reveal that the major contributions to the positive heat release are the reactions including R10, R284, R84, R98, R99, R168, R101, R58, and R46. The major negative contributors are R38, R166, and R167. The contribution of heat release from R99 increases with increasing CO content. It reaches to a maximum value at the condition where maximum burning velocity occurs and then decreases as the CO is further increased.

3-11 Sebsitivity Analysis

In order to understand the effect of H_2 addition on the reaction steps, the sensitivity analysis with respect to temperature are made and shown in Figs. 31-33. Fig. 31 shows that with 0% of H_2 addition, the sensitivity of (R38) is the highest for 10% CO–90% CH_4 and 50% CO–50% CH_4 flames and it becomes lower as the CO is increased over 80%. When the concentration of CO is larger than 80%, the oxidation of CO through R99 becomes the dominant reaction. Figs. 32 and 33 also show similar results for 10% and 20% H_2 additions. This fact suggests that the addition of H_2 does not affect the transition of dominant reaction steps as that for CH_4/CO/air flames.

3-12 Pollutant Emissions

The pollutant emissions of CO, NO_x, and CO_2 are measured for the the premixed stoichiometric H_2/CH_4/CO/air flames. Fig. 34 shows that with 10% and 20% of H_2 additions the CO emissions are lower than those without H_2 addition. And, as expected, the CO emission increases with increasing CO content in the fuel mixture. Fig. 35 shows the measured NO_x emissions for flames with 0%, 10%, and 20% of H_2 additions. It can be seen that with H_2 addition to the fuel the NO_x emissions are higher than those without H_2 addition

for the CO content in fuel mixture up to 80%. The flame with H_2 addition results in lower NO_x emissions than that without H_2 addition when the CO volume fraction is larger than 80%. This could be due to the effect of the change of dominant reaction steps. In general, the increase of H_2 in fuel would increase the adiabatic flame temperature, and hence, increase the NO_x emission. For the CO_2 emission, it increases with increasing CO content in fuel mixture as shown in Fig. 36. The addition of H_2 (up to 30%) to the fuel mixture does not reduce the CO_2 emission.

CHAPTER IV
CONCLUSIONS

In the present study, the effect of H_2 and CO additions on the characteristics of methane/air flames is examined systematically. The study is divided into two parts due to thermophysical complexity of the blended fuel. The first part focuses on experimental measurements and numerical simulations of the flame front position, temperature, and velocity in the *stoichiometric* CH_4/CO/air opposed-jet flames with various CO contents in the fuel. While the second part concentrates on experimental and numerical studies of the *stoichiometric* H_2/CH_4/CO/air opposed-jet flames.

The laminar burning velocities of the CH_4/CO/air flames under various equivalence ratios and fuel compositions are firstly calculated using the PREMIX code of Chemkin collection 3.5. Computed results show that for a fixed fuel composition the maximum burning velocity occurs at the rich side of stoichiometry. The maximum burning velocity increases with increasing CO concentration in the fuel mixture, and it reaches its highest value (77.43 cm/s) at φ = 1.9 (6% CH_4–94% CO in the fuel mixture) and then decreases as CO is further increased. The calculated results are also in good agreement with reported experimental data [44].

In order to investigate the effect of fuel variations on the flame structure, *stoichiometric* CH_4/CO/air opposed-jet flames are examined in detail. Experimental measurements and numerical simulations of the flame front position, temperature, and velocity under various fuel compositions are performed. The flame structures are simulated using the OPPDIF package with GRI-Mech 3.0 mechanisms and detailed transport properties. Computed results, again, show that the laminar burning velocity increases monotonically with increasing CO content in the CH_4–air mixtures, and it reaches a maximum value (57.5 cm/s) at the condition of 80% of CO in fuel and then decreases rapidly as CO is further increased. In contrast to these results, the flame-temperature-based mixing rule predicts a monotonic decrease of the burning velocities with increasing CO content in the blended fuel, indicating the invalidity of the mixing rule for laminar burning velocity predictions in CH_4/CO/air flames. Comparisons of the predicted flame front position, temperature, and velocity with the measured data indicate that the numerical model can accurately predict the general flame characteristics. This, in turn, validates the correct settings of the boundary conditions in the model and also shows the capability of the GRI-Mech 3.0 mechanisms for CH_4/CO/air flame calculations.

Finally, the calculated chemical kinetic structures for flames 1 (100% CH_4–0% CO), 5 (60% CH_4–40% CO), 9 (20% CH_4–80% CO), and 12 (4% CH_4–96% CO) are compared and the key reactions that affect the flame structure and laminar flame speed are identified. For flame 1, both reactions (R98) and (R53) play an equivalent role in the dehydrogenation of methane in CH_4/air flame, the reaction (R98) occurs slightly prior to the reaction (R53). The

production of the intermediate CO is mainly from the reactions (R284) and (R168). The oxidation of CO is mainly through reaction (R99) and its rate is slow until the CH4 has been consumed through (R98) and (R53) to a large extent. As 40% of CO is added to the fuel mixture, the oxidation of the additive CO does not occur during the methane oxidation stage in which intermediate CO is also produced. However, the rate of CO oxidation (R99) increases significantly and contributes to a significant amount of heat-release as compared to the premixed pure methane flame. As the volume fraction of CO is increased to 80% in the fuel mixture, the chemistry of this flame shifts toward the kinetics of the additive CO. Thereby, the reaction (R99) almost dominates the overall reaction rate and contributes to most of the positive heat-release in the preheated and oxidation zones. As the concentration of CO is further increased to 96%, the rate of methane dehydrogenation reactions (R98) and (R53) is much less than the rate of OH production reactions (R38) and (R46). The produced OH radicals accelerate the CO oxidation through reaction (R99) which still contributes to the overall heat release to this flame even though reaction (R99) is not dominant. Comparison of the computed laminar burning velocity, flame temperature, and CO consumption rate (R99) reveals that the effect of CO addition on the laminar burning velocity of the stoichiometric CH_4/CO/air flames is due mostly to the transition of the dominant chemical kinetic steps.

For H_2/CH_4/CO/air flames, the addition of H_2 to the fuel mixture not only increases the overall burning velocity, but also changes the characteristics of flame velocity. When 10% and 20% of H_2 are added to the CH_4/CO fuel mixture, the maximum laminar burning velocity occurs at 90% CO–10% CH_4 and 94% CO–6% CH_4, respectively. This is also confirmed by experimental measurements of temperature and flame front position.

Computed chemical kinetic structures indicate that with H_2 addition, the reaction (R38) dominates the overall reaction for the CO volume fraction less than 90%. The maximum reaction rate of R38 occurs at 20% H_2 and 80% CO. When the CO is increased to 90% and higher, the reaction rate of R99 exceeds that of R38. The maximum reaction rate of R99 appears at the condition where the maximum laminar burning velocity occurs, i.e. at 10% H_2–90% CO–10% CH_4 and 20% H_2–94% CO–6% CH_4. The reaction rate of R84 is always higher than that of R53 and R98, but its reaction location occurs later than R53 and R98 for CH_4/CO/air flames. When H_2 is added to the fuel, the reaction location of R84 shifts closer to that of R98. The reactions (R84) and (R98) occur at the same location when the maximum burning velocity also occurs. As the CO is increased to 98%, the reaction (R84) occurs before the reaction (R98). When 20% of H_2 is added to the fuel, the reaction location of R84 is different from that with 10% H_2 addition. The reactions (R84) and (R98) occur at the same location at 80% CO. As the CO is increased to 94%, the reaction (R84) occurs before the reaction (R98) and its rate is also higher in the preheated zone. It is noted that the addition of H_2 increases the overall reaction rate, especially for the reactions (R38) and (R84). The major contributions to the positive heat release are the reactions including R10, R284, R84, R98, R99, R168, R101, R58, and R46. The major negative contributors are R38, R166, and R167.

The contribution of heat release from R99 increases with increasing CO content. It reaches to a maximum value at the condition where maximum burning velocity occurs and then decreases as the CO is further increased. Sensitivity analysis suggests that the addition of H_2 does not affect the transition of dominant reaction steps as that for CH_4/CO/air flames. Pollutant emission measurements indicate that the addition of H_2 to the fuel mixture reduces CO emission, but increases NO_x emission due to increased flame temperature. In addition, the addition of H_2 (up to 30%) to the fuel mixture does not reduce CO_2 emission for stoichiometric H_2/CH_4/CO/air flames.

REFERENCES

[1] Bureau of Energy, Ministry of Economic Affairs. http://www.moeaec.gov.tw/ecw.asp

[2] IPCC, http://www.ipcc.ch

[3] Energy Policy White Paper, Bureau of Energy, Ministry of Economic Affairs. http://www.moeaec.gov.tw/policy/EnergyWhitePaper/94/main/main.html

[4] Demirbas, A., Global energy sources, energy usage and future development, *Energy Sources*, **26,** 2004, 191-204.

[5] Demirbas, A., Potential Applications of Renewable Energy Sources, Biomass Combustion Problems in Boiler Power Systems and Combustion Related Environmental Issues. *Progress in Energy and Combustion Science*, **31,** 2005, 171-192.

[6] The President's Hydrogen Fuel Initiative. http://www.hydrogen.gov./president.html

[7] Quakernaat, J., Hydrogen in a global long-term perspective. *Int. J. Hydrogen Energy*, **20**: 485-492 (1995).

[8] Demirbas, A., Combustion characteristics of different biomass fuels. *Progress in Energy and Combustion Science*, **30,** 2004, 219-230.

[9] Johnson, C. E., Neumeier, Y., Lieuwen, T. and Zinn, B. T., Experimental Determination of the Stability Margin of a Combustor Using Exhaust Flow and Fuel Injection Rate Modulations. *Proc. Comb. Inst*. **28**: 757-763 (2000).

[10] Neumeier, Y. and Zinn, B. T., Active Control of Combustion Instabilities with Real Time Observation of Unstable Combustor Modes. AIAA-96-0758 (1996).

[11] Lefebvre, A. H., *Gas Turbine Combustion* (2nd Ed.). Taylor & Francis, Philadelphia, 1999.

[12] Grosshandler, W., Hamins, A., McGrattan, K. and Rao Charagundla, S. and Presser, C., Suppression of a Non-Premixed Flame behind a Step. *Proc. Comb. Inst.* **28**: 2957-2964 (2000).

[13] Demayo, T. N., Miyasato, M. M. and Samuelsen, G. S., Hazardous Air Pollutant and Ozone Precursor Emissions From a Low-NOx Natural Gas-Fired Industrial Burner. *Proc. Comb. Inst*. **27**: 1283-1291 (1998).

[14] Kuo, K. K., *Principles of Combustion*. John Wiley and Sons, Inc., NY, 1986.

[15] Hayashi, S., Yamada, H., Shimodaira, K. and Machida, T., NOx Emissions From Non-Premixed, Direct Fuel Injection Methane Burners at High-Temperature and Elevated Pressure Conditions. *Proc. Comb. Inst.* **27**: 1833-1839 (1998).

[16] Lieuwen, T. and Zinn, B. T., The Role of Equivalence Ratio Oscillations in Driving Combustion Instabilities in Low NOx Gas Turbines. *Proc. Comb. Inst.* **27**: 1809-1816 (1998).

[17] Paschereit, C. O., Gutmark, E., and Weisenstein, W., Control of Thermoacoustic Instabilities and Emissions an Industrial-Type Gas-Turbine Combustor. *Proc. Comb. Inst.* **27**: 1817-1824 (2000).

[18] Karner, D. and Francfort, J., Low-Percentage Hydrogen/CNG Blend Ford F-150 Operations Summary. U.S. Department of Energy, FreedomCAR & Vehicle Technologies, Advanced Vehicle Testing Activity, Report INEEL/EXT-03-00007~8 (2003).

[19] Todd, D. M. and Battista, R. A., Demonstrated Applicability of Hydrogen Fuel for Gas Turbines. *Proceedings of Gasification 4 the Future*, Noordwijk, The Netherlands, (2000).

[20] Chiesa, P., Lozza, G. and Mazzocchi, L., Using Hydrogen as Gas Turbine Fuel. *J. of Engineering for Gas Turbines and Power*, **127**: 73-80 (2005).

[21] Schefer, R. W., Wicksall, D. M. and Agrawal, A. K., Combustion of Hydrogen-Enriched Methane in a Lean Premixed Swirl-Stabilized Burner. *Proc.*

Comb. Inst. **29**: 843-851 (2002).
[22] Choudhuri, A. R. and Gollahalli, S. R., Intermediate radical concentrations in hydrogen-natural gas blended fuel jet flames. *Int. J. Hydrogen Energy*, **29**: 1293-1302 (2004).
[23] Juste, G. L., Hydrogen injection as additional fuel in gas turbine combustor: Evaluation of effects. *Int. J. Hydrogen Energy*, **31**: 2112-2121 (2006).
[24] Law, C. K. and Sung, C. J., Structure, aerodynamics, and geometry of premixed flamelets. *Progress in Energy and Combustion Science*, *26*: 459-505 (2000).
[25] Vagelopoulos, C. M. and Egolfopoulos, Laminar Flame Speeds and extinction Strain rates of Mixtures of Carbon Monoxide with Hydrogen, Methane, and Air. *Proc. Combust. Inst*. **25**: 1317-1323 (1994).
[26] Papas, P., Glassman, I. And Law, C. K., Effects of Pressure and Dilution on the Extinction of Counterflow Nonpremixed Hydrogen-Air Flames. *Proc. Combust. Inst*. **25**: 1333-1339 (1994).
[27] Ren, J.-Y., Qin, W., Egolfopoulos, F. F. and Tsotsis, T. T., Strain-Rate Effects on Hydrogen-Enhanced Lean premixed Combustion. *Combust. Flame*, **124**: 717-720 (2001).
[28] Sankaran, R. and Im, H. G., Effect of Hydrogen Addition on the Flammability Limit of Stretched Methane/Air premixed Flames. *Proceedings of the Third Joint Meeting of the U.S. Section of the Combustion Institute*, (2003).
[29] Hawkes, E. R. and Chen, J. H., Turbulent Stretch Effects on Hydrogen Enriched Lean Premixed Methane-Air Flames. *Proceedings of the Third Joint Meeting of the U.S. Section of the Combustion Institute*, (2003).
[30] Jackson, G. S., Sai, R., Plaia, J. M., Boggs, C. M. and Kiger, K. T., Influence of H_2 on the response of lean premixed CH_4 flames to high strained flows. *Combust. Flame*, **132**: 503-511 (2003).
[31] Seshadri, K., Counterflow Extinction of Premixed and Nonpremixed Methanol and Ethanol Flames. Report, University of California Energy Institute, paper FSE007, (2005).
[32] Kent, J.H., A noncatalytic coating for platinum-rhodium thermocouple. Combust. Flame 14:279–281 (1970).
[33] Becker, H.A., Yamazaki, S., Entrainment, momentum flux and temperature in vertical free turbulent diffusion flames. Combust. Flame 33:123–149 (1978).
[34] Chao, Y.-C., Jeng, M.S., Behavior of lifted jet flame under acoustic excitation. Proc. Combust. Inst. 24:333–340 (1992).
[35] Andresen, P., Bath, A., Gröger, W., Lülf, H. W., Meijer, G., and ter Meulen, J. J., Laser-induced fluorescence with tunable excimer lasers as a possible method for instantaneous temperature field measurements at high pressure: checks with an atmospheric flame. *Appl. Opt.* **27**, 365-378 (1988).
[36] Cheng, T.S., Chao, Y.-C., Wu, D.-C., Yuan, T., Lu, C.-C., Cheng, C.-K., Chang, J.-M., Effects of Fuel-Air Mixing on Flame Structures and NOx Formations in Swirling Methane Jet Flames.Proc. Combust. Inst. 27:1229–1237 (1998).
[37] Cheng, T.S., Wu, C.-Y., Chen, C.-P., Li, Y.-H., Chao, Y.-C., Yuan, T., Leu, T.S., Detailed measurement and assessment of laminar hydrogen jet diffusion flames. Combust. Flame 146:268–282 (2006).
[38] Smith, G., Golden, D., Frenklach, M., Moriaty, N., Eiteneer, B., Goldenber, M., Bowman, C., Hanson, R., Song, S., Gardiner, W., Lissianski, V., Qin, Z., GRI-Mech 3.0, 1999, http://euler.me.berkeley.edu/gri_mech.
[39] Rightley, M.L., Williams, F.A., Burning velocities of CO flames. Combust. Flame 110:285–297 (1997).
[40] Hirasawa, T., Sung, C.J., Joshi, A., Yang, Z., Wang, H., Law, C.K., Determination of

laminar flame speeds using digital particle image velocimetry: binary fuel blends of ethylene, n-butane, and toluene. Proc. Combust. Inst. 29:1427–1434 (2002).
[41] Spalding, D.B., Fuel 35:347–351 (1956).
[42] Payman, W., Wheeler, R.V., Fuel (London) 1:185 (1922).
[43] Yumlu, V.S., Prediction of burning velocity of carbon monoxide-hydrogen-air flames. Combust. Flame 11:190–194 (1967).
[44] Scholte, T.G., Vaags, P.B., Burning vlocity of mixtures of hydrogen, carbon monoxide and methane with air. Combust. Flame 3:511–524 (1959).
[45] Huang, Y., Sung, C.J., Eng, J.A., Laminar flame speeds of primary reference fuels and reformer gas mixtures Combust. Flame 139:239–251 (2004).
[46] Williams, T.C., Shaddix, C.R., Contamination of carbon monoxide with metal carbonyls: Implications for combustion research. Combust. Sci. Technol. 179:1225–1230 (2007).
[47] Lask, G., Wagner, H.G., Influence of Additives on the Velocity of Laminar Flames. Proc. Combust. Inst. 8:432–438 (1960).
[48] Wyse, C., Vininski, J., Watanabe, T., Solid State Technol. 45 (2002) 125–129.
[49] Schefer, R.W., Goix, P.J., Mechanism of flame stabilization in turbulent, lifted-jet flames. Combust. Flame 112:559–574 (1998).
[50] Sung, C.J., Huang, Y., Eng, J.A., Laminar flame speeds of primary reference fuels and reformer gas mixtures. Combust. Flame 126:1699–1713 (2001).
[51] 張彥丞，"氫氣加入一氧化碳與甲烷混合燃料對火焰結構影響之研究"，國立成功大學航空太空工程學系碩士論文(2010)。

Table 1 Experimental condition of the premixed stoichiometric CH_4/CO/air opposed-jet flames

Flame	Fuel		Mixture	*Net heating value (MJ/nm^3) ($\phi = 1$)	Adiabatic flame temperature (K) ($\phi = 1$)	Le_{O2}	Le_{CH4}	Le_{CO}
	CH_4 (vol%)	CO(vol%)	Air(vol%)					
1	100	0	90.49	3.4106	2258.3	1.08	0.89	N/A
2	90	10	89.80	3.4218	2263.8	1.08	0.90	1.02
3	80	20	89.00	3.4346	2270.2	1.07	0.90	1.02
4	70	30	88.06	3.4497	2277.6	1.07	0.90	1.02
5	60	40	86.95	3.4676	2286.2	1.07	0.90	1.03
6	50	50	85.61	3.4891	2296.5	1.07	0.91	1.03
7	40	60	83.96	3.5156	2308.8	1.07	0.91	1.03
8	30	70	81.89	3.5489	2323.8	1.07	0.92	1.03
9	20	80	79.20	3.5922	2342.6	1.07	0.93	1.03
10	10	90	75.57	3.6505	2366.8	1.07	0.94	1.04
11	6	94	73.74	3.6799	2378.6	1.07	0.94	1.04
12	4	96	72.72	3.6964	2384.8	1.07	0.95	1.04
13	0	100	70.41	3.7334	2398.9	1.07	N/A	1.04

*Net heating value: CH_4=35.88MJ/nm^3; CO=12.62 MJ/nm^3

Table 2 Summary of the major reaction steps.

Reaction number	Reaction step
R10	$O + CH_3 \leftrightarrow H + CH_2O$
R12	$O+CO(+M) \leftrightarrow CO_2 (+M)$
R38	$H + O_2 \leftrightarrow OH + O$
R46	$HO_2 + H \leftrightarrow OH + OH$
R53	$H + CH_4 \leftrightarrow H_2 + CH_3$
R58	$H + CH_2O \leftrightarrow H_2 + HCO$
R84	$OH + H_2 \leftrightarrow H + H_2O$
R97	$OH + CH_3 \leftrightarrow CH_2(S) + H_2O$
R98	$OH + CH_4 \leftrightarrow CH_3 + H_2O$
R99	$OH + CO \leftrightarrow H + CO_2$
R101	$OH + CH_2O \leftrightarrow HCO + H_2O$
R119	$HO_2 + CH_3 \leftrightarrow OH + CH_3O$
R166	$HCO + H_2O \leftrightarrow H + CO + H_2O$
R167	$HCO + M \leftrightarrow H + CO + M$
R168	$O_2 + HCO \leftrightarrow HO_2 + CO$
R284	$O + CH_3 \rightarrow H + H_2 + CO$

Table 3 Experimental condition of the premixed stoichiometric $H_2/CH_4/CO$/air opposed-jet flames.

$H_2/CO/CH_4$ Fuel mixture (vol%)			CO/CH_4 Fuel mixture (vol%)		Air (vol%)	$(F/A)_{stoich}$
H_2	CO	CH_4	CO	CH_4		
0	0	100	0	100	90.49	0.1050
0	10	90	10	90	89.80	0.1136
0	50	50	50	50	85.61	0.1681
0	80	20	80	20	79.20	0.2626
0	85	15	85	15	77.53	0.2898
0	90	10	90	10	75.57	0.3232
0	94	6	94	6	73.74	0.3561
0	98	2	98	2	71.61	0.3964
0	100	0	100	0	70.41	0.4202
10	0	90	0	100	89.80	0.1136
10	9	81	10	90	89.09	0.1225
10	45	45	50	50	84.83	0.1788
10	72	18	80	20	78.56	0.2728
10	76.5	13.5	85	15	76.98	0.2991
10	81	9	90	10	75.14	0.3308
10	84.6	5.4	94	6	73.44	0.3616
10	88.2	1.8	98	2	71.50	0.3986
10	90	0	100	0	70.41	0.4202
20	0	80	0	100	89.00	0.1236
20	8	72	10	90	88.26	0.1330
20	40	40.0	50	50	83.96	0.1910
20	64	16	80	20	77.89	0.2839
20	68	12	85	15	76.40	0.3089
20	72	8	90	10	74.69	0.3388
20	75.2	4.8	94	6	73.14	0.3673
20	78.4	1.6	98	2	71.38	0.4009
20	80	0	100	0	70.41	0.4202

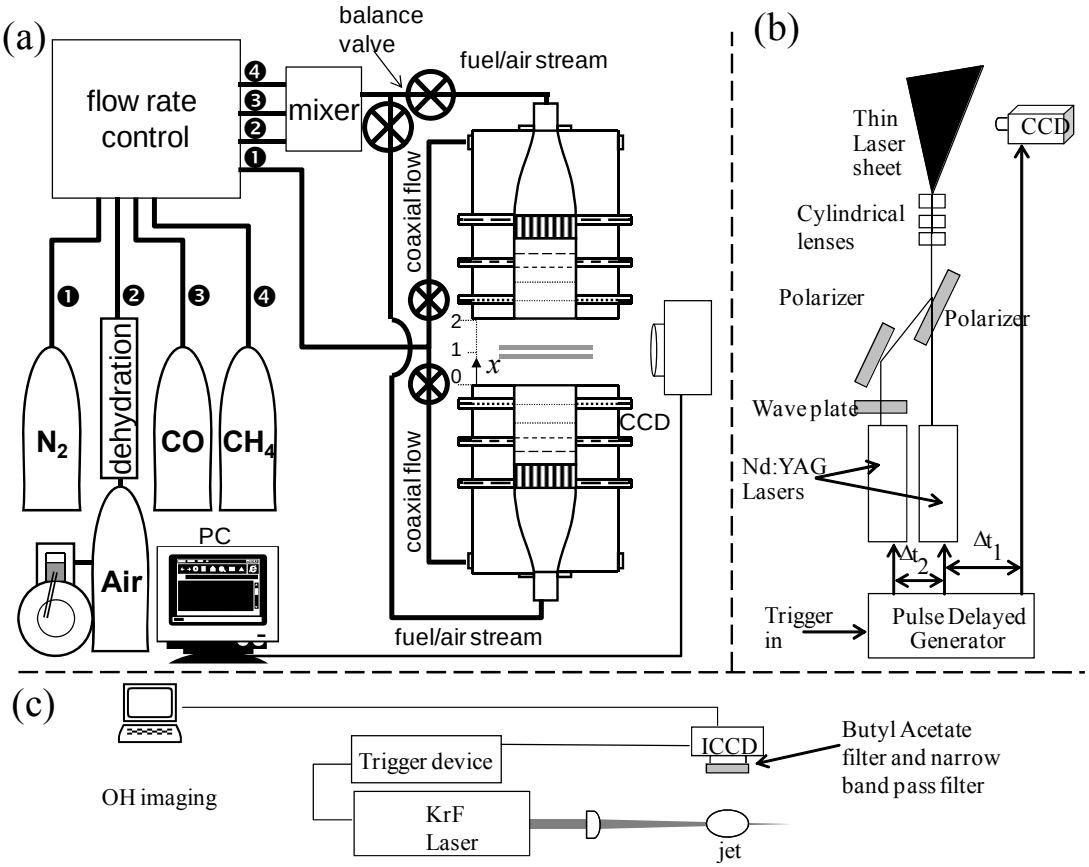

Fig. 1. Experimental apparatus: (a) fuel supply system and opposed-jet burner; (b) particle image velocimetry system; (c) LIPF-OH imaging system.

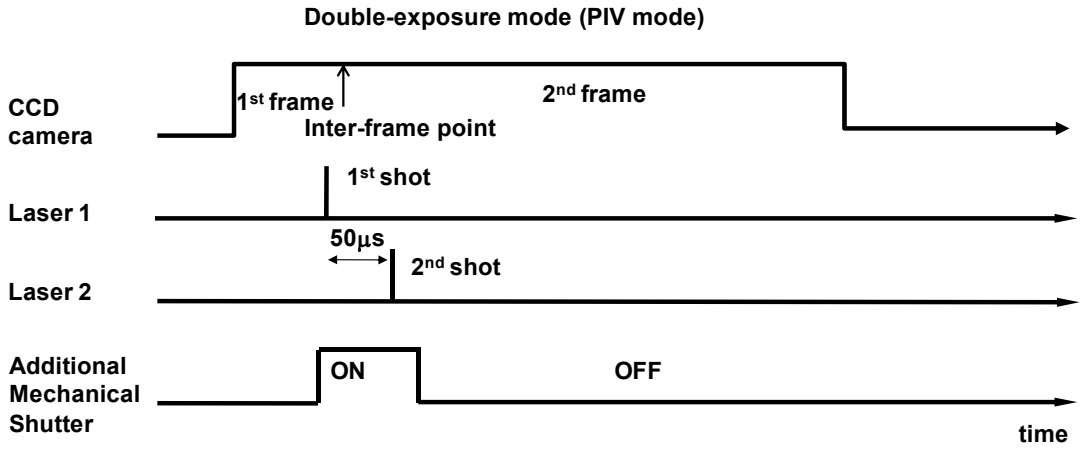

Fig. 2. Schematic plot of CCD control and triggering sequence for PIV measurement.

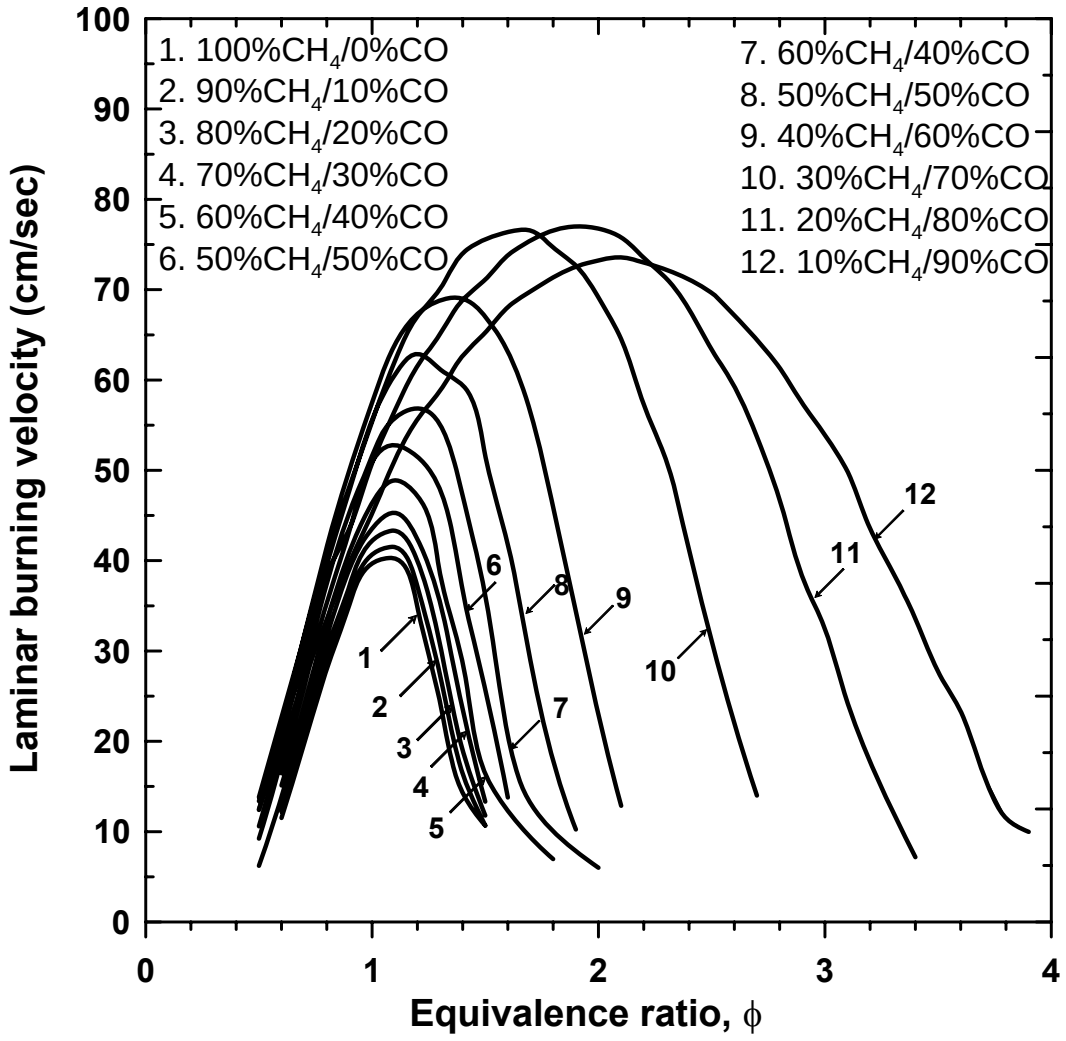

Fig. 3. Computed laminar burning velocity of the CH_4/CO/air flames as a function of equivalence ratio with various CO content in the fuel mixture.

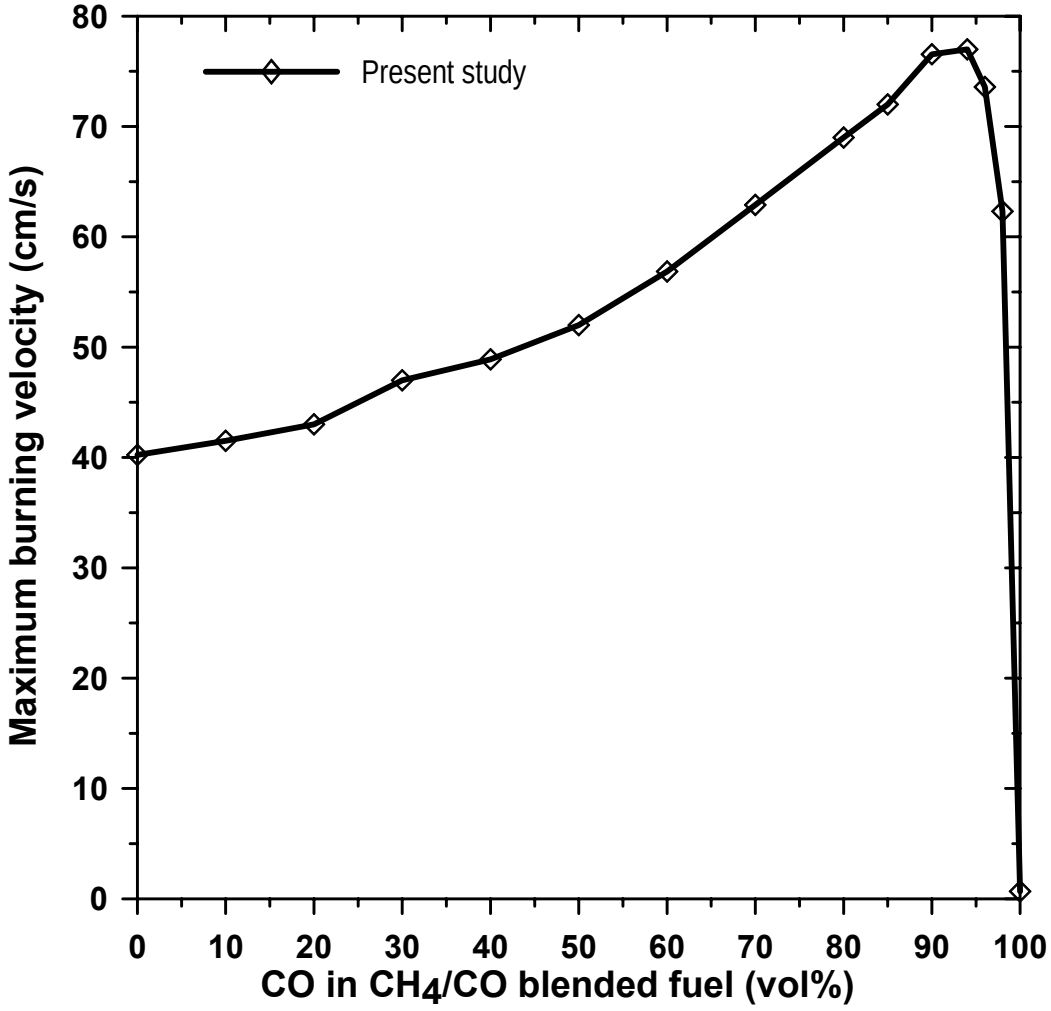

Fig. 4. The computed maximum burning velocities.

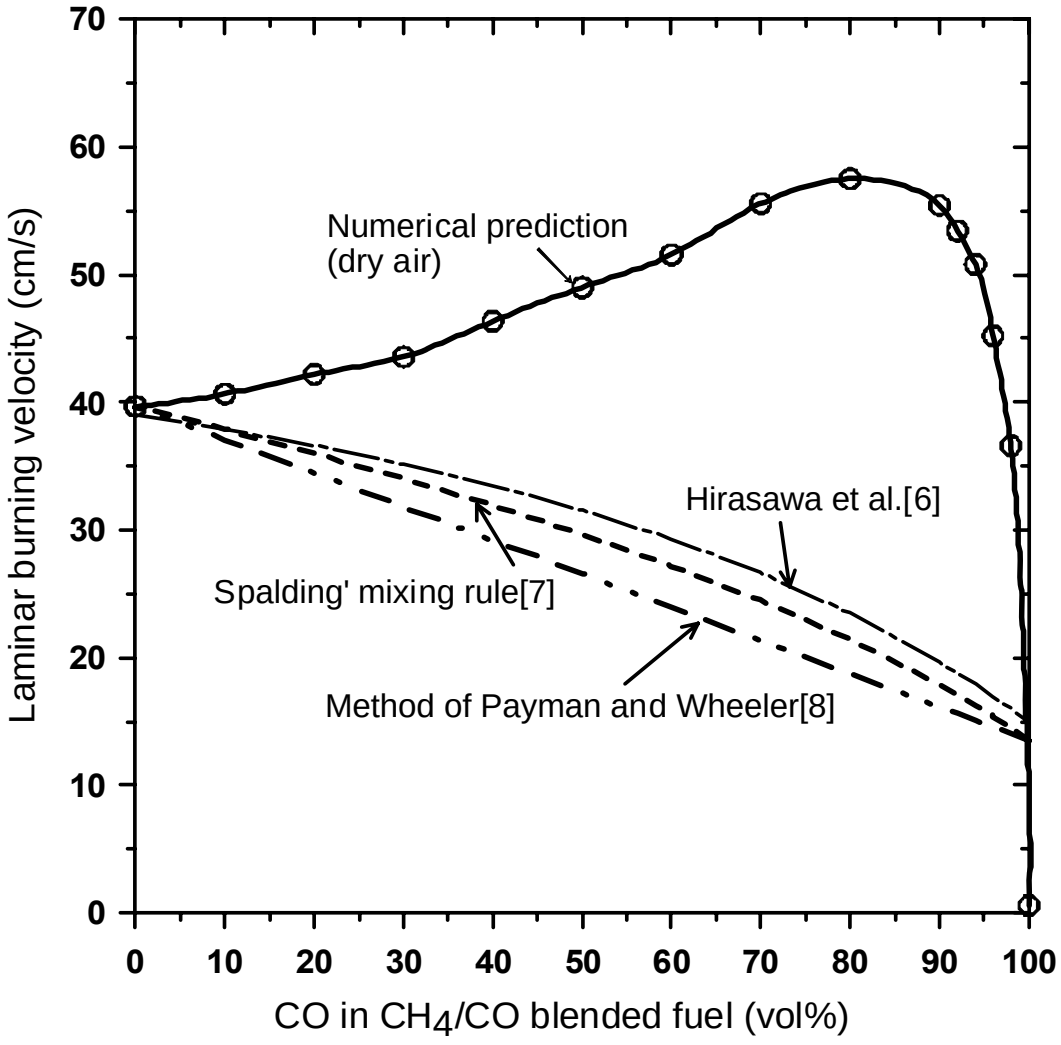

Fig. 5. Comparison of the calculated laminar burning velocities with mixing rule predictions for the stoichiometric CH_4/CO/air flames with various CO contents in the fuel mixture.

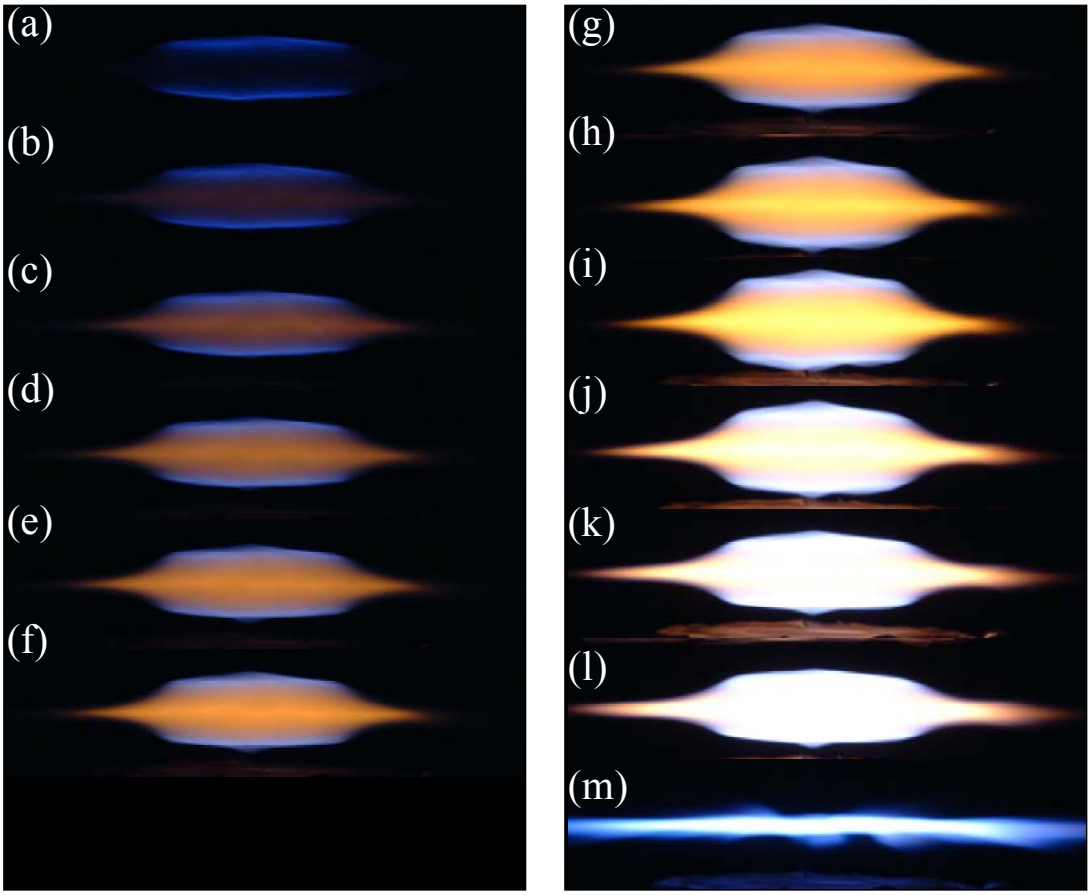

Fig. 6. Photographs of the premixed stoichiometric CH_4/CO/air opposed-jet flames (a): flame 1 (100%CH_4–0%CO), (b): flame 2 (90%CH_4–10%CO), (c): flame 3 (80%CH_4–20%CO), (d): flame 4 (70%CH_4–30%CO), (e): flame 5 (60%CH_4–40%CO), (f): flame 6 (50%CH_4–50%CO), (g): flame 7 (40%CH_4–60%CO), (h): flame 8 (30%CH_4–70%CO), (i): flame 9 (20%CH_4–80%CO), (j): flame 10 (10%CH_4–90%CO), (k): flame 11 (6%CH_4–94%CO), (l): flame 12 (4%CH_4–96%CO), (m): flame 13 (0%CH_4–100%CO).

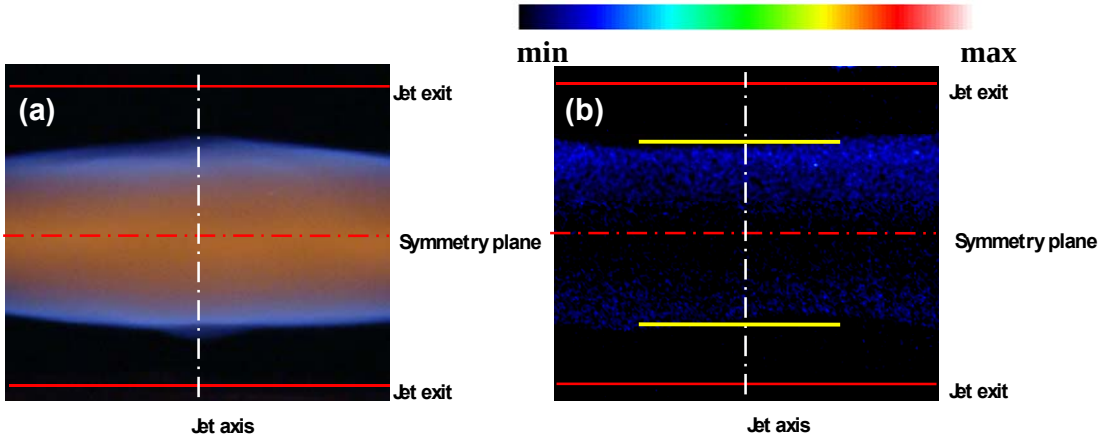

Fig. 7. (a) Photograph and (b) LIPF-OH imaging for flame 4 (70%CH_4-30%CO).

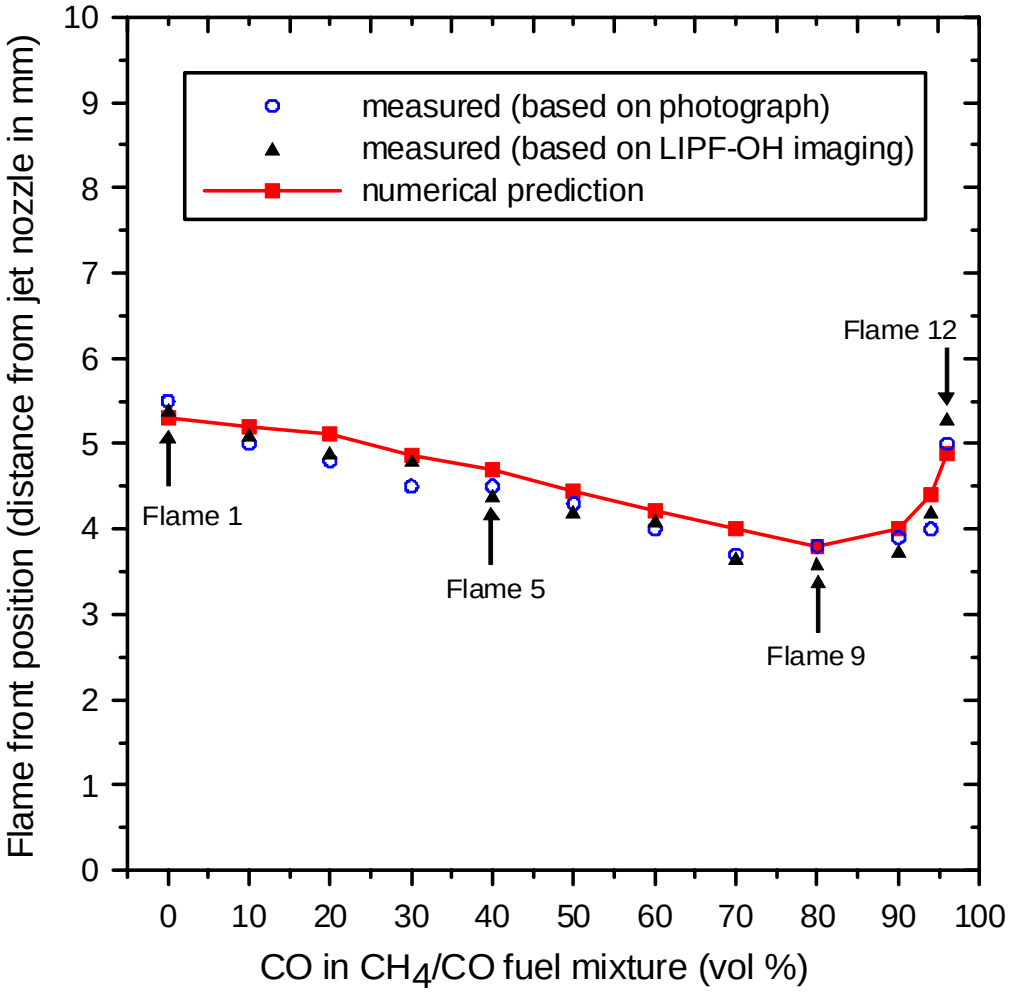

Fig. 8. Comparison of the calculated and measured flame front position for premixed stoichiometric CH_4/CO/air flames.

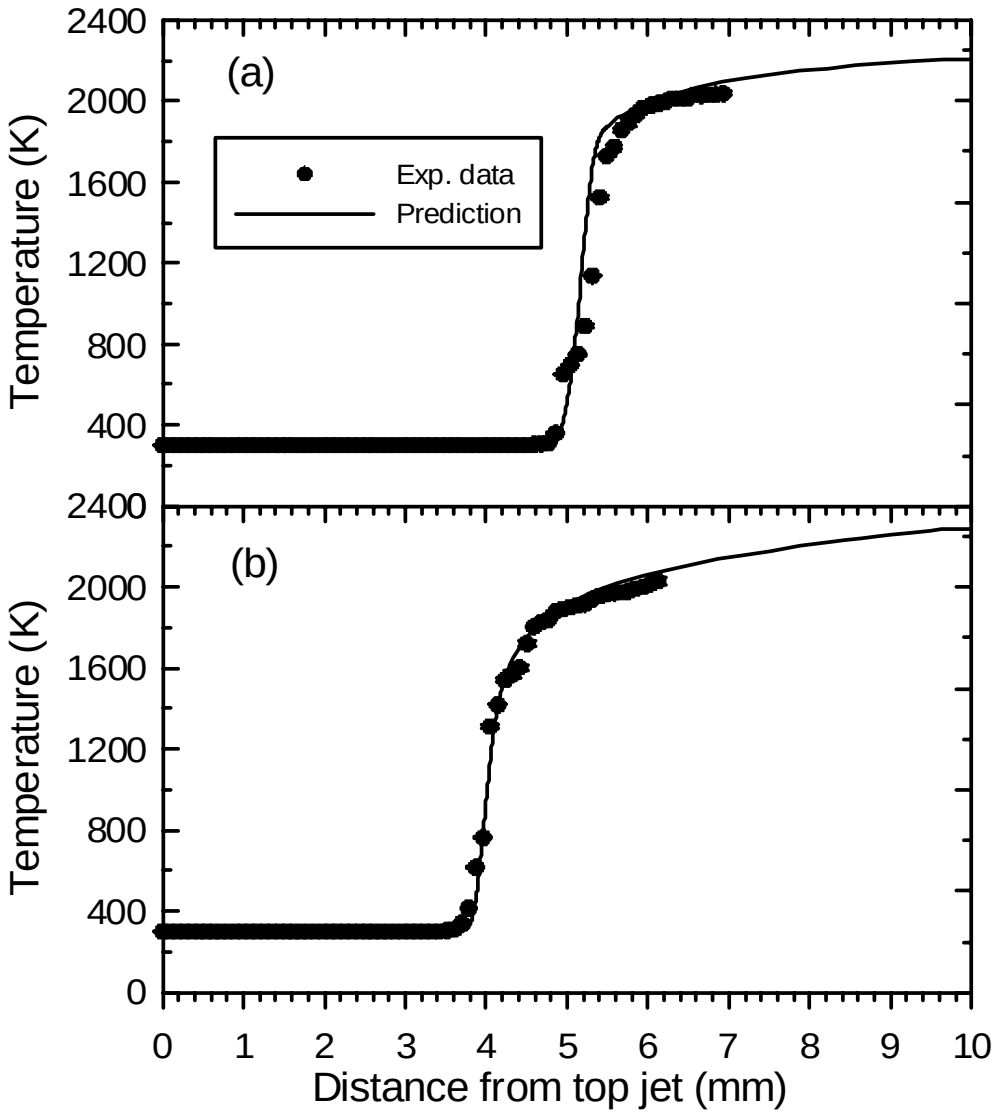

Fig. 9. Comparison of the measured and predicted flame temperatures. (a) flame 2 (90%CH_4-10%CO) and (b) flame 10 (10%CH_4-90%CO).

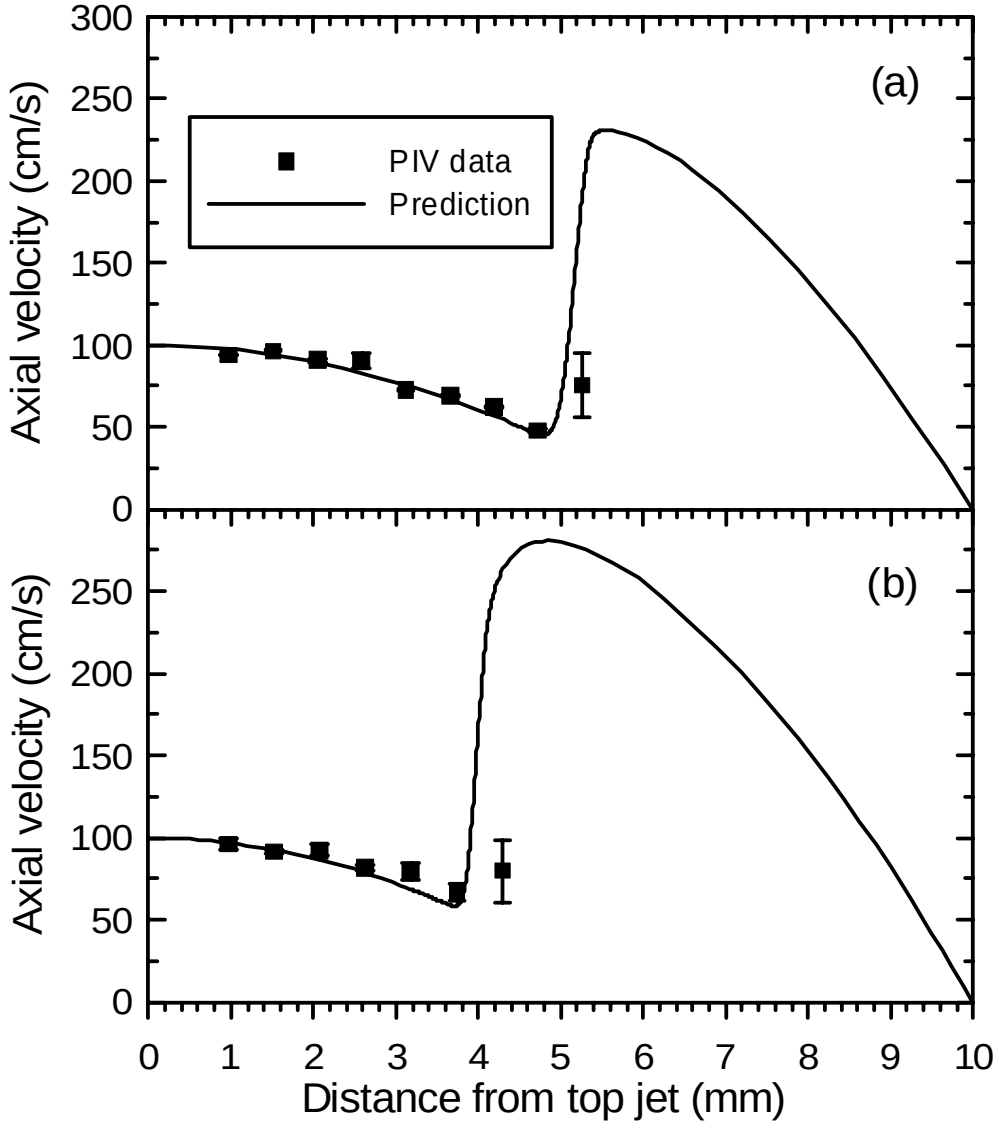

Fig. 10. Comparison of the measured and predicted velocity distributions. (a) flame 2 (90%CH_4-10%CO) and (b) flame 10 (10%CH_4-90%CO).

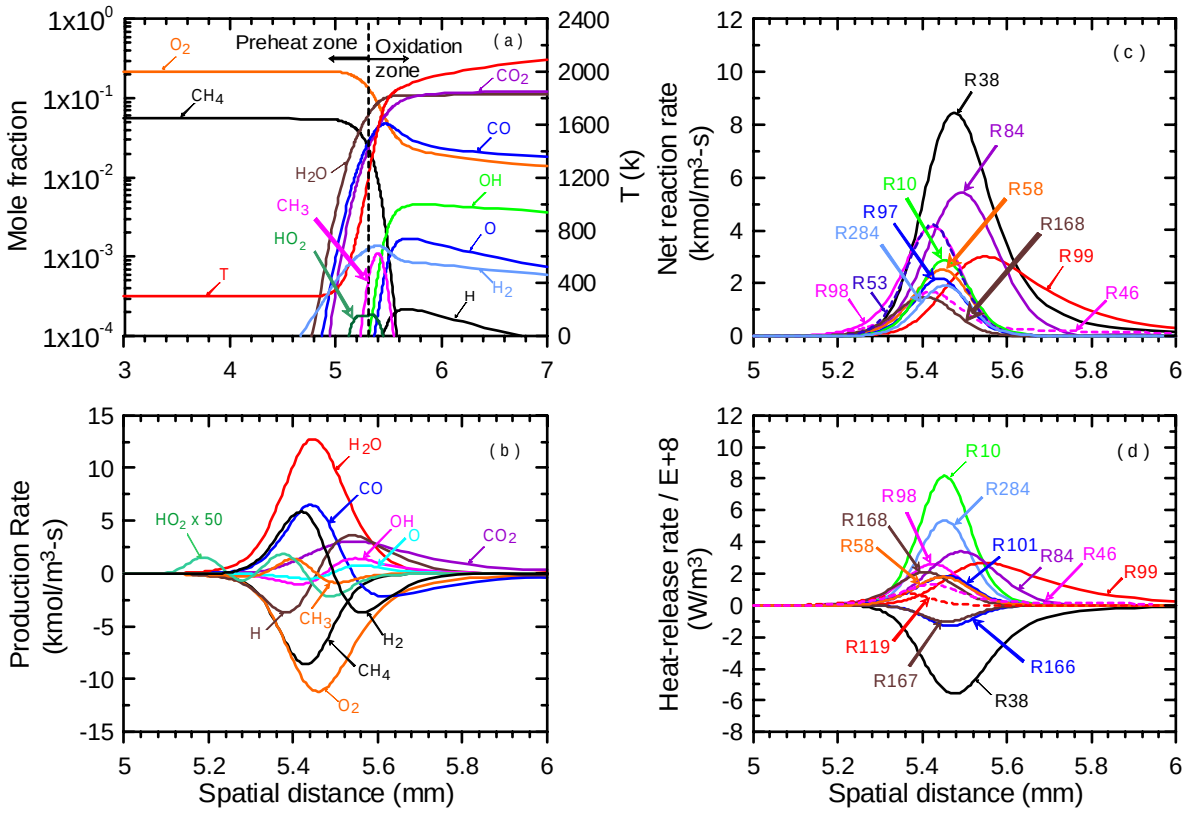

Fig. 11. Computed axial distributions of temperature, species mole fraction, production rate, net reaction rate and heat-release rate for flame 1 (100%CH_4-0%CO).

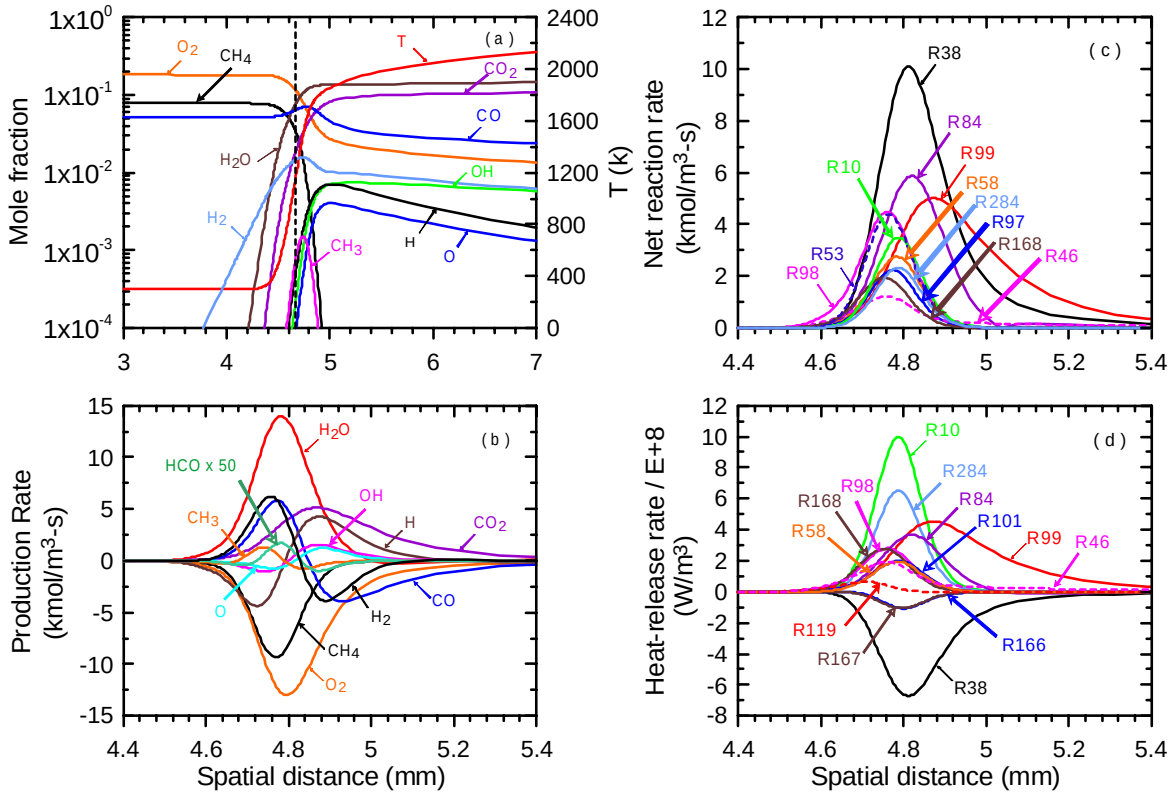

Fig. 12. Computed axial distributions of temperature, species mole fraction, production rate, net reaction rate and heat-release rate for flame 5 (60%CH_4-40%CO).

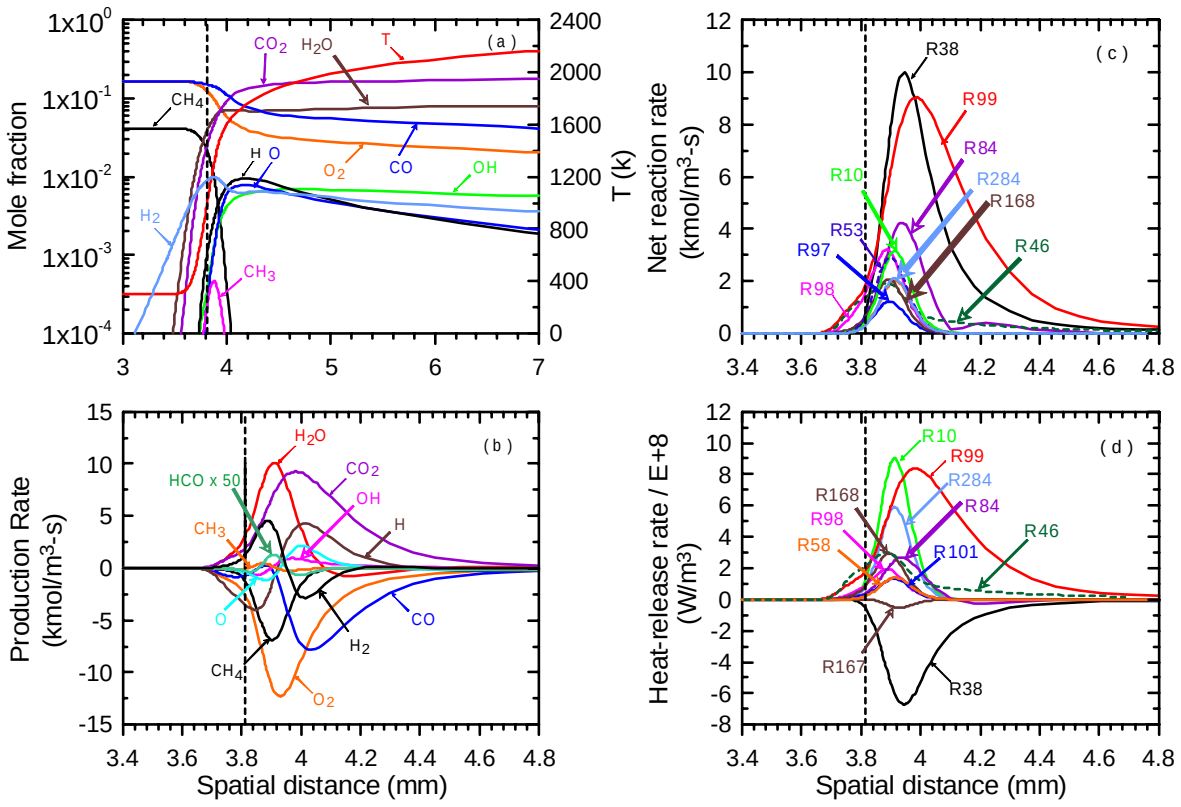

Fig. 13. Computed axial distributions of temperature, species mole fraction, production rate, net reaction rate and heat-release rate for flame 9 (20%CH_4-80%CO).

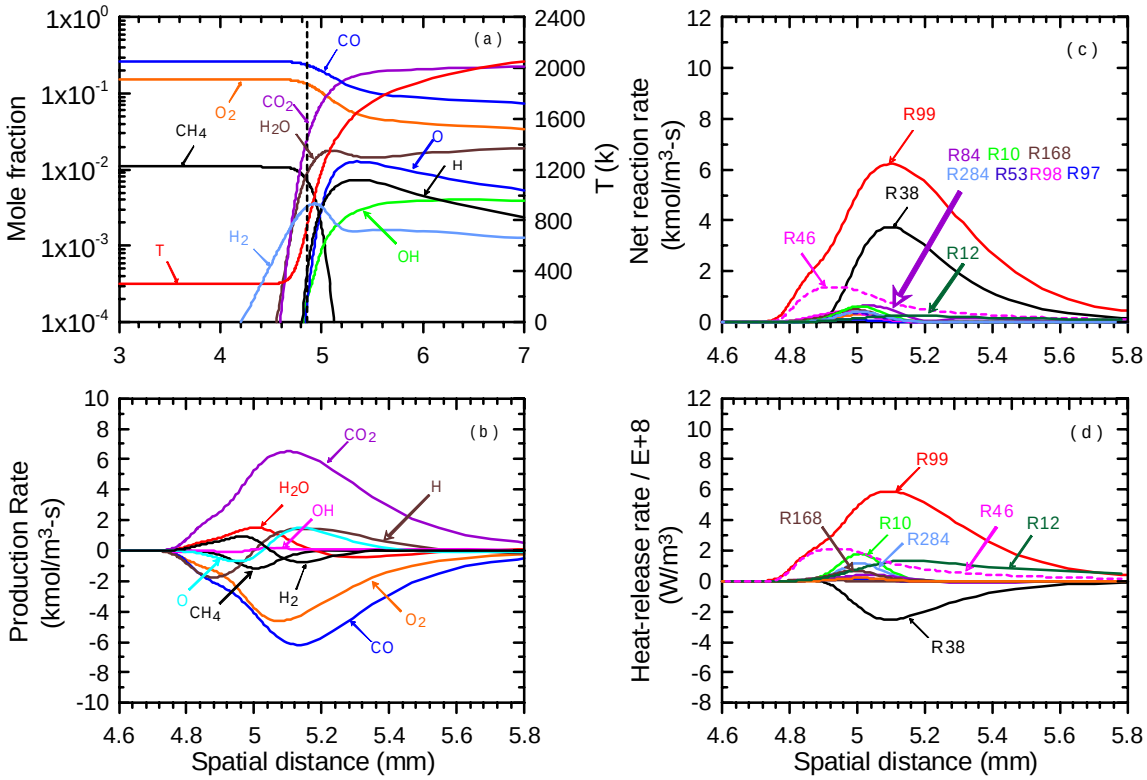

Fig. 14. Computed axial distributions of temperature, species mole fraction, production rate, net reaction rate and heat-release rate for flame 12 (4%CH_4-96%CO).

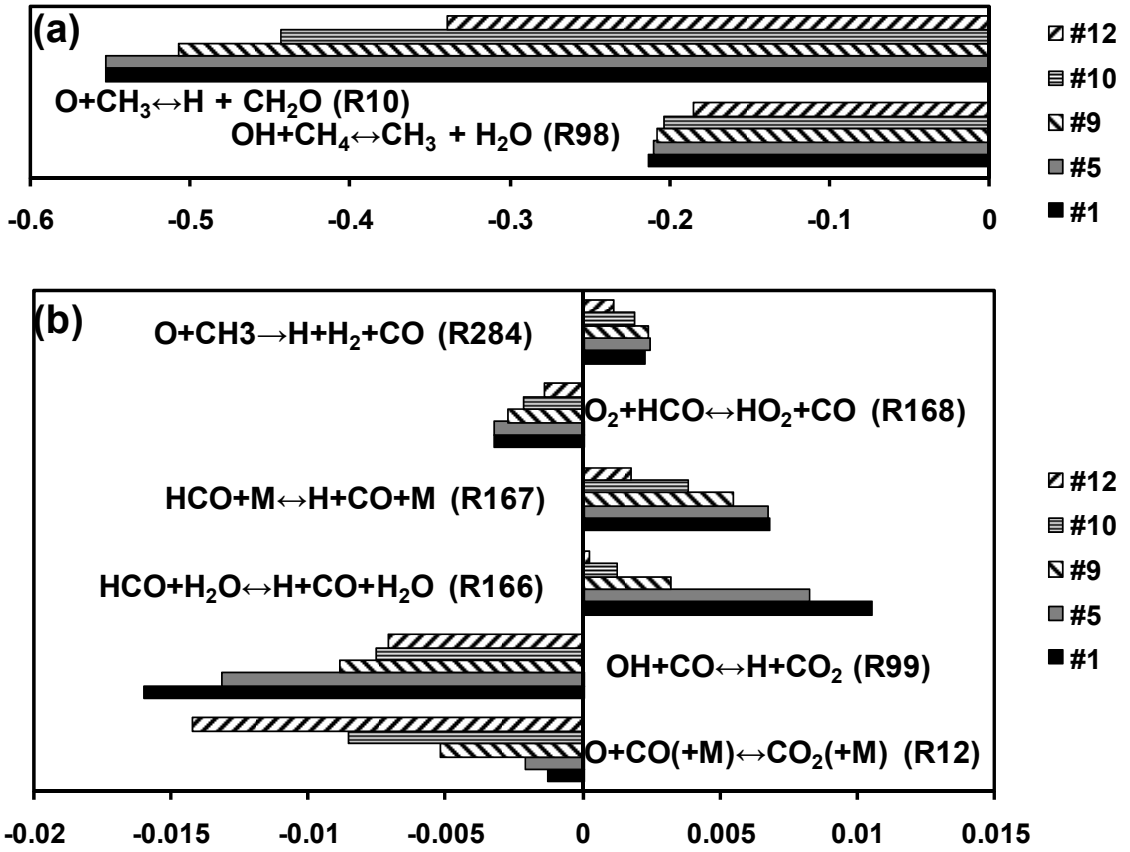

Fig. 15. The first-order sensitivity coefficients with respect to the chemistry reaction rate constants for (a) CH_4 and (b) CO.

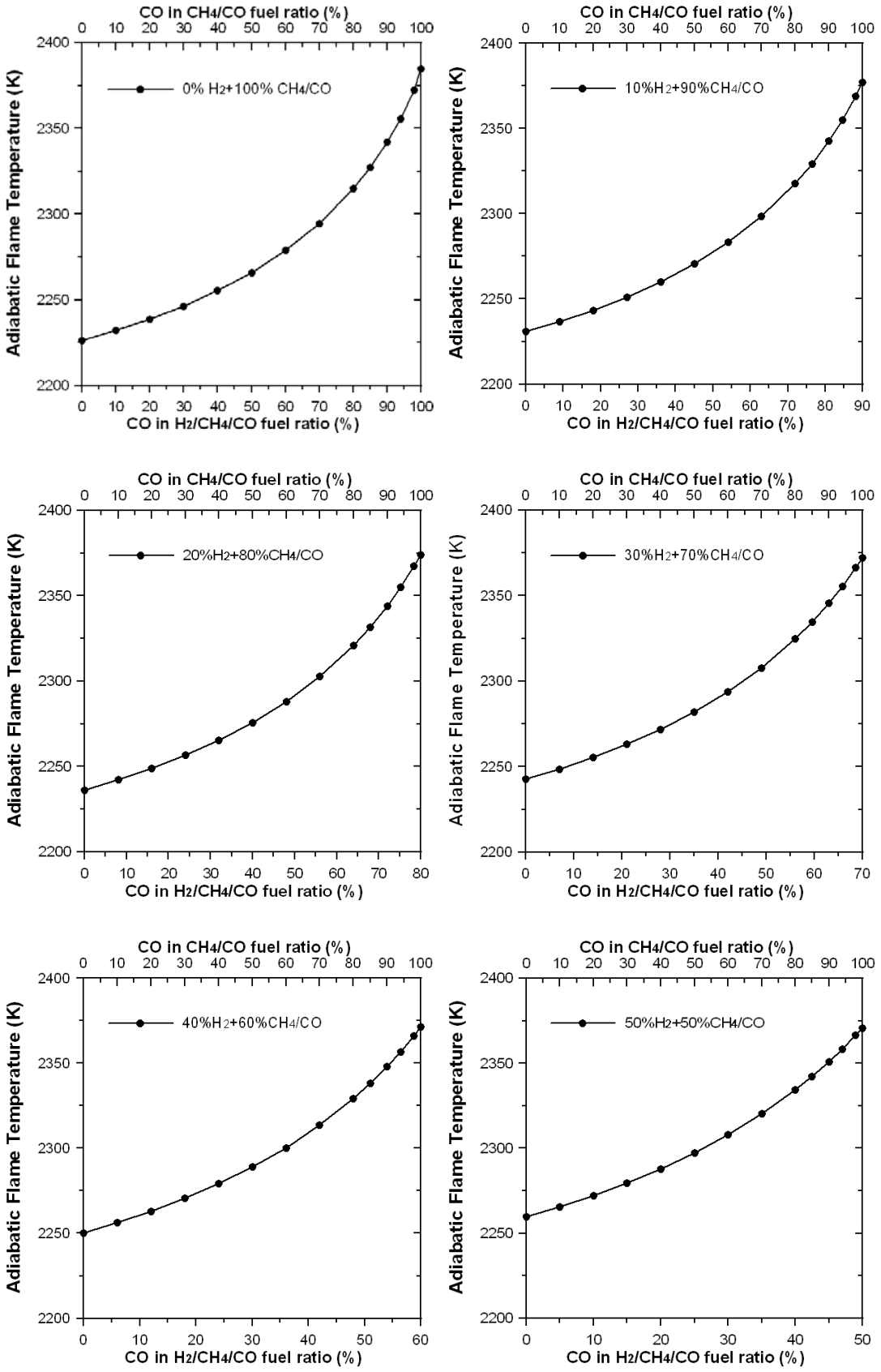

Fig. 16. Computed adiabatic flame temperature of the premixed stoichiometric $H_2/CH_4/CO$ flames with various H_2 and CO contents in the fuel mixture.

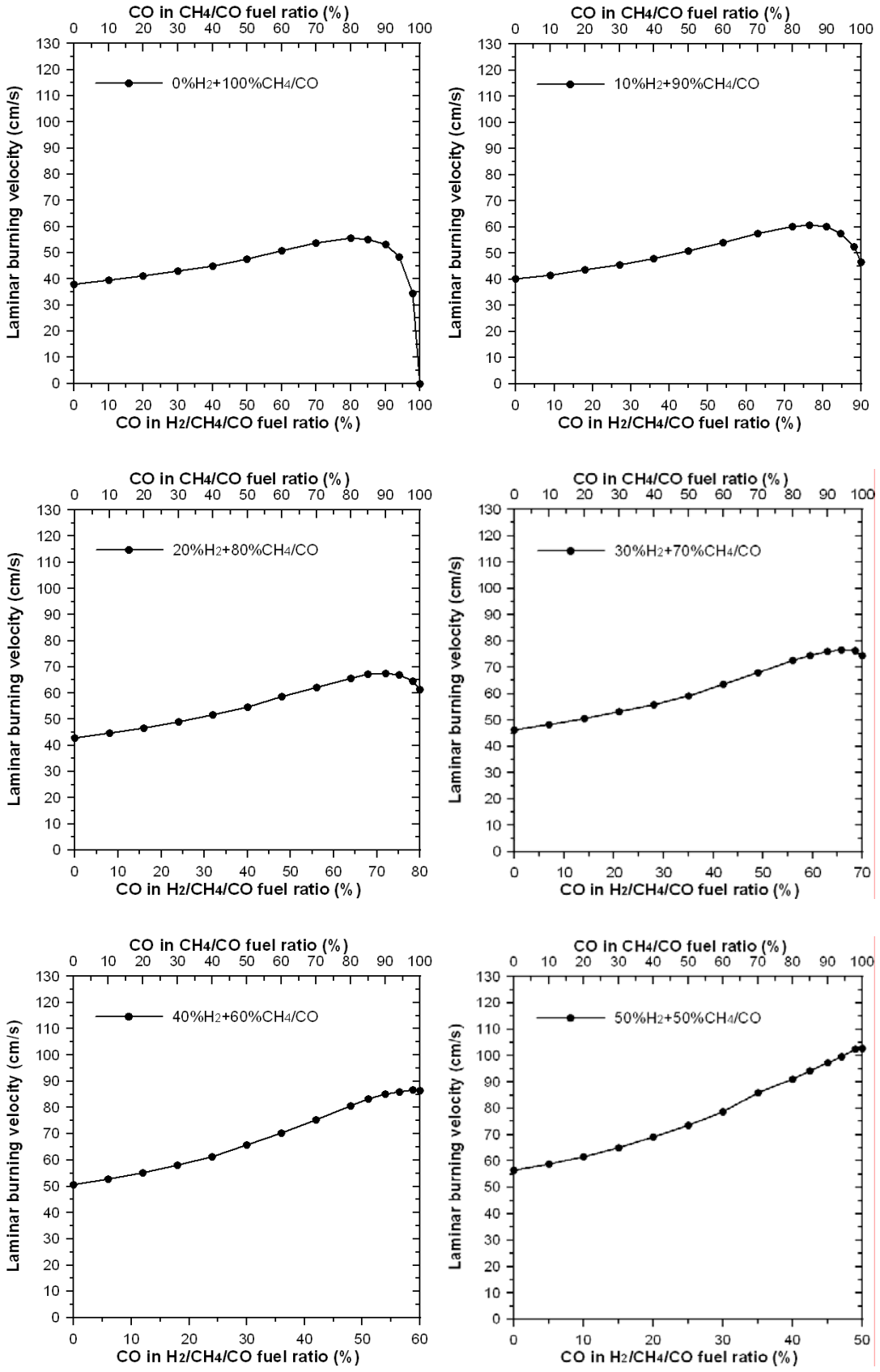

Fig. 17. Computed laminar burning velocity of the premixed stoichiometric $H_2/CH_4/CO$ flames with various H_2 and CO contents in the fuel mixture.

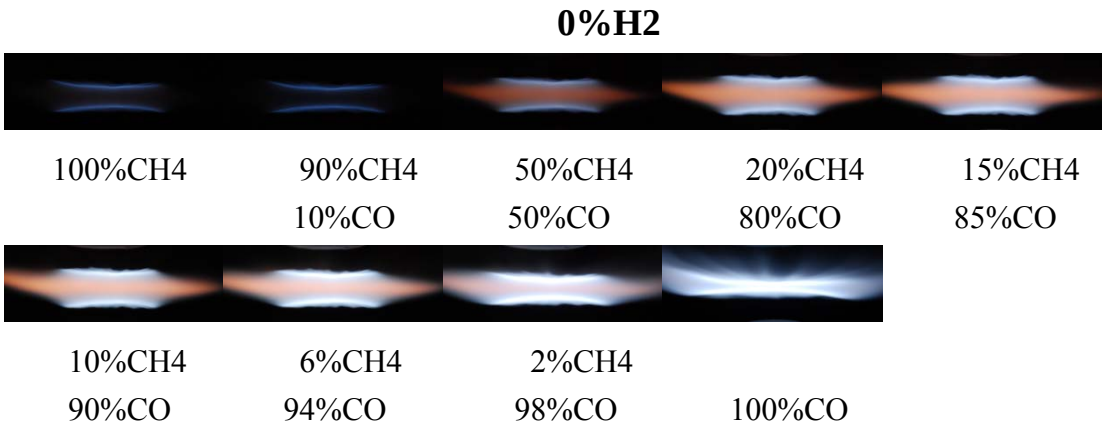

Fig. 18. Photographs of the premixed stoichiometric $H_2/CH_4/CO$ flames with 0%, 10% and 20% of H_2 and various CO contents in the fuel mixture.

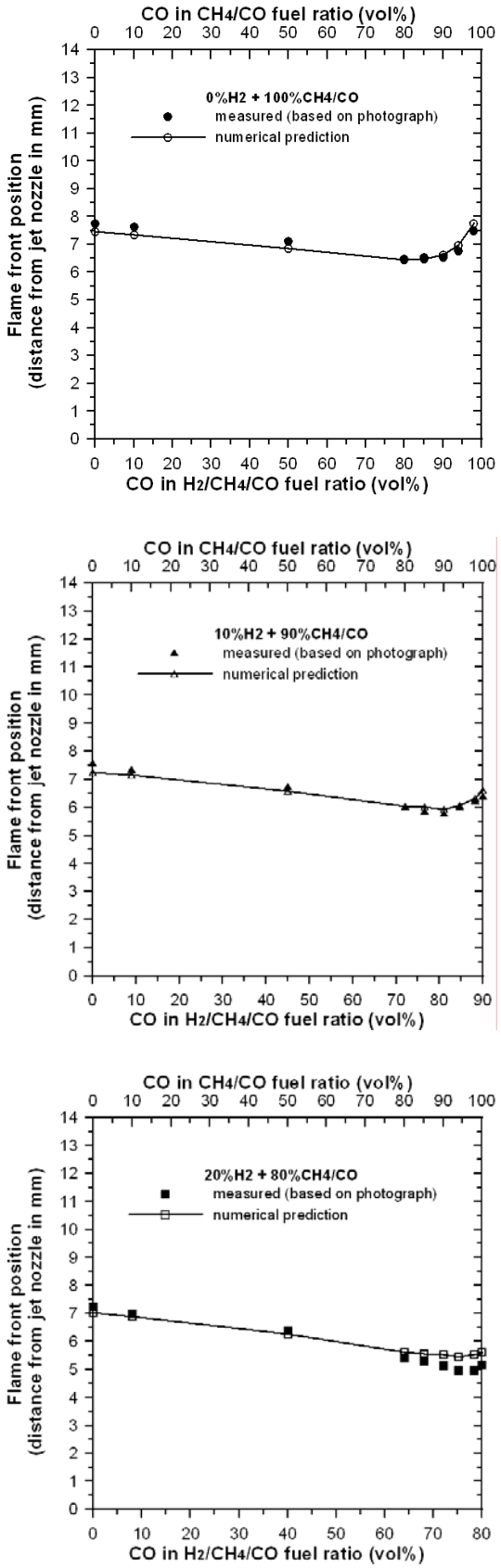

Fig. 19. Comparison of the measured and calculated flame front positions for premixed stoichiometric $H_2/CH_4/CO$ flames with 0%, 10% and 20% of H_2 and various CO contents in the fuel mixture.

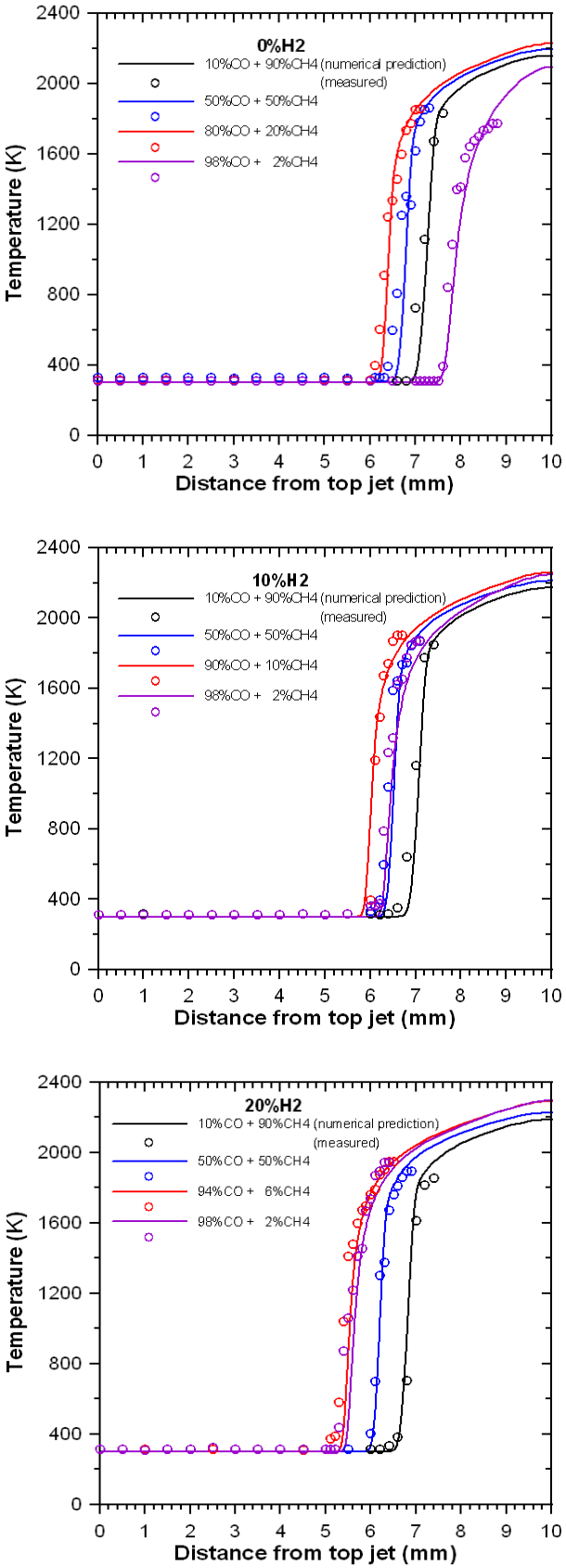

Fig. 20. Comparison of the measured and calculated temperatures for premixed stoichiometric $H_2/CH_4/CO$ flames with 0%, 10% and 20% of H_2 and various CO contents in the fuel mixture.

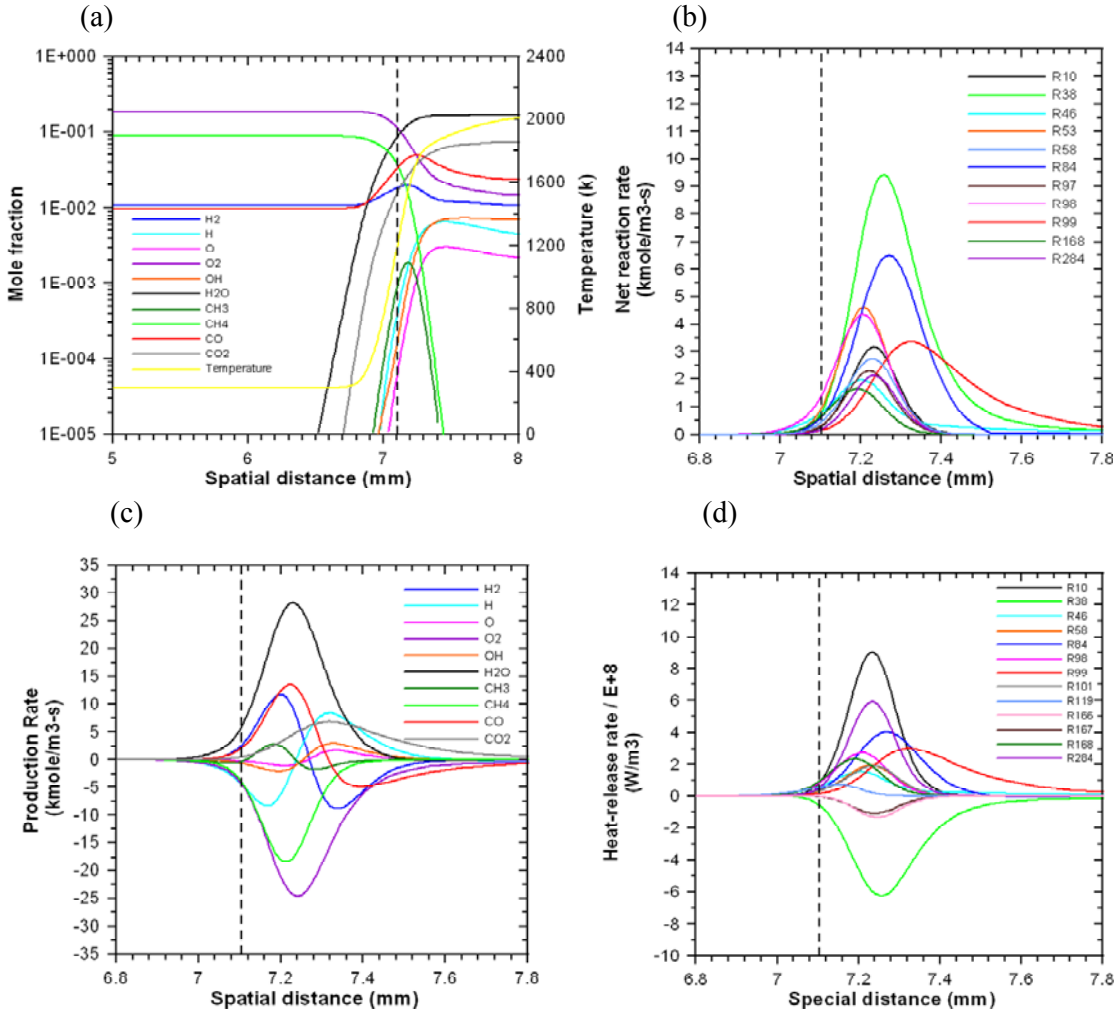

Fig. 21. Computed axial distributions of temperature, species mole fraction, production rate, net reaction rate and heat-release rate for 10%H_2– (90%CH_4–10%CO) flame.

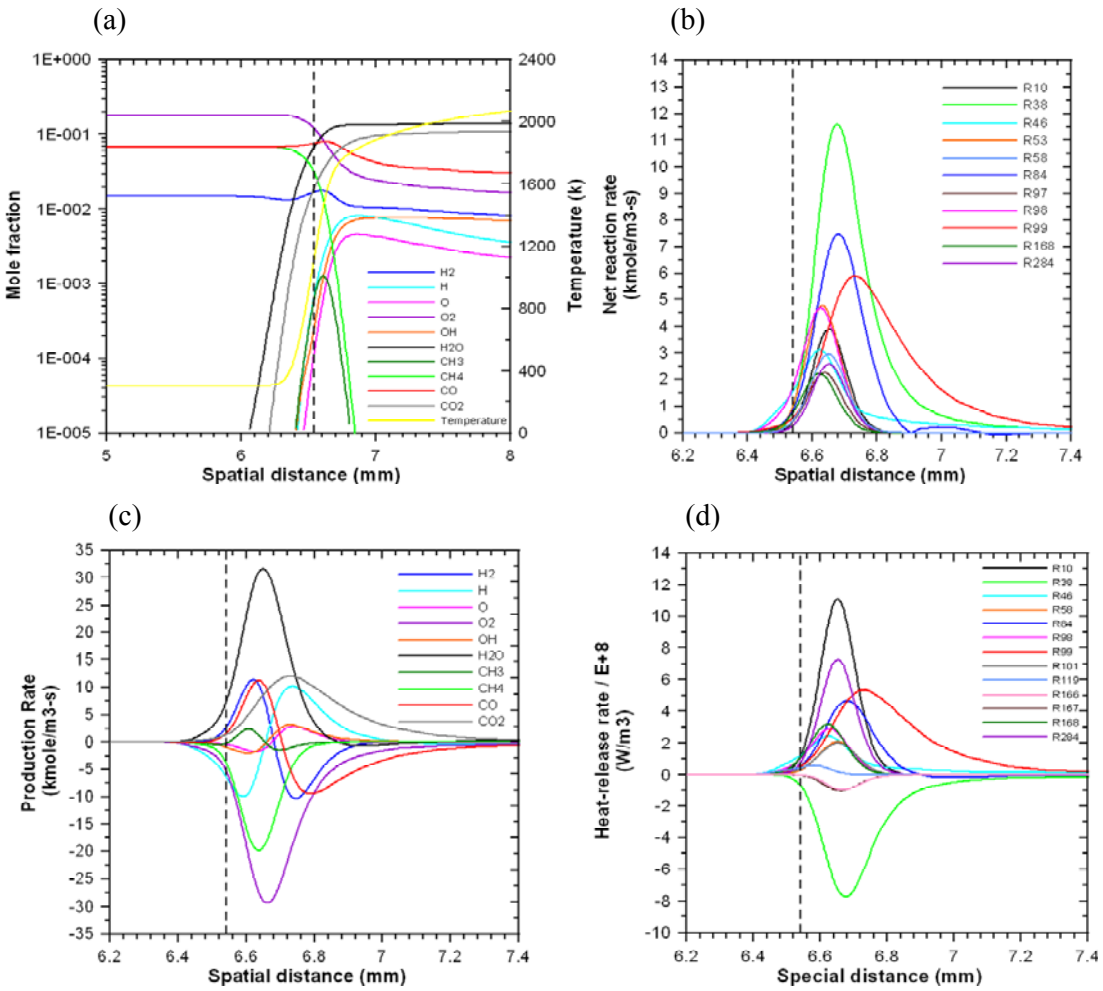

Fig. 22. Computed axial distributions of temperature, species mole fraction, production rate, net reaction rate and heat-release rate for 10%H_2– (50%CH_4–50%CO) flame.

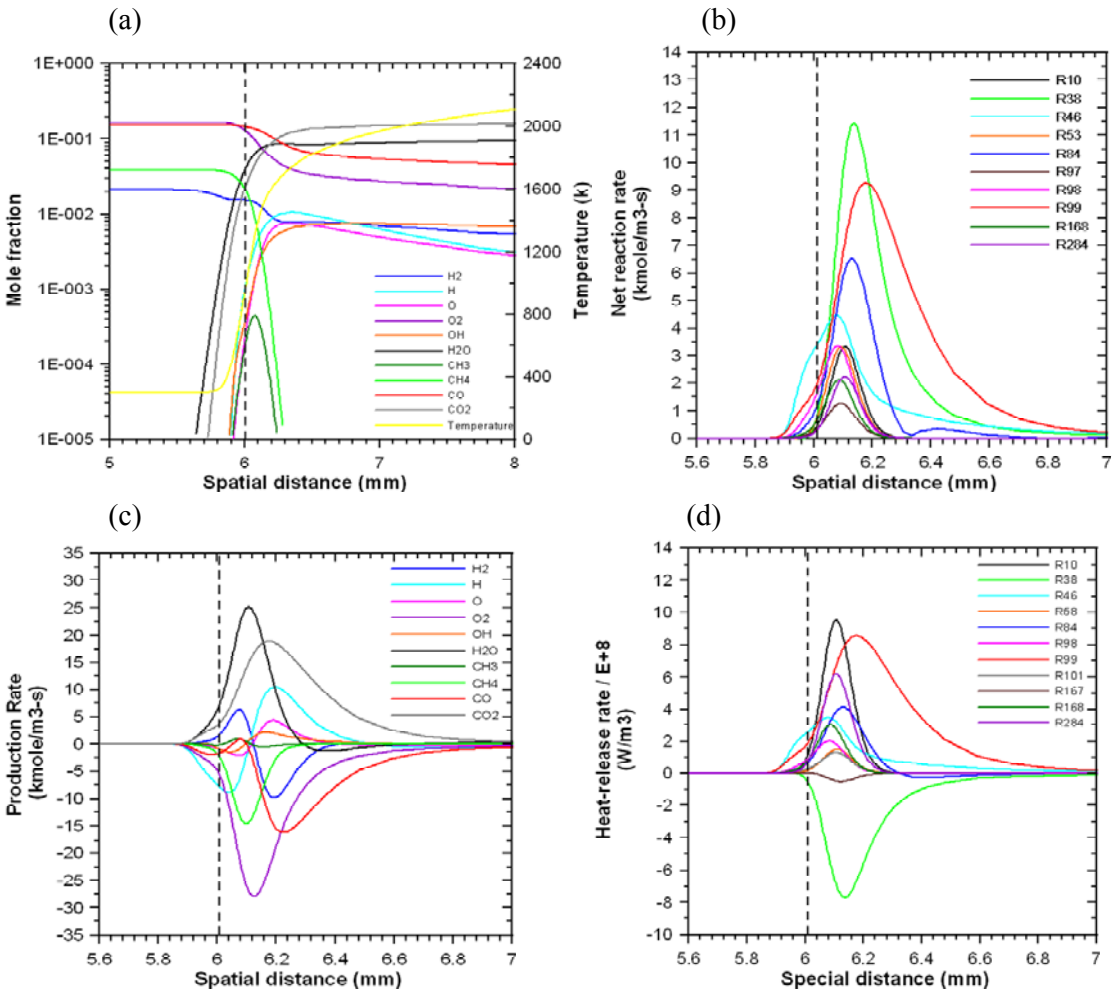

Fig. 23. Computed axial distributions of temperature, species mole fraction, production rate, net reaction rate and heat-release rate for 10%H_2– (20%CH_4–80%CO) flame.

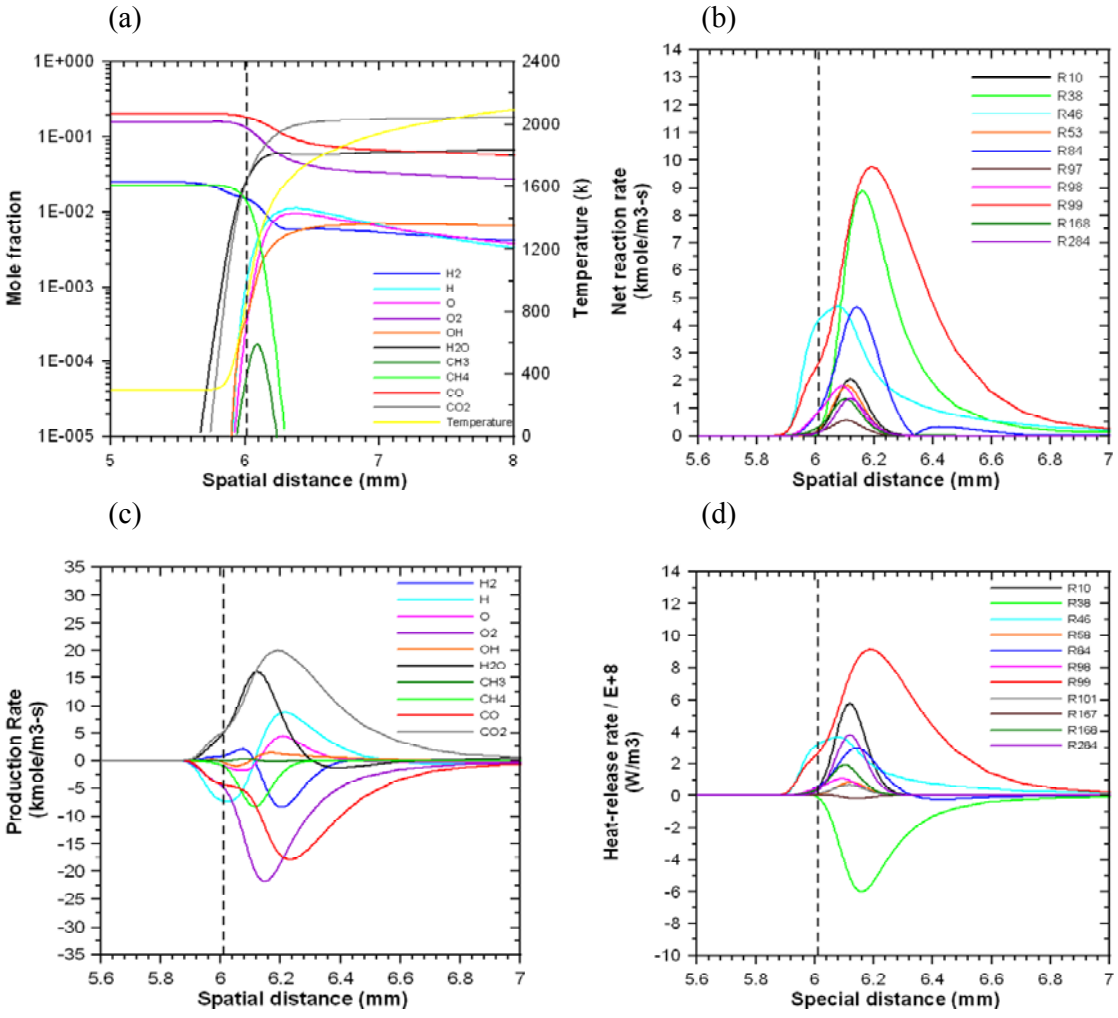

Fig. 24. Computed axial distributions of temperature, species mole fraction, production rate, net reaction rate and heat-release rate for 10%H_2– (10%CH_4–90%CO) flame.

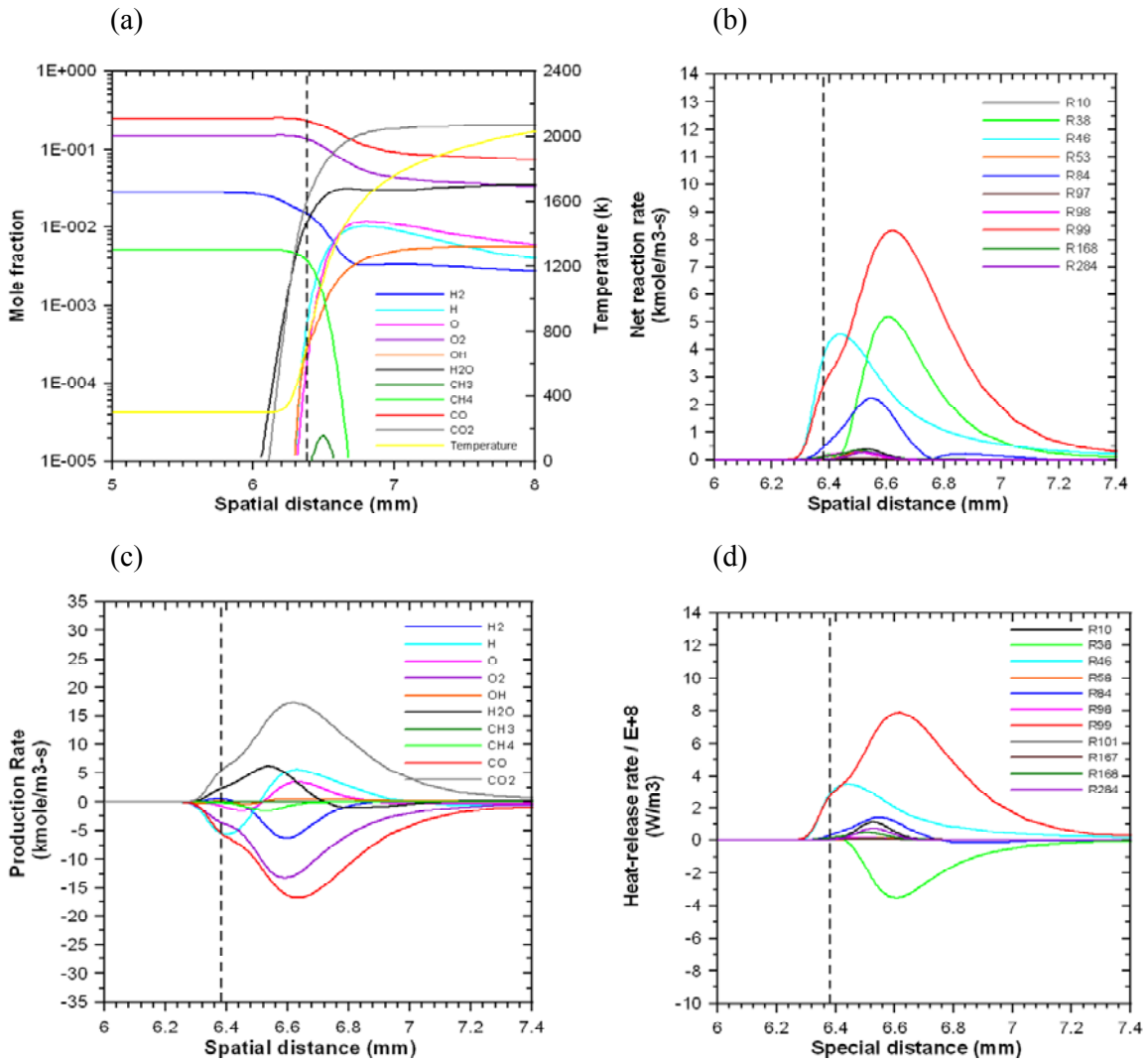

Fig. 25. Computed axial distributions of temperature, species mole fraction, production rate, net reaction rate and heat-release rate for 10%H_2– (2%CH_4–98%CO) flame.

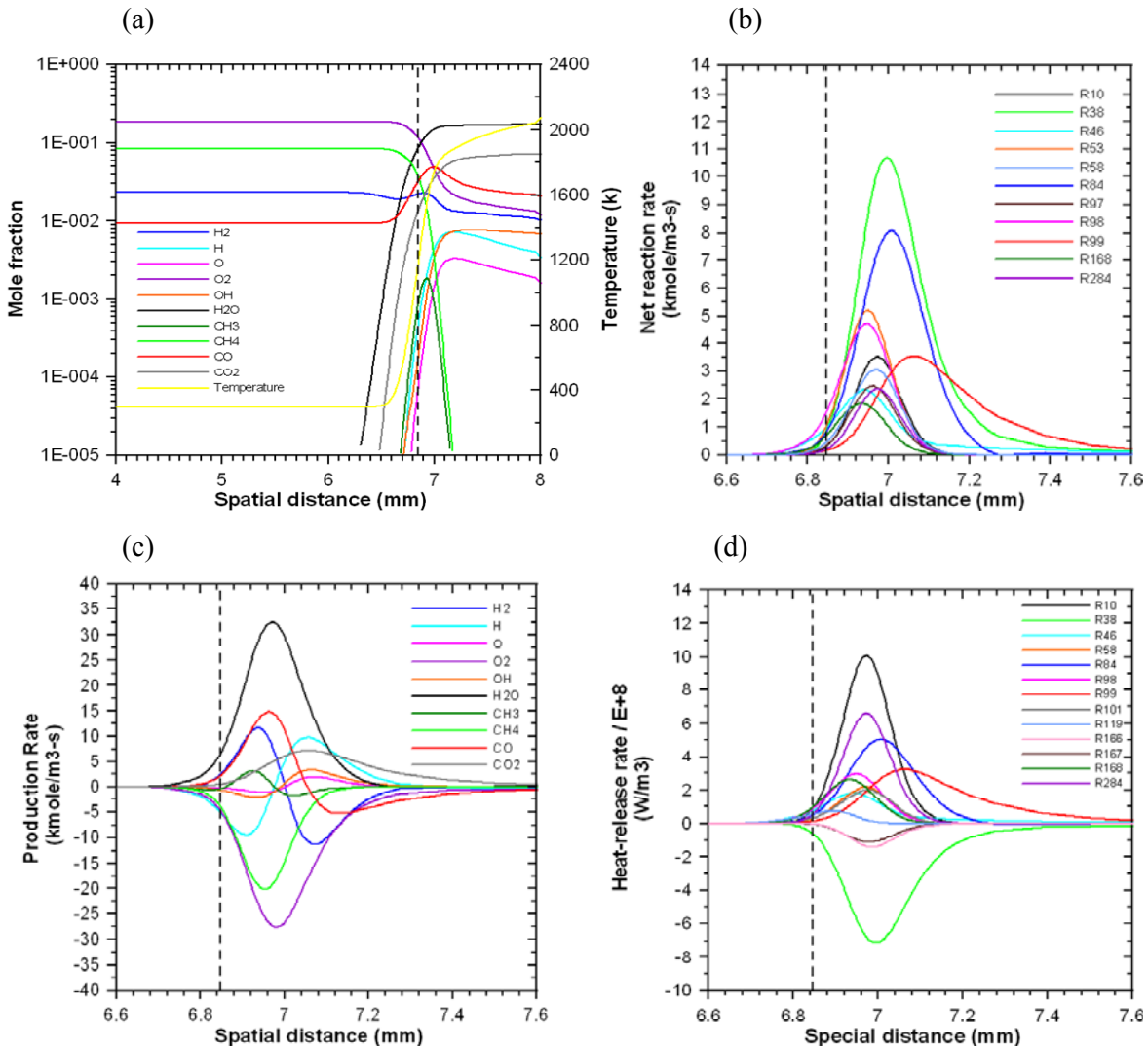

Fig. 26. Computed axial distributions of temperature, species mole fraction, production rate, net reaction rate and heat-release rate for 20%H_2– (90%CH_4–10%CO) flame.

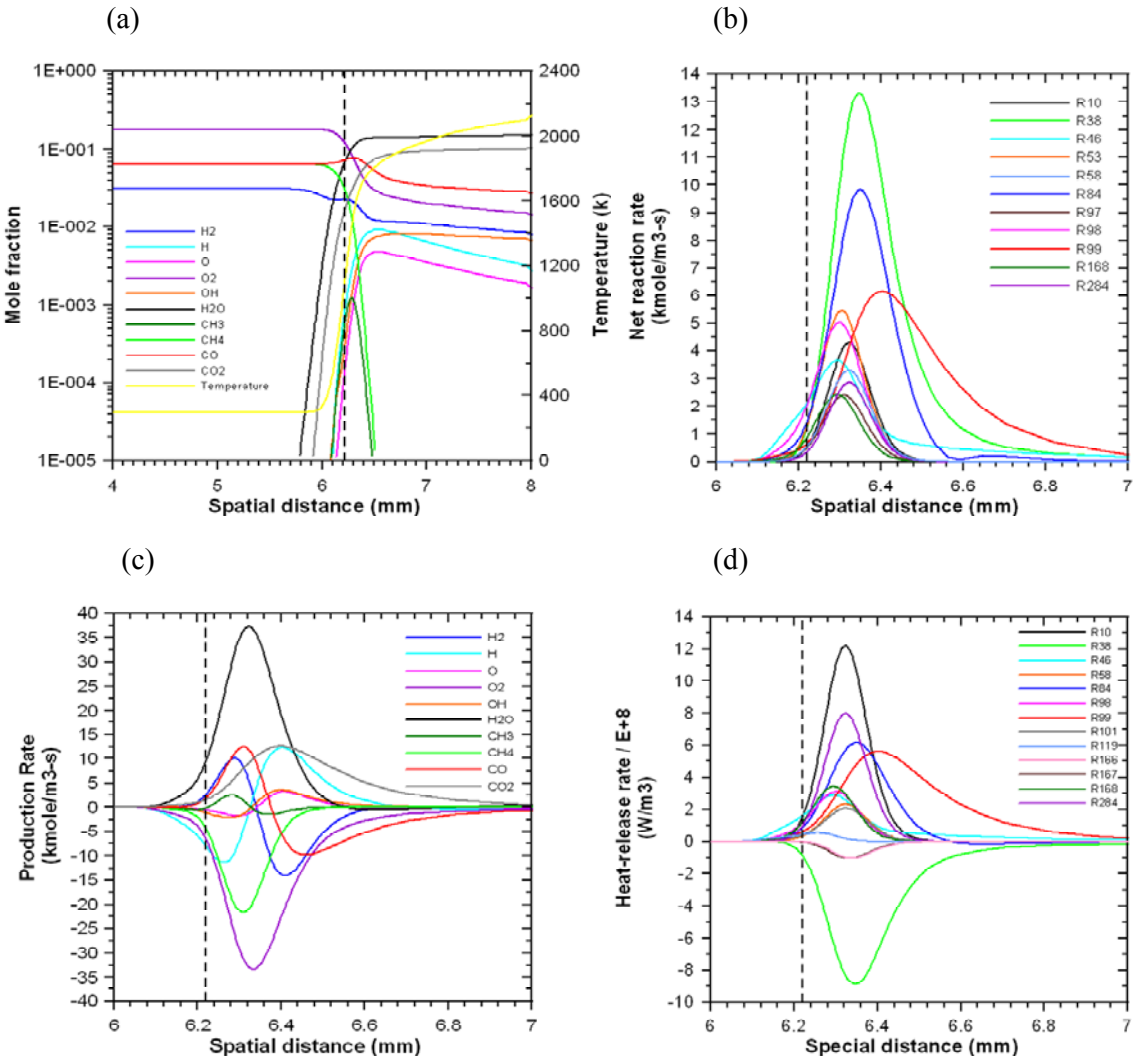

Fig. 27. Computed axial distributions of temperature, species mole fraction, production rate, net reaction rate and heat-release rate for 20%H_2– (50%CH_4–50%CO) flame.

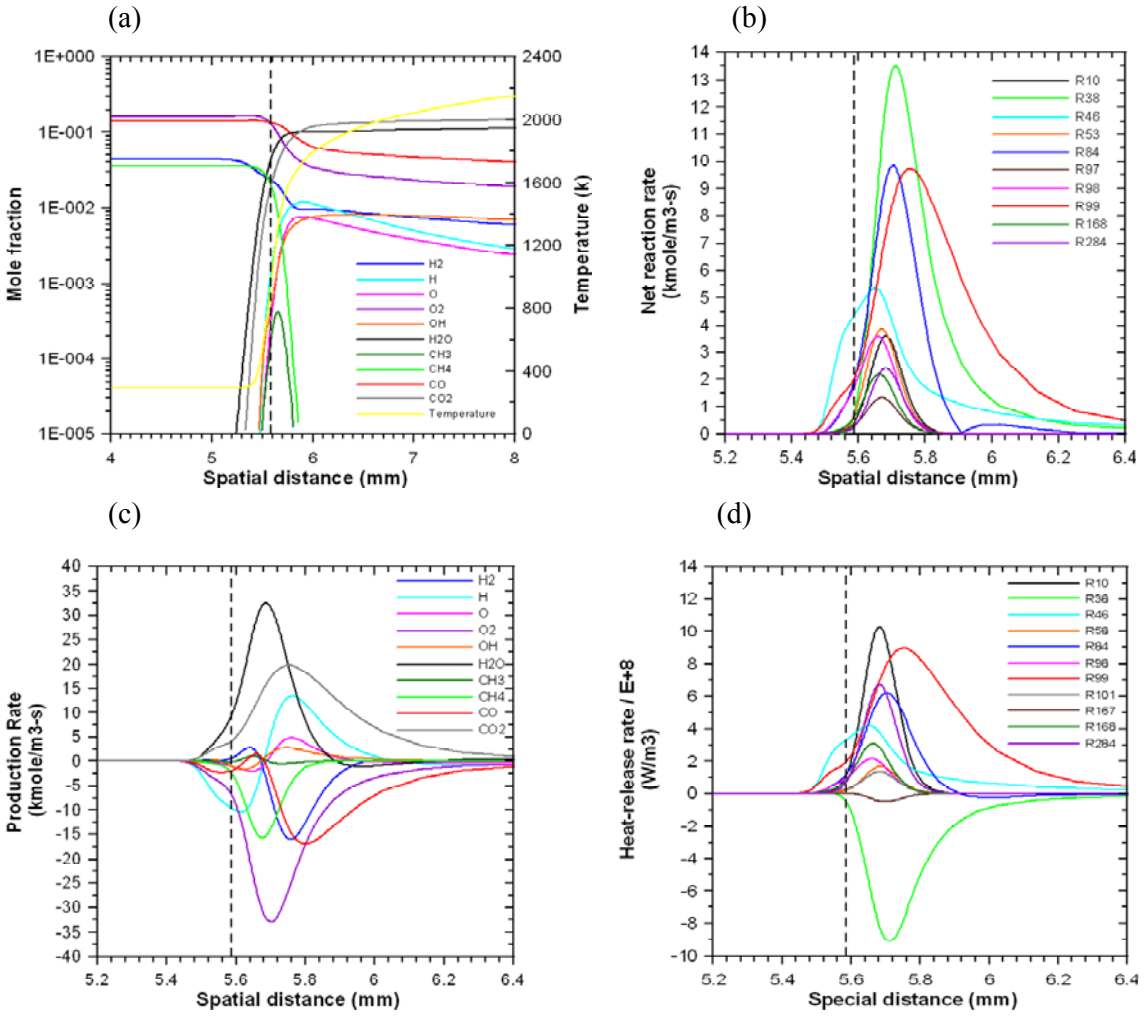

Fig. 28. Computed axial distributions of temperature, species mole fraction, production rate, net reaction rate and heat-release rate for 20%H_2– (20%CH_4–80%CO) flame.

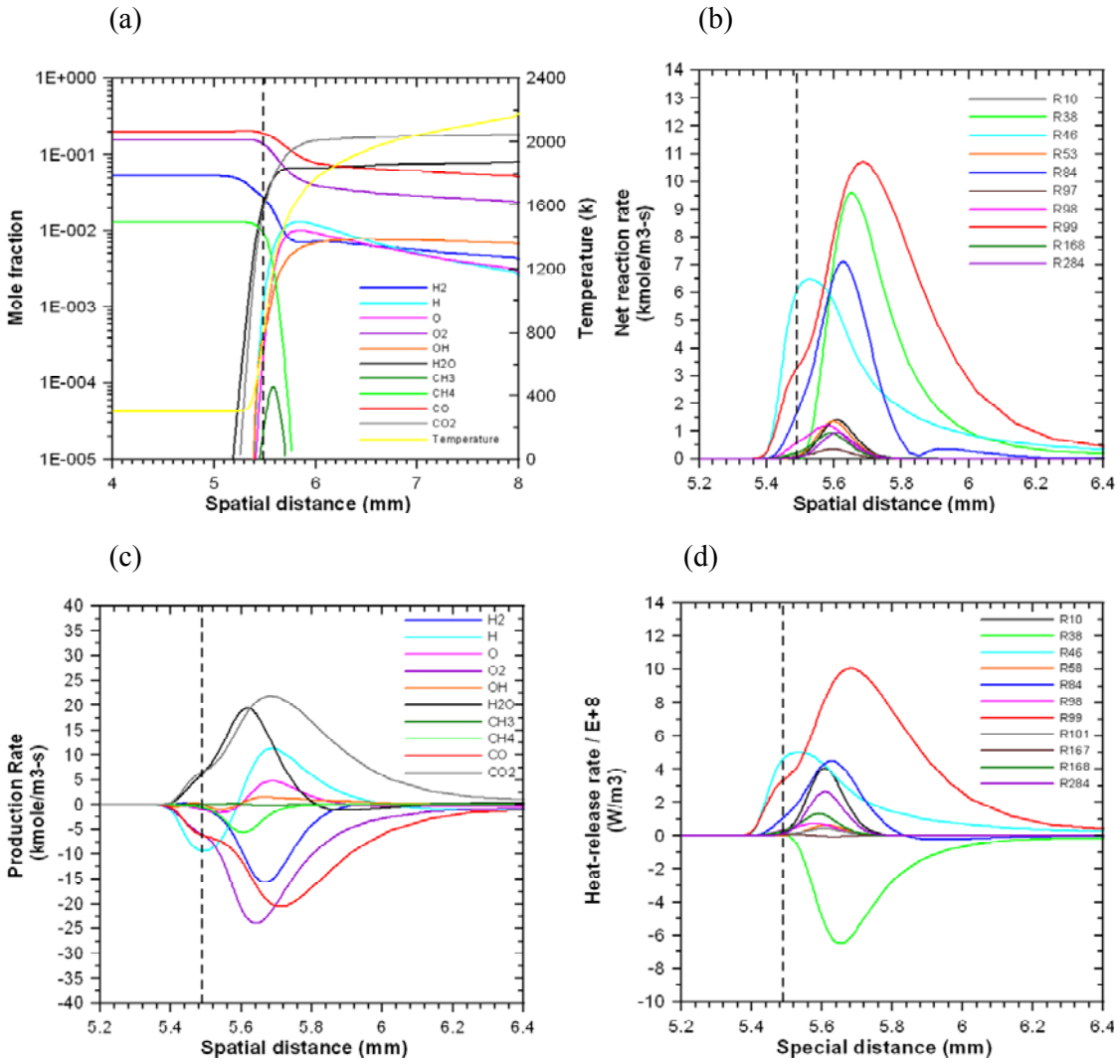

Fig. 29. Computed axial distributions of temperature, species mole fraction, production rate, net reaction rate and heat-release rate for 20%H_2– (6%CH_4–94%CO) flame.

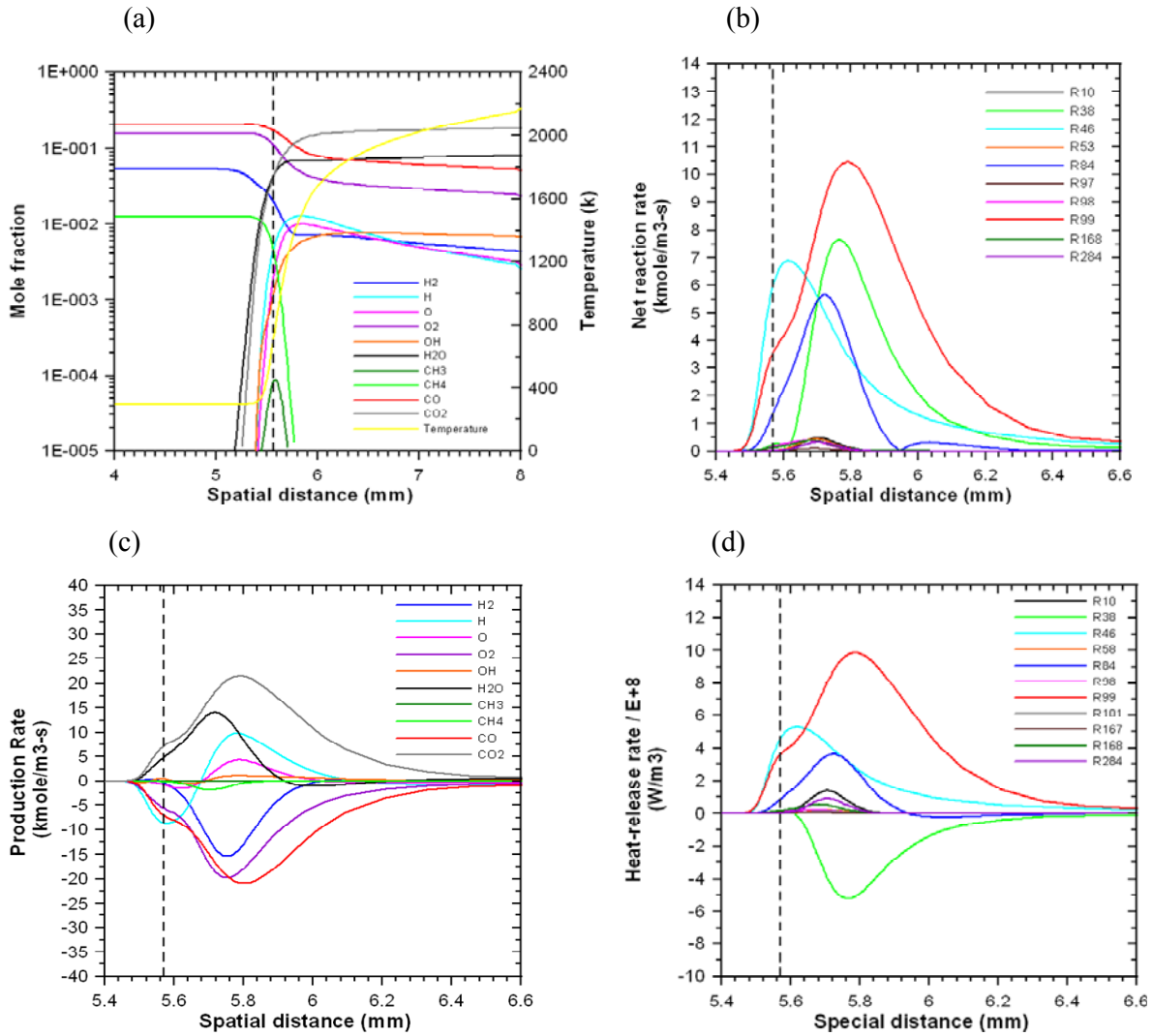

Fig. 30. Computed axial distributions of temperature, species mole fraction, production rate, net reaction rate and heat-release rate for 20%H_2– (2%CH_4–98%CO) flame.

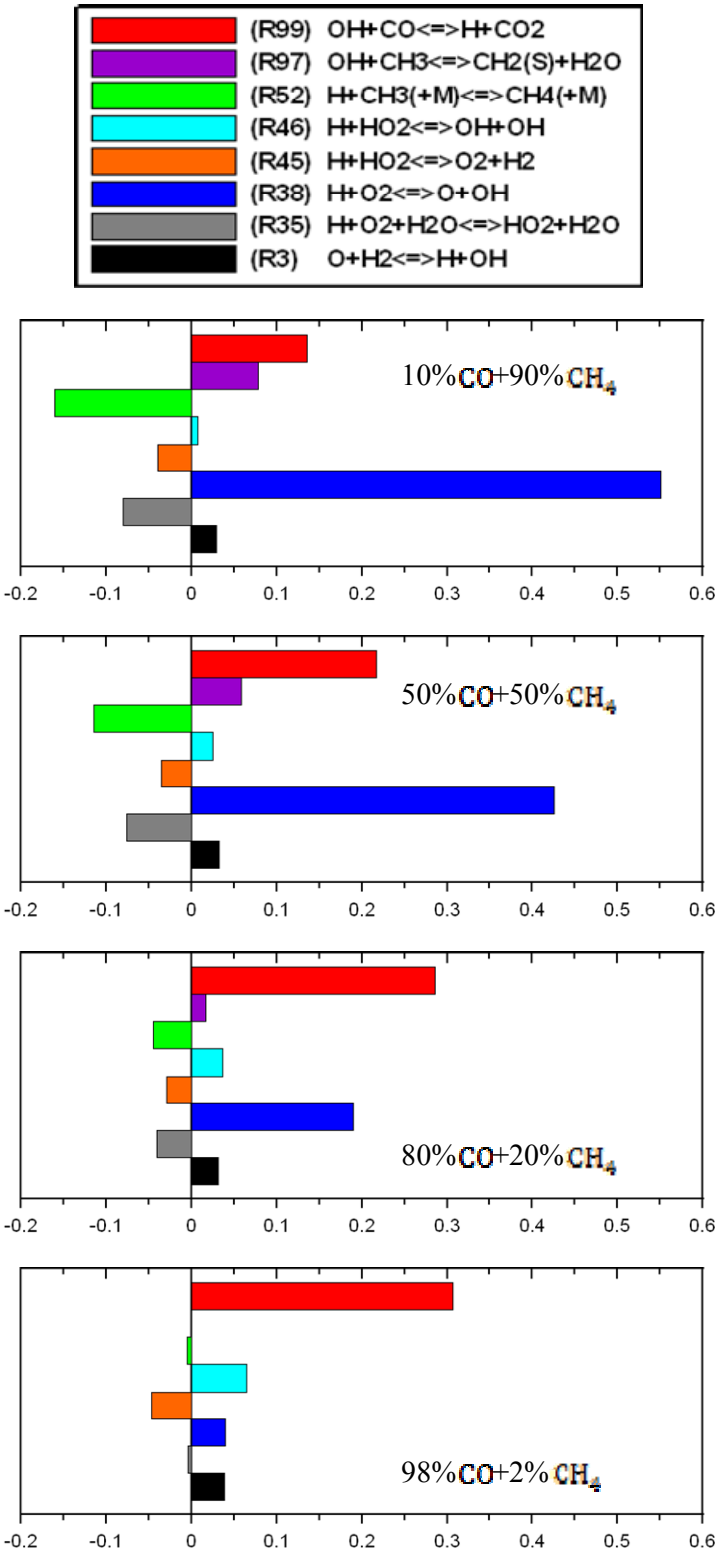

Fig. 31. The first-order sensitivity analysis with respect to temperature for premixed stoichiometric CH_4/COair flames.

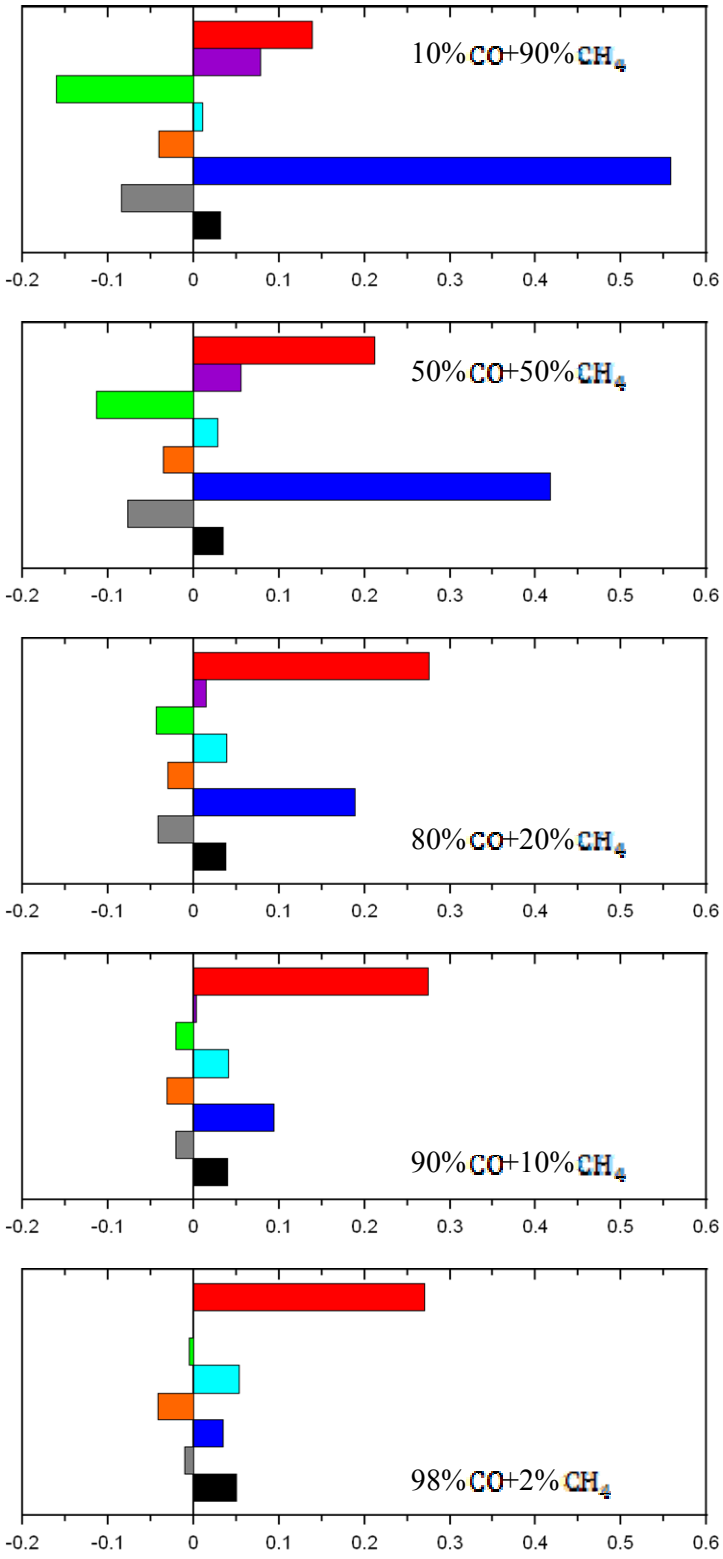

Fig. 32. The first-order sensitivity analysis with respect to temperature for premixed stoichiometric $H_2/CH_4/CO$air flames (10% H_2).

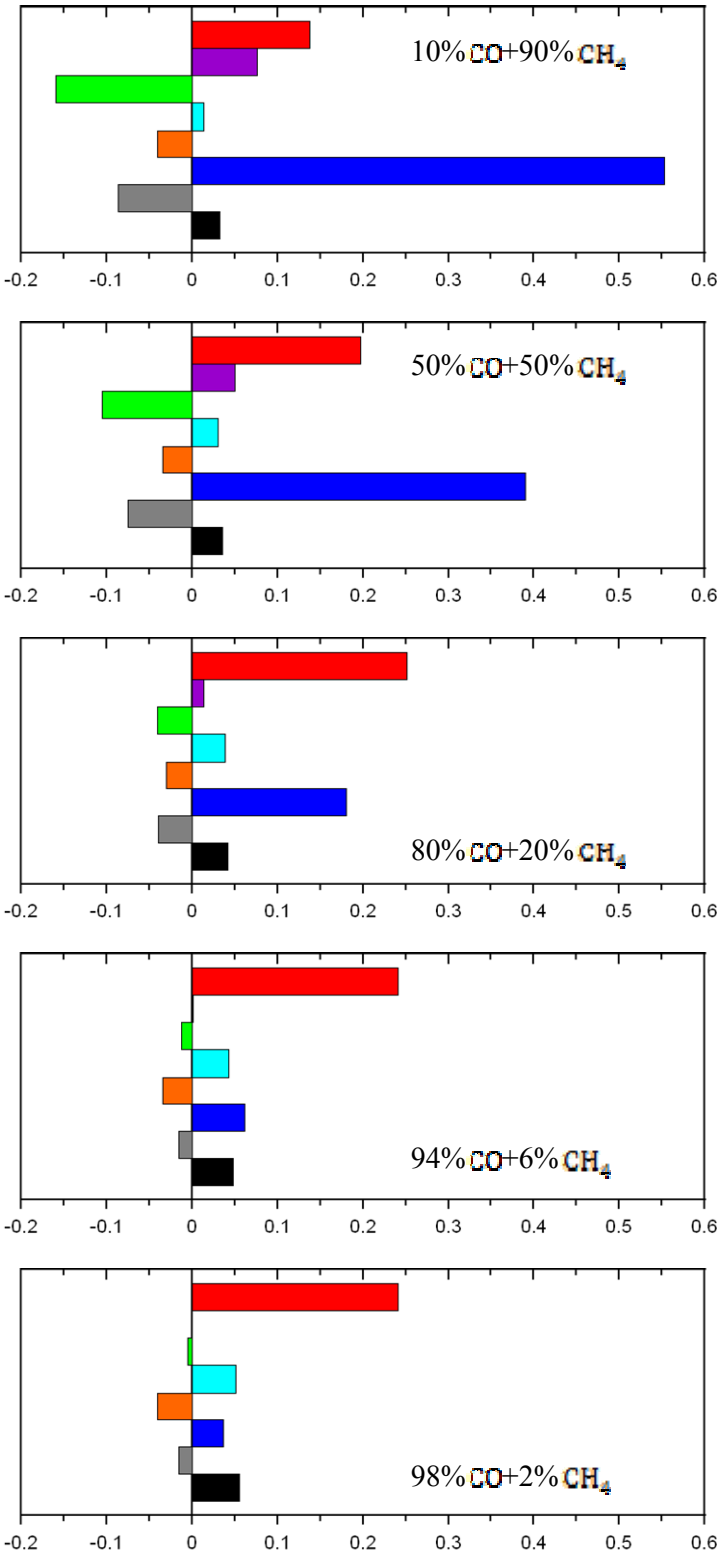

Fig. 33. The first-order sensitivity analysis with respect to temperature for premixed stoichiometric $H_2/CH_4/CO$air flames (20% H_2).

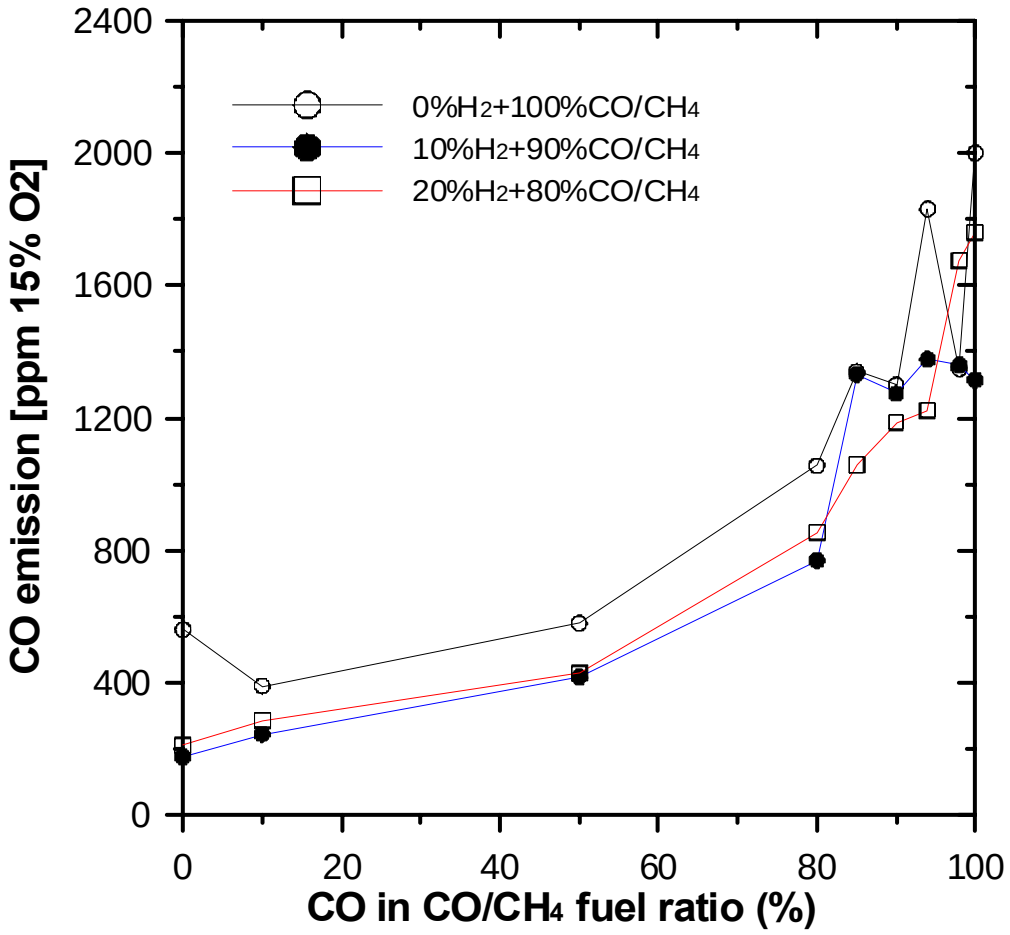

Fig. 34. The CO emission measurements for premixed stoichiometric H_2/CH_4/COair flames with various H_2 (0%, 10%, and 20%) and CO contents in fuel mixture.

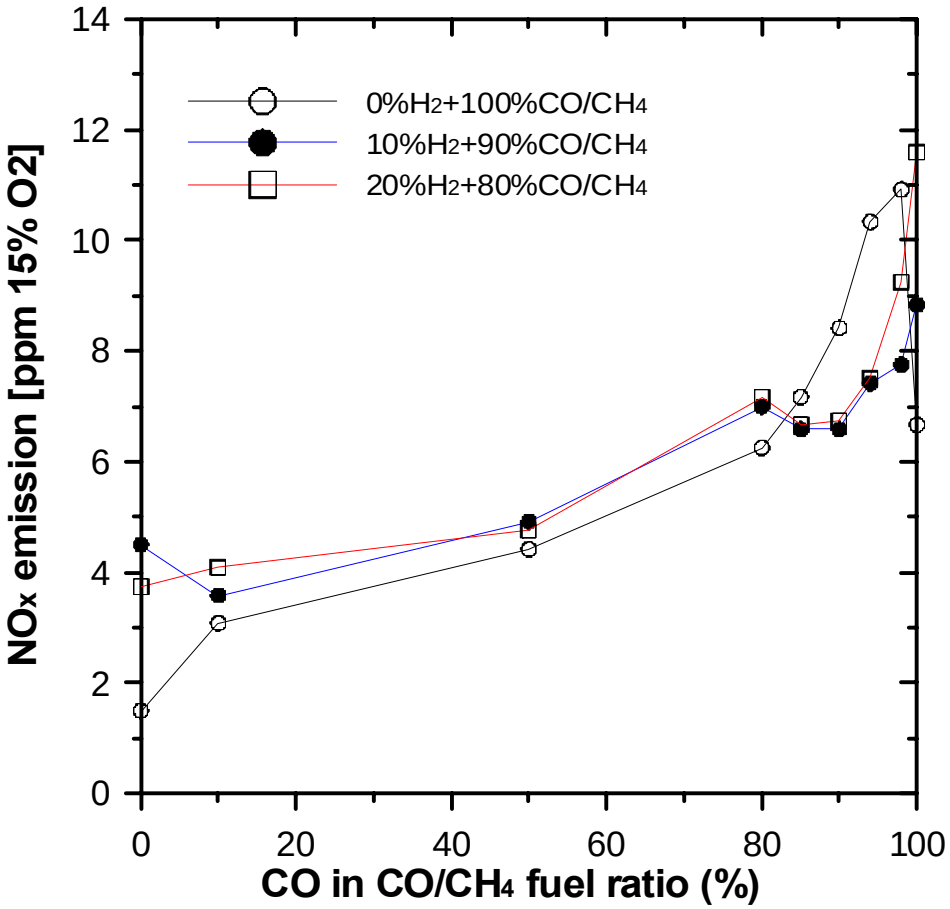

Fig. 35. The NO_x emission measurements for premixed stoichiometric H_2/CH_4/COair flames with various H_2 (0%, 10%, and 20%) and CO contents in fuel mixture.

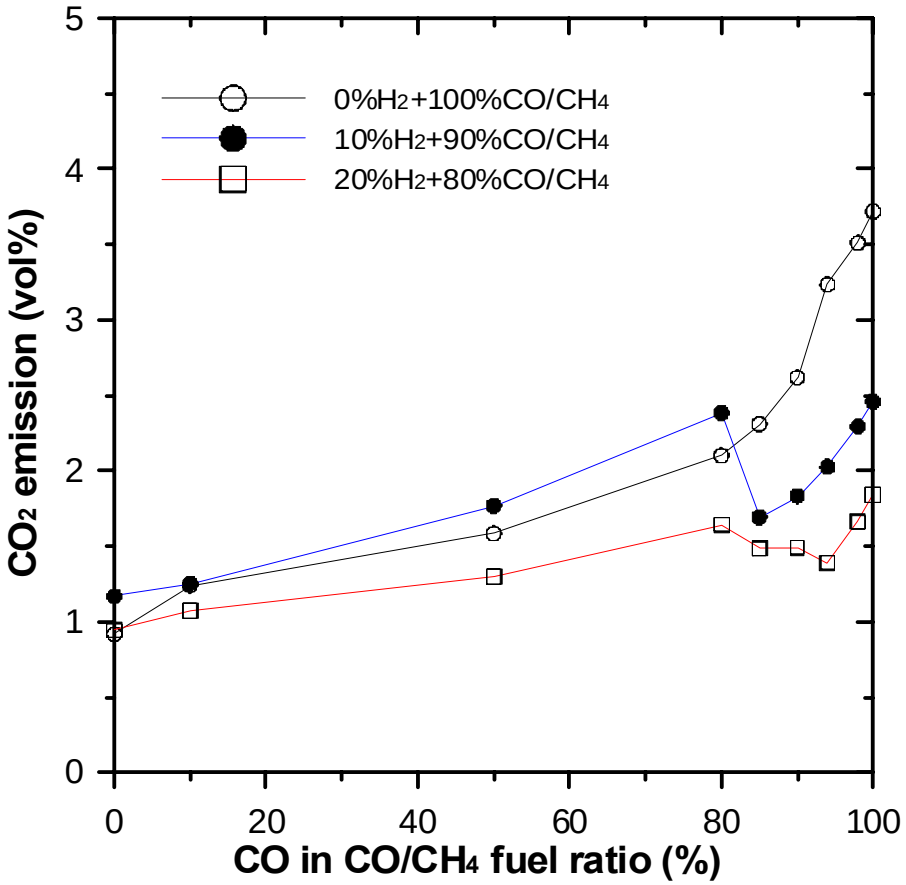

Fig. 36. The CO_2 emission measurements for premixed stoichiometric H_2/CH_4/COair flames with various H_2 (0%, 10%, and 20%) and CO contents in fuel mixture.

國科會補助專題研究計畫成果報告自評表

請就研究內容與原計畫相符程度、達成預期目標情況、研究成果之學術或應用價值（簡要敘述成果所代表之意義、價值、影響或進一步發展之可能性）、是否適合在學術期刊發表或申請專利、主要發現或其他有關價值等，作一綜合評估。

1. 請就研究內容與原計畫相符程度、達成預期目標情況作一綜合評估

■ 達成目標

□ 未達成目標（請說明，以 100 字為限）

□ 實驗失敗

□ 因故實驗中斷

□ 其他原因

說明：

2. 研究成果在學術期刊發表或申請專利等情形：

論文：■已發表 □未發表之文稿 ■撰寫中 □無

專利：□已獲得 □申請中 □無

技轉：□已技轉 □洽談中 □無

其他：（以 100 字為限）

本計畫研究成果分為兩部分：第一部份為探討在甲烷燃料中加入不同比例之一氧化碳，以瞭解一氧化碳含量對 CH_4/CO/air 當量預混火焰之層流火焰速度、火焰形狀、火焰前端位置、火焰溫度、火焰結構及化學動力結構之影響，此部分之研究成果已發表在高等級之燃燒期刊 (Combustion Flame, Vol. 156, pp. 362-373, 2009, SCI, IF: 2.923)。第二部份為探討在甲烷/一氧化碳燃料中加入不同比例之氫氣，以瞭解氫氣含量對 H_2/CH_4/CO/air 當量預混火焰之層流火焰速度、火焰形狀、火焰前端位置、火焰溫度、火焰結構及化學動力結構之影響，此部分之研究成果目前正在撰寫成論文，將先投稿至明年七月在美國 UC Irvine 舉行的第 23 屆國際爆炸與反應系統動力會議發表，之後再轉投至國際期刊。

3. 請依學術成就、技術創新、社會影響等方面，評估研究成果之學術或應用價值（簡要敘述成果所代表之意義、價值、影響或進一步發展之可能性）（以500字為限）

本研究主要在探討氫氣、甲烷及一氧化碳重組燃料之燃燒特性，氫氣、甲烷及一氧化碳為生質材料氣化後之主要成分，而生質能為綠能之一，燃燒生質能可有效降低二氧化碳排放，然因生質能之熱值較低，且各組成份含量不一，容易造成燃燒不穩定現象。因此探討三種主要氣體在不同混合比例下，其對火焰燃燒速度、燃燒穩定性、化學動力及火焰結構等核心機制之影響，以瞭解重組(混合)燃料之關鍵特性、建立替代能源燃燒特性資料庫及作為將來設計無碳燃燒系統之參考，是本研究的目的。由於氫氣、甲烷及一氧化碳個別的可燃極限、燃燒速度及化學特性不同，相互混合之後的燃燒特性亦不相同，因此本研究初期先進行甲烷及一氧化碳混合燃料的燃燒特性研究，之後再進行將氫氣加入甲烷及一氧化碳混合燃料中，以瞭解加氫對火焰結構及化學動力之影響。經由實驗量測與數值模擬之研究結果顯示，在當量(Stoichiometric)混合之 CH_4/CO/air 火焰中，當 CH_4/CO 燃料體積比為1：4時，燃燒速度達到最大值，此結果乃是因主宰之化學反應動力機制由甲烷轉換至一氧化碳，並由 $OH + CO \leftrightarrow H + CO_2$ 反應式主宰反應速率及熱釋放率。而當10%及20%的氫氣加入 CH_4/CO 燃料時，最大燃燒速度分別發生在 CH_4/CO 燃料體積比為1：9及1：15.67時，此結果乃是因主宰之化學反應動力機制由甲烷轉換至氫氣及一氧化碳，並由 $OH + CO \leftrightarrow H + CO_2$、$OH + H_2 \leftrightarrow H + H_2O$ 及 $HO_2 + H \leftrightarrow OH + OH$ 反應式主宰反應速率及熱釋放率。本研究第一部份成果已發表在國際知名燃燒期刊，顯見其學術價值相當高。第二部份之研究成果將先投稿至明年七月在美國 UC Irvine 舉行的第23屆國際爆炸與反應系統動力會議發表，之後再轉投至國際期刊。

誌謝

感謝國科會對本計畫全程三年(96/8~98/8)之經費補助，計畫編號 NSC 96-2221-E-216-016-MY3，同時也感謝成大航太系趙怡欽教授多年來在實驗儀器設備上及研究生人力（吳志勇、李約亨、陳志鵬、林河川、侯俊慶、蘇佑翔、張彥丞、鄭雅云）所提供的協助，使得本計畫得以順利完成。

行政院國家科學委員會補助國內專家學者出席國際學術會議報告

98 年 8 月 6 日

附件三

報告人姓名	鄭藏勝	服務機構及職稱	中華大學機械系 教授
時間 會議 地點	98.7.27~98.7.31 白俄羅斯、明斯克市	本會核定補助文號	NSC 96-2212-E-216-016-MY3
會議名稱	(中文)第 22 屆國際爆炸與反應系統動力會議 (英文)22nd International Colloquium on the Dynamics of Explosions and Reactive Systems		
發表論文題目	(中文)1.同步量測紊流碳氫火焰當量比及溫度之自然螢光感測器研發 2.層流甲烷/一氧化碳與空氣對衝擴散火焰之化學結構研究 (英文)1. Development of Chemiluminescence Sensor for Equivalence Ratio and Temperature Measurements in Turbulent Hydrocarbon Flames 2. The Chemical Structures of Laminar Opposed-Jet Diffusion Flames of CH_4/CO Versus Air		

一、參加會議經過

本次第二十二屆國際爆炸與反應系統動力研討會(International Colloquium on the Dynamics of Explosions and Reactive Systems, ICDERS)係由白俄羅斯國家科學院 A. V. Luikov 熱與質傳研究所(A. V. Luikov Heat and Mass Transfer Institute of National Academy of Science of Belarus)承辦，於 2009 年 7 月 26 日至 7 月 31 日在白俄羅斯首都明斯克市的國家聯合貿易館舉行。此會議是由設於西雅圖的爆炸與反應系統動力學會(Institute of Dynamics of Explosion and Reactive Systems, IDERS)每兩年於世界各地定期主辦，是國際上有關爆炸與燃燒反應動力系統歷史最悠久的主要國際會議，剛好與國際燃燒會議(International Symposium on Combustion)隔年錯開，此會議由國際燃燒學會(The International Combustion Institute)認可為偏重於燃燒之流體動態影響方面之專家會議(A Specialist Meeting on the Fluid-Dynamic Aspects of Combustion)，比較著重於爆炸、爆震與燃燒動態反應方面，與國際燃燒會議在主題強調上有明顯的區隔，所以這個會議是爆炸、爆震、反應動力與動態燃燒反應界兩年一次重要的聚會。此次研討會共有 231 篇相關論文發表，其中 171 篇論文以口述發表，60 篇以海報發表，可見其規模之完整以及普受重視。

明斯克市是白俄羅斯的首都，由於台灣沒有到明斯克的直飛班機，因此

必須在維也納轉機，雖然曾多次出國參加國際會議，但到東歐國家開會還是第一次，所以利用此機會與成功大學航太系趙怡欽教授及其博士後研究員李約亨博士、博士生連永生、利鴻源、許耀中等人提早於 7 月 22 日早上到達維也納，並在維也納停留一晚，隔天早上搭 2 個半小時的火車到匈牙利的首都布達佩斯，去拜訪這個曾在好幾世紀前遭蒙古人蹂躪的美麗雙子城。布達是山城，佩斯是平原，兩個城市隔著多瑙河遙遙相對，橫跨多瑙河的鐵鍊橋造好之後，也將兩個城市連成一個城市。我們在布達佩斯住兩個晚上，第一天下午瀏覽布達城上的古老教堂、漁夫堡、總理府及皇宮建築之後就回旅館休息，隔天再去參觀佩斯城裡的傳統市場、國會大廈及踏步鐵鍊橋，晚上搭船沿著藍色多瑙河瀏覽兩岸的夜景。

我們於 7 月 26 日早上在維也納搭機前往明斯克，在機場候機室與任職於高苑科技大學的吳志勇博士、任職於成大航太中心的許紘瑋博士、中央大學機械系施聖洋教授及其博士生劉建嘉同學碰面，搭同班機前往明斯克。抵達明斯克是下午當地時間四點半，但我們一行十人辦理落地簽證卻花了將近兩個小時的時間，出海關後又等了主辦單位派來的巴士，到達旅館辦理完住宿手續已八點多，匆忙趕到會場辦理報到手續後，大會舉辦的歡迎酒會也已結束，由於大家都尚未用餐，因此只好將酒會所剩的炒飯帶回旅館當晚餐。抵達明斯克第一天就領教到前共產國家的辦事態度及效率，第一印象就不是很好。

7 月 27 日至 7 月 31 日為正式會議議程，7 月 27 日上午 8:30 開幕儀式後隨即在 9:10 開始論文宣讀，此次會議之論文宣讀安排三個不同場地同時有三篇論文同時發表，其主題及進行時程如下:

Monday, July 27			
8:30	Welcome		
9:10~10:50	(1A) DDT 1	(1B) Modeling of Reactive System	(1C) Flames in IC Engines
10:50	Break/Poster Session		
11:45~13:00	(2A) DDT 2	(2B) Jet Ignition	(2C) Multiphase Reactive System 1
13:00	Lunch		
14:40~15:55	(3A) Detonation Structure 1	(3B) Combustion Induced Vortex Breakdown 1	(3C) Diagnostics
15:55	Break		
16:20~18:00	(4A) Detonation Structure 2	(3B) Combustion Induced Vortex	(3C) Fires

		Breakdown 2	
Tuesday, July 28			
8:30~11:00	R. Soloukhin Memorial Session		
11:00	Break		
11:45~13:00	(5A) PDE and RDE 1	(5B) Fast Flame 1	(5C) Soot
13:00	Lunch		
14:40~15:55	(6A) PDE and RDE 2	(6B) Fast Flame 2	(6C) Flames 1
15:55	Break/Work-in-Progress Session		
17:00~18:15	(7A) PDE and RDE 3	(7B) Ignition	(7C) Hydrocarbons Ignition and Combustion
Wednesday, July 29			
8:30~11:00	H. Edwards Memorial Session		
11:45~13:00	(8A) Detonation Structure 3	(8B) Detonation Initiation 1	(8C) Numerical Simulation 1
13:00	Lunch		
Thursday July 30			
8:30~9:20	A. K. Oppenheim Memorial Session		
9:20~11:00	(9A) Detonation Structure 4	(9B) Explosions 1	(9C) Multiphase Combustion
11:00	Break		
11:45~13:00	(10A)Detonation Initiation 2	(10B) Explosions 2	(10C) Chemical Kinetics 1
13:00	Lunch		
14:40~15:55	(11A) Detonation Initiation 3	(11B) Flame Instabilities 1	(11C) Numerical Simulation 2
15:55	Break		
16:20~18:00	(12A) Detonation Structure 5	(12B) Micro and Mesoscale Combustion	(12C) Flames 2
Friday July 31			
8:55~10:35	(13A) Detonation Structure and	(13B) Electric and	(13C) Flames in

	Chemical Reaction	Magnetic Effects	Channels
10:35	Break		
11:00~13:00	(14A) Detonation Multiphase 1	(14B) Flame Instabilities 2	(14C) Chemical Kinetics 2
13:00	Lunch		
14:40~15:55	(15A) Detonation Multiphase 2	(15B) Flame Instabilities 3	(15C) various Topic 1
15:55	Break		
16:20~17:35	(16A) Detonation Multiphase 3		(16C) various Topic 2
18:00~20:00	Farewell Party		

會議除了論文宣讀還有二場張貼海報(Poster)外，大會亦安排三場 Memorial Sessions，分別是 1. R. Soloukhin Memorial Session，有三位學者各以 25 分鐘的報告來紀念 Prof. Soloukhin 在 Shock wave 及 Detonation 研究上的貢獻；2. H. Edwards Memorial Session，本來這個紀念會是由美國海軍研究中心的 Dr. Elan Oran 負責報告，但聽說是因 Dr. Oran 任職國防部門，沒拿到白俄羅斯的簽證，若這是事實的話，那麼以後有關的國際研討會大概也不會再到白俄羅斯來舉行，二年前 Board Meeting 在法國討論是否讓白俄羅斯舉辦時，就有 Board Member 反對，不過因有歐洲及東歐國家的支持，最後才決定由白俄羅斯負責舉辦這一屆的會議。3. A. K. Oppenheim Memorial Session，Dr. Oppenheim 是波蘭籍的加州大學柏克萊分校教授，去年過世，2005 年第 20 屆會議在加拿大蒙特婁舉年時，還以 90 高齡出席會議，一生對燃燒與爆炸氣動力的研究不遺餘力，桃李滿天下，本人有幸於 1997 到波蘭克拉克第一次參加這個會議時認識他，在會議結束後參加搭竹筏沿著波蘭與斯洛伐克兩國邊境旅遊的活動還跟他們夫婦同舟，他說曾到工研院訪問，對台灣印象非常好。

大會的主要活動尚包括：7 月 27 日晚上在會場大廳舉辦的音樂會，由深具白俄羅斯傳統的歌舞劇團負責演出。7 月 29 日星期三下午的搭車遠足(Excursion)，到 Dudutki 農莊品嚐伏特加、香檳、紅酒及白酒，並在那裡 BBQ 直到晚上十點半看完煙火秀之後才回旅館。以及 7 月 30 日星期四晚上在獨立紀念館舉行的大會晚宴(Banquet)及音樂、歌舞表演，星期五下午的歡送酒會。

從以上會議主題可以明顯分類出四個主要主題：(i)爆震(Detonation)，(ii)火焰基礎(Flames)，(iii)點燃(Ignition)，(iv)爆炸(Explosions)。會議中主要行程在於聽取專題演講與分組論文發表，在分組發表部分來說，主要聽取火

焰結構(Flame structure)、微型燃燒器燃燒(Microscale Combustion)及數值模擬(Numerical Simulation)等，因比較少接觸爆震與反應動力方面的研究，所以這方面場次也比較少參加。著重的方面在於應用診測技術於火焰的量測；在微尺寸與小尺寸的燃燒現象與研究與觸媒燃燒方面也是興趣所在。此次共發表 2 篇與成功大學航太所趙怡欽教授合作的論文，第一篇“Development of Chemiluminescence Sensor for Equivalence Ratio and Temperature Measurements in Turbulent Hydrocarbon Flames”是於 7 月 27 日下午發表，第二篇海報論文“The Chemical Structures of Laminar Opposed-Jet Diffusion Flames of CH_4/CO Versus Air” 於 7 月 27 日早上發表，第一篇論文由成大航太系博士後研究員李約亨博士做口頭報告。李約亨博士從博士班學生就參與本人與趙怡欽教授之整合型研究計畫，並曾多次出國參加國際性學術研討會，所以表現相當平穩。除了聆聽專題演講分組發表之外，亦參觀許許多多其他學者張貼之海報，尤其是有關應用 CARS 雷射光學技術量測超過 10000K 高溫電漿之成果，不僅僅與張貼之作者當面討論之外，亦留下聯絡之方式以便將來能夠做技術上面的交流。整個會議行程相當緊湊，然而所獲得之資料與資訊卻相當的豐富。

二、與會心得及建議

有關燃燒與爆震方面的研究在各界努力經多年灌溉耕耘已漸漸開花結果，此次我國計有 7 篇論文發表，也有 10 位學者與研究人員參加，與會之陣容及發表論文數在大會開幕時被主辦單位提及，表示肯定，論文發表也表現平順。成大航太系趙怡欽教授在第 20 屆會議時就被選為 Board member，中央大學機械系施聖洋教授於本屆亦被選為 Board member，同時趙怡欽教授又被推舉為下一屆 2011 年在 UC Irvine 舉行時的 Program Chair，可見我國學者在此國際會議組織也漸嶄露頭角，大會方面也一直希望我國可以接辦 2013 年或以後的會議，代表團不敢貿然答應，答應帶回討論再議。近年來國科會與教育部正大力推廣的鼓勵博士班研究生出國參加國際會議並親自發表論文以及出國參加知名教授研究的千里馬計畫，是相當值得肯定的，對學生一生的影響不是補助的旅費所可以衡量的，但是去年以來國科會或其他基金會去大幅減低出國補助經費，而教育部補助也納入各學校經費由學校統籌，如此讓這些博士後研究員與博士班學生出國參加會議申請補助處處碰壁，幾乎無法成行，還得靠自己家裡與平時積蓄始得勉強成行，政府對這些年輕有潛力的新力軍的關注與實質補助與其在會場上的表現幾乎不成比例，而這個現象幾乎沒有轉變的跡象，只有越來越遭，希望在上位者對花小錢培育人才能有突破現行制度盲點的看法。此次博士後研究員李約亨博士在學期間已有數次參加國際會議經驗，所以表現相當平穩，而且會場內外與其他國學者也建立相當友誼。參加這次會議的博士生中，成大航太系有兩位，中央機械系有一位，都是第一次以英文作

口頭報告，國內博士生第一次用英文演講難免緊張，現場問答會有些支拙，但讓學生於國際會議場合加以磨練，熟悉論文發表程序以及方法，增進其經驗，培養其獨立思考的能力，這是在課堂上無法傳授的經驗，這是培養一位從事研究的專家不可或缺的經驗，所以個人認為應該在經費補助與管道上多多鼓勵學生參加國際性研討會，絕對有助於培養獨立研究的人才。

近兩三年來國際上不論美國或日本在燃燒與航太研究方面在經費上都受到相當程度的排擠，所以研究方面受到一定程度的影響，連帶影響到學者出席會議的意願明顯降低，而且國際爆炸與反應系統動力研討會所匯集的教授學者均是各國在燃燒學或者是化學反應動力學方面上頗具成就之人士，發現研究人口有日益老化的趨勢，而且有大幅退休的風潮，這在日本近年來相當明顯，但是歐洲國家則比較平穩，他們比較重視長遠的基礎研究，比較不受研究經費波動的影響。由於各國燃燒與國防相關經費削減，燃燒研究大受影響，爆炸與燃燒相關研究漸漸往兩個主要方向集中即:火焰基礎與爆震(Detonation)，充分反應出國防與太空方面的相關燃燒推進方面研究經費的緊縮，漸漸往比較小規模的基礎研究與兼顧實用上發展的現實，國內燃燒方面的研究宜早注意此趨勢。

另一重要的方向就是國際燃燒界近年來一直努力在尋求新的有創意的燃燒研究(Novel combustion methods)與應用的主題方向，今年是國際爆炸與反應系統動力研討會有多個這方面主題分組，反應出美、歐、日等主要先進燃燒研究國家對尋找新的燃燒研究方向的努力與殷切，這個趨勢也值得我們注意。國內這兩年進行的觸媒燃燒與微燃燒現象研究今年發表多篇論文，引起相當廣泛的注意，而這兩方面卻是目前幾乎還沒有開發的燃燒研究處女地，目前在儀器量測上相當困難，有其研究上的瓶頸，但是未來可能的發展與影響卻無可限量，對人類未來廣泛的能源應用，會有相當大的影響，值得我們及早加以注意。

三、攜回資料名稱及內容

所攜回資料詳列如下：

會議之論文光碟：其中包含所有口頭發表論文與海報論文，可供查詢此次研討會所發表論文之查詢；另外有最近會議資訊海報，以及最新的相關化學反應模擬軟體等資料。

四、感謝

在此衷心感謝國科會提供經費補助機票、生活費與註冊費用，始能順利參與此次國際爆炸與反應系統動力研討會，在此特別誌謝。

行政院國家科學委員會補助國內專家學者出席國際學術會議報告

99 年 8 月 14 日

附件三

報告人姓名	鄭藏勝	服務機構及職稱	中華大學機械工程學系教授
會議時間地點	99.8.1~99.8.6 大陸、北京	本會核定補助文號	NSC 96-2212-E-216-0016-MY3
會議名稱	(中文)第 33 屆國際燃燒會議 (英文)Thirty-third International Symposium on Combustion		
發表論文題目	(中文)1.熱光電動力系統之管式燃燒器研發 (英文)1.Development of a tubular-flame combustor for thermophotovoltaic power systems		

一、參加會議經過

本次第三十三屆國際燃燒會議(The 33rd International Symposium on Combustion)係由北京清華大學承辦，於 2010 年 8 月 1 日至 8 月 6 日在清華大學的主樓及第六教學大樓舉行。本人於 7 月 31 日早上與成功大學航太系趙怡欽教授、副研究員陳冠邦博士及趙老師之博士後研究員李約亨、博士生連永生、利鴻源、許耀中、張子威、碩士生伍芳嫻及高苑科技大學吳志勇助理教授一起搭乘長榮航空公司班機啟程直飛北京首都國際機場，由於直飛的關係，從桃園到北京只需 2 小時 40 分左右，抵達北京首都機場之後再分批搭計程車到清華大學的「甲所」旅館辦理住宿手續，當天下午稍事休息之後，一群人開始認識清華大學的周遭環境。北京清華大學的校園比台灣的清大要大上好幾倍，光是從住宿旅館走到會議場館就要花 20 分鐘左右。雖然是暑假期間，校園內人山人海，絕大部分是外來觀光客，最主要的觀光照相景點就是立有「清華園」牌樓的第二校門，從早到晚都有人在那取景照相，外來觀光客中有不少是帶著小孩來的，我們想應該是父母要讓小孩瞭解，清華是大陸理工科的第一學府，也是他們未來努力的目標。清華大學可說是大陸的重點大學中的重點，近幾年獲得的資源相當多，走過一些大樓都可看到標示著「國家重點實驗室」的牌示，高科技園區的「中關村」就設在清華旁邊，同時除了香港邵逸夫捐款蓋大樓之外，富士康及寶成也都各捐了一棟非常現代化的教學或研究大樓，這一次會議的主要場所第六教學大樓就是由寶成企業所捐獻的。

此次前往北京參與會議的人員尚有中央大學機械系施聖洋教授及其一位博士生與三位碩士生，台灣大學機械系王興華教授與潘國隆副教授及其一位碩士生，成功大學機械系吳明勳助理教授，高雄第一科大蔡匡忠助理教授，以及虎尾科技大學楊碩印助理教授等共 21 人，陣容是歷年來最龐大的一次，值得一提的是成功大學機械系吳明勳助理教授是此次獲得 Bernard Lewis Fellowship Award 五位青年得獎人之一，真是與有榮焉。8 月 1 日上午與趙怡欽老師及其研究生一行人一起去遊覽頤和園，下午五點到清華大學美術學院辦理報到手續之後，並參加主辦單位所舉辦之歡迎酒會，在酒會中遇到燃燒總會前任主席普林斯頓大學的 Prof. C. K. Law，加州大學柏克萊機械系的陳志源(J.-Y. Chen)教授，Stanford 大學的 Professor Ron Hanson，雪梨大學的 Prof. Masri，首爾國立大學的鄭仁碩教授，從首爾國立大學轉任至沙烏地阿拉伯阿布杜拉國王科技大學擔任潔淨燃燒研究中心主任的鄭石浩教授，加州大學爾灣分校的 Professor Derek Dunn-Rankin 及美國 Sandia 國家實驗室的 Dr. Rob Barlow 與 Dr. Bill Pitz 等人。

8 月 2 日起至 8 月 6 日連續五天論文發表及海報張貼，這次會議共有 1123 多位來自 30 多個不同國家的學者專家參與，大部份來自美國、日本、法國、德國及其他歐洲國家，由於大陸是主辦國，因此參加會議的人數也不少。依據大會 Technical Program 主席南加大機械系 Prof. Paul Ronney 的報告，本次會議投稿共 1051 篇，接受發表 439 篇，可刊載在 Proceeding 的約 370 幾篇，可見論文審查之嚴謹度。

此次會議每天安排七個不同主題同時進行論文宣讀，主題及進行時程如下:

Monday	Hottel Lecture						
am	Break						
	Turbulent Flames: Modeling	Reaction Kinetics: Large Alkanes	Laminar Flame: Burning Velocities Small Fuels	Stationary Combustion	Gas Turbine Combustion	Coal Combustion	Detonations: Modeling
pm	Topical review Turbulent Flames: Acoustics	Reaction Kinetics: C_3 Compounds	Laminar Flames	Stationary Combustion	Engine Combustion: Diagnostics	Coal Combustion	Detonations
	Break						
	Turbulent Flames: Modeling	Reaction Kinetics: Alcohols	Laminar Flames	Stationary Combustion: Mercury	Engine Combustion: LES	Coal Combustion	Detonations: Scramjets
All Day Work-in-Progress Poster Presentations							
Tuesday	Plenary Lecture						
am	Turbulent Combustion: Extinction	Reaction Kinetics : Propyl Chemistry	Laminar Flames: Coflow	Stationary Combustion: Metals	I.C. Engines: Emissions	Heterogeneous Combustion: Explosives	Detonations
	Break						
	Turbulent Flames: Burning Velocities	Reaction Kinetics: Methyl Esters	Laminar Flames: Additivies	Stationary Combustion: Ash	I.C. Engines: Emissions	Heterogeneous Combustion: Catalysis	Detonations
pm	Topic review Turbulent	Reaction Kinetics:	Laminar Flames:	Stationary Combustion:	I.C. Engines: Modeling	Heterogeneous Combustion:	Detonations

	Flames: Stabilization	NO_x & Si	Large Fuels	Particulates		Surface Reactions	
	Break						
	Turbulent Flames: Stabilization	Reaction Kinetics: N-C-H Chemistry	Laminar Flames: Jet Fuels	New Technology: Catalysis	I.C. Engines: Modeling	Heterogeneous Combustion: Synthesis	Detonations
All Day Work-in-Progress Poster Presentations							
Wednesday	Plenary Lecture						
am	Turbulent Combustion: LES	Reaction Kinetics: Surrogate Fuels	Laminar Flames: Lifted Flames	Soot	I.C. Engines: HCCI	Heterogeneous Combustion: Metals	Detonations
	Break						
	Turbulent Combustion: LES	Reaction Kinetics: Aromatics	Laminar Flames: Spherical Flames	Soot Formation	I.C. Engines: Ignition	Heterogeneous Combustion: Metals	Fire
Thursday	Plenary Lecture						
am	Turbulent Combustion: LES	Reaction Kinetics: Low Temperature Oxidation	New Technology: Micro-combustors	Soot: Liquid Fuels	Heterogeneous Combustion: Metals	Spray & Droplets: Diagnostics	Fire: Electric Fields
	Break						
	Turbulent Combustion: Jet Flames	Reaction Kinetics: Small Fuels	New Technology: Micro-combustors	Soot: Liquid Fuels	Heterogeneous Combustion: Metals	Spray & Droplets	Fire: Extinction
pm	Topical Review Turbulent Combustion: Jet Flames	Reaction Kinetics: NO_x-Hydrocarbon Interactions	New Technology: Microchannel combustion	Soot: Characterization	Diagnostics: Temperature	Spray & Droplets: Large Fuels	Fire
	Break						
	Turbulent Combustion: Jet Flames	Reaction Kinetics: n-Alkanes	New Technology:	I.C. Engines: HCCI	Diagnostics	Spray & Droplets	Fire
All Day Work-in-Progress Poster Presentations							
am	Plenary Lecture						
am	Turbulent Combustion: Modeling	Reaction Kinetics: Optimization	Laminar Flames: DME	Soot: Oxidation	Diagnostics	Spray & Droplets: Simulation	Fire
	Break						
	Turbulent Combustion: DNS	New Technology: Oxy Fuel Combustion	Laminar Flames: Ethanol	Soot: Growth	Diagnostics	Spray & Droplets: Diesel	Fire
pm	Turbulent Combustion: Modeling	New Technology: Oxy Fuel Combustion	Laminar Flames	New Technology: Plasma/Flame Interaction	Diagnostics: LIF	Spray & Droplets: Diesel	Fire
	Break						
	Turbulent Combustion: Modeling	New Technology: MILD Combustion	Laminar Flames: Butanol	New Technology	Diagnostics: Soot	New Technology: Power Generation	Fire
All Day Work-in-Progress Poster Presentations							

由本人與成大航太所趙怡欽老師及其博士後研究員、研究生共同發表之論文被安排在最後一天(8 月 6 日)下午以口頭報告方式進行，題目是 Development of a tubular-flame combustor for thermophotovoltaic power systems，由博士生利鴻源進行報告，因利同學曾在去年的國際爆炸與反應

系統動力會議做過口頭報告，口語表達與臨場反應皆比去年進步許多。由於國際燃燒會議兩年出版一次的論文集(Proceedings of the Combustion Institute) Impact Factor 非常高，2007 年的 Impact Factor 為 2.647，2008 年為 1.906，2009 年 Impact Factor 為 3.256，此 Impact Factor 高於燃燒著名期刊 Combustion and Flame 之 Impact Factor，由此可見國際燃燒會議所出版之論文集的重要性。

二、 與會心得

有關燃燒方面的研究在各界努力經多年灌溉耕耘已漸漸開花結果，此次我國計有 7 篇論文被接受發表，也有 21 位學者與研究生參加，與會之陣容及發表論文數可說是本人自 1994 年參加國際燃燒會議以來之最，論文發表也表現平順。近年來國科會與教育部正大力推廣的鼓勵博士班研究生出國參加國際會議並親自發表論文，是相當值得肯定的，對學生一生的影響不是補助的旅費所可以衡量的，但是去年以來國科會或其他基金會去大幅減低出國補助經費，而教育部補助也納入各學校經費由學校統籌，如此讓這些博士後研究員與博士班學生出國參加會議申請補助處處碰壁，幾乎無法成行，還得靠自己家裡與平時積蓄始得勉強成行，政府對這些年輕有潛力的新力軍的關注與實質補助與其在會場上的表現幾乎不成比例，而這個現象幾乎沒有轉變的跡象，只有越來越遭，希望在上位者對花小錢培育人才能有突破現行制度盲點的看法。此次博士後研究員李約亨博士在學期間已有數次參加國際會議經驗，所以表現相當平穩，而且會場內外與其他國學者也建立相當友誼。參加這次會議的博士生中，成大航太系有利鴻源及張子威兩位上台報告，張子威是第一次以英文作口頭報告，國內博士生第一次用英文演講難免緊張，現場問答會有些支拙，但讓學生於國際會議場合加以磨練，熟悉論文發表程序以及方法，增進其經驗，培養其獨立思考的能力，這是在課堂上無法傳授的經驗，這是培養一位從事研究的專家不可或缺的經驗，所以個人認為應該在經費補助與管道上多多鼓勵學生參加國際性研討會，絕對有助於培養獨立研究的人才。同時由這次會議更讓我覺得從事燃燒實驗或是數值模擬研究早已走向合作研究的方向，尤其是光學量測燃燒流場的研究更非合作不可，昂貴儀器設備的購買與維護已不再是每個研究單位都可負擔，共同合作一起發表論文才能提升我們的學術國際聲望，本人十幾年來與成大航太系趙怡欽老師的合作就是最好的例子。

三、攜回資料名稱及內容

此次會議所攜回的資料是與會者通訊錄及海報摘要各一本。

四、感謝

在此衷心感謝國科會提供經費補助機票、生活費與註冊費用，始能順利參與此次國際燃燒會議，在此特別誌謝。

行政院國家科學委員會補助國內專家學者出席國際學術會議報告

99 年 8 月 14 日

附件三

報告人姓名	鄭藏勝	服務機構及職稱	中華大學機械工程學系教授
時間 會議 地點	99.8.1~99.8.6 大陸、北京	本會核定 補助文號	NSC 96-2212-E-216-0016-MY3
會議名稱	(中文)第 33 屆國際燃燒會議 (英文)Thirty-third International Symposium on Combustion		
發表論文題目	(中文)1.熱光電動力系統之管式燃燒器研發 (英文)1.Development of a tubular-flame combustor for thermophotovoltaic power systems		

報告內容應包括下列各項：

一、參加會議經過

二、與會心得

三、考察參觀活動(無是項活動者省略)

四、建議

五、攜回資料名稱及內容

六、其他

一、參加會議經過

本次第三十三屆國際燃燒會議(The 33rd International Symposium on Combustion)係由北京清華大學承辦，於 2010 年 8 月 1 日至 8 月 6 日在清華大學的主樓及第六教學大樓舉行。本人於 7 月 31 日早上與成功大學航太系趙怡欽教授、副研究員陳冠邦博士及趙老師之博士後研究員李約亨、博士生連永生、利鴻源、許耀中、張子威、碩士生伍芳嫻及高苑科技大學吳志勇助理教授一起搭乘長榮航空公司班機啟程直飛北京首都國際機場，由於直飛的關係，從桃園到北京只需 2 小時 40 分左右，抵達北京首都機場之後再分批搭計程車到清華大學的「甲所」旅館辦理住宿手續，當天下午稍事休息之後，一群人開始認識清華大學的周遭環境。北京清華大學的校園比台灣的清大要大上好幾倍，光是從住宿旅館走到會議場館就要花 20 分鐘左右。雖然是暑假期間，校園內人山人海，絕大部分是外來觀光客，最主要的觀光照相景點就是立有「清華園」牌樓的第二校門，從早到晚都有人在那取景照相，外來觀光客中有不少是帶著小孩來的，我們想應該是父母要讓小孩瞭解，清華是大陸理工科的第一學府，也是他們未來努力的目標。清華大學可說是大陸的重點大學中的重點，近幾年獲得的資源相當多，走過一些大樓都可看到標示著「國家重點實驗室」的牌示，高科技園區的「中關村」就設在清華旁邊，同時除了香港邵逸夫捐款蓋大樓之外，富士康及寶成也都各捐了一棟非常現代化的教學或研究大樓，這一次會議的主要場所第六教學大樓就是由寶成企業所捐獻的。

此次前往北京參與會議的人員尚有中央大學機械系施聖洋教授及其一位博士生與三位碩士生，台灣大學機械系王興華教授與潘國隆副教授及其一位碩士生，成功大學機械系吳明勳助理教授，高雄第一科大蔡匡忠助理教授，以及虎尾科技大學楊碩印助理教授等共 21 人，陣容是歷年來最龐大的一次，值得一提的是成功大學機械系吳明勳助理教授是此次獲得 Bernard Lewis Fellowship Award 五位青年得獎人之一，真是與有榮焉。8 月 1 日上午與趙怡欽老師及其研究生一行人一起去遊覽頤和園，下午五點到清華大學美術學院辦理報到手續之後，並參加主辦單位所舉辦之歡迎酒會，在酒會中遇到燃燒總會前任主席普林斯頓大學的 Prof. C. K. Law，加州大學柏克萊機械系的陳志源(J.-Y. Chen)教授，Stanford 大學的 Professor Ron Hanson，雪梨大學的 Prof. Masri，首爾國立大學的鄭仁碩教授，從首爾國立大學轉任至沙烏地阿拉伯阿布杜拉國王科技大學擔任潔淨燃燒研究中心主任的鄭石浩教授，加州大學爾灣分校的 Professor Derek Dunn-Rankin 及美國 Sandia 國家實驗室的 Dr. Rob Barlow 與 Dr. Bill Pitz 等人。

8 月 2 日起至 8 月 6 日連續五天論文發表及海報張貼，這次會議共有 1123 多位來自 30 多個不同國家的學者專家參與，大部份來自美國、日本、法國、德國及其他歐洲國家，由於大陸是主辦國，因此參加會議的人數也不少。依據大會 Technical Program 主席南加大機械系 Prof. Paul Ronney 的報告，本次會議投稿共 1051 篇，接受發表 439 篇，可刊載在 Proceeding 的約 370 幾篇，可見論文審查之嚴謹度。

此次會議每天安排七個不同主題同時進行論文宣讀，主題及進行時程如下:

Monday	Hottel Lecture						
am	Break						
	Turbulent Flames: Modeling	Reaction Kinetics: Large Alkanes	Laminar Flame: Burning Velocities Small Fuels	Stationary Combustion	Gas Turbine Combustion	Coal Combustion	Detonations: Modeling
pm	Topical review Turbulent Flames: Acoustics	Reaction Kinetics: C_3 Compounds	Laminar Flames	Stationary Combustion	Engine Combustion: Diagnostics	Coal Combustion	Detonations
	Break						
	Turbulent Flames: Modeling	Reaction Kinetics: Alcohols	Laminar Flames	Stationary Combustion: Mercury	Engine Combustion: LES	Coal Combustion	Detonations: Scramjets
All Day Work-in-Progress Poster Presentations							
Tuesday	Plenary Lecture						
am	Turbulent Combustion: Extinction	Reaction Kinetics : Propyl Chemistry	Laminar Flames: Coflow	Stationary Combustion: Metals	I.C. Engines: Emissions	Heterogeneous Combustion: Explosives	Detonations
	Break						
	Turbulent Flames: Burning Velocities	Reaction Kinetics: Methyl Esters	Laminar Flames: Additivies	Stationary Combustion: Ash	I.C. Engines: Emissions	Heterogeneous Combustion: Catalysis	Detonations
pm	Topic review Turbulent Flames: Stabilization	Reaction Kinetics: NO_x & Si	Laminar Flames: Large Fuels	Stationary Combustion: Particulates	I.C. Engines: Modeling	Heterogeneous Combustion: Surface Reactions	Detonations
	Break						
	Turbulent Flames: Stabilization	Reaction Kinetics: N-C-H Chemistry	Laminar Flames: Jet Fuels	New Technology: Catalysis	I.C. Engines: Modeling	Heterogeneous Combustion: Synthesis	Detonations
All Day Work-in-Progress Poster Presentations							
Wednesday	Plenary Lecture						
am	Turbulent Combustion: LES	Reaction Kinetics: Surrogate Fuels	Laminar Flames: Lifted Flames	Soot	I.C. Engines: HCCI	Heterogeneous Combustion: Metals	Detonations
	Break						
	Turbulent Combustion: LES	Reaction Kinetics: Aromatics	Laminar Flames: Spherical Flames	Soot Formation	I.C. Engines: Ignition	Heterogeneous Combustion: Metals	Fire
Thursday	Plenary Lecture						
am	Turbulent Combustion: LES	Reaction Kinetics: Low Temperature Oxidation	New Technology: Micro-combustors	Soot: Liquid Fuels	Heterogeneous Combustion: Metals	Spray & Droplets: Diagnostics	Fire: Electric Fields
	Break						
	Turbulent Combustion: Jet Flames	Reaction Kinetics: Small Fuels	New Technology: Micro-combustors	Soot: Liquid Fuels	Heterogeneous Combustion: Metals	Spray & Droplets	Fire: Extinction
pm	Topical Review Turbulent Combustion: Jet Flames	Reaction Kinetics: NO_x-Hydrocarbon Interactions	New Technology: Microchannel combustion	Soot: Characterization	Diagnostics: Temperature	Spray & Droplets: Large Fuels	Fire
	Break						
	Turbulent Combustion: Jet Flames	Reaction Kinetics: n-Alkanes	New Technology:	I.C. Engines: HCCI	Diagnostics	Spray & Droplets	Fire
All Day Work-in-Progress Poster Presentations							
am	Plenary Lecture						
am	Turbulent	Reaction	Laminar	Soot:	Diagnostics	Spray &	Fire

表 Y04

	Combustion: Modeling	Kinetics: Optimization	Flames: DME	Oxidation		Droplets: Simulation	
	Break						
	Turbulent Combustion: DNS	New Technology: Oxy Fuel Combustion	Laminar Flames: Ethanol	Soot: Growth	Diagnostics	Spray & Droplets: Diesel	Fire
pm	Turbulent Combustion: Modeling	New Technology: Oxy Fuel Combustion	Laminar Flames	New Technology: Plasma/Flame Interaction	Diagnostics: LIF	Spray & Droplets: Diesel	Fire
	Break						
	Turbulent Combustion: Modeling	New Technology: MILD Combustion	Laminar Flames: Butanol	New Technology	Diagnostics: Soot	New Technology: Power Generation	Fire
All Day Work-in-Progress Poster Presentations							

由本人與成大航太所趙怡欽老師及其博士後研究員、研究生共同發表之論文被安排在最後一天(8 月 6 日)下午以口頭報告方式進行，題目是 Development of a tubular-flame combustor for thermophotovoltaic power systems，由博士生利鴻源進行報告，因利同學曾在去年的國際爆炸與反應系統動力會議做過口頭報告，口語表達與臨場反應皆比去年進步許多。由於國際燃燒會議兩年出版一次的論文集(Proceedings of the Combustion Institute) Impact Factor 非常高，2007 年的 Impact Factor 為 2.647，2008 年為 1.906，2009 年 Impact Factor 為 3.256，此 Impact Factor 高於燃燒著名期刊 Combustion and Flame 之 Impact Factor，由此可見國際燃燒會議所出版之論文集的重要性。

二、 與會心得

有關燃燒方面的研究在各界努力經多年灌溉耕耘已漸漸開花結果，此次我國計有 7 篇論文被接受發表，也有 21 位學者與研究生參加，與會之陣容及發表論文數可說是本人自 1994 年參加國際燃燒會議以來之最，論文發表也表現平順。近年來國科會與教育部正大力推廣的鼓勵博士班研究生出國參加國際會議並親自發表論文，是相當值得肯定的，對學生一生的影響不是補助的旅費所可以衡量的，但是去年以來國科會或其他基金會去大幅減低出國補助經費，而教育部補助也納入各學校經費由學校統籌，如此讓這些博士後研究員與博士班學生出國參加會議申請補助處處碰壁，幾乎無法成行，還得靠自己家裡與平時積蓄始得勉強成行，政府對這些年輕有潛力的新力軍的關注與實質補助與其在會場上的表現幾乎不成比例，而這個現象幾乎沒有轉變的跡象，只有越來越遭，希望在上位者對花小錢培育人才能有突破現行制度盲點的看法。此次博士後研究員李約亨博士在學期間已有數次參加國際會議經驗，所以表現相當平穩，而且會場內外與其他國學者也建立相當友誼。參加這次會議的博士生中，成大航太系有利鴻源及張子威兩位上台報告，張子威是第一次以英文作口頭報告，國內博士生第一次用英文演講難免緊張，現場問答會有些支拙，但讓學生於國際會議場合加以磨練，熟悉論文發表程序以及方法，增進其經驗，培養其獨立思考的能力，這是在課堂上無法傳授的經驗，這是培養一位從事研究的專家不可或缺的經驗，所以個人認為應該在經費補助與管道上多多鼓勵學生參加國際性研討

會，絕對有助於培養獨立研究的人才。同時由這次會議更讓我覺得從事燃燒實驗或是數值模擬研究早已走向合作研究的方向，尤其是光學量測燃燒流場的研究更非合作不可，昂貴儀器設備的購買與維護已不再是每個研究單位都可負擔，共同合作一起發表論文才能提升我們的學術國際聲望，本人十幾年來與成大航太系趙怡欽老師的合作就是最好的例子。

三、攜回資料名稱及內容

此次會議所攜回的資料是與會者通訊錄及海報摘要各一本。

四、感謝

在此衷心感謝國科會提供經費補助機票、生活費與註冊費用，始能順利參與此次國際燃燒會議，在此特別誌謝。

國科會補助計畫衍生研發成果推廣資料表

日期:2010/11/04

國科會補助計畫	計畫名稱: 重組燃料燃燒之實驗與數值研究--加氫對混合燃料火焰穩定性、化學動力、火焰結構及污染排放之影響
	計畫主持人: 鄭藏勝
	計畫編號: 96-2221-E-216-016-MY3　　學門領域: 能源科技

無研發成果推廣資料

96 年度專題研究計畫研究成果彙整表

計畫主持人：鄭藏勝	計畫編號：96-2221-E-216-016-MY3
計畫名稱：重組燃料燃燒之實驗與數值研究--加氫對混合燃料火焰穩定性、化學動力、火焰結構及污染排放之影響	

成果項目			量化			單位	備註（質化說明：如數個計畫共同成果、成果列為該期刊之封面故事...等）
			實際已達成數（被接受或已發表）	預期總達成數(含實際已達成數)	本計畫實際貢獻百分比		
國內	論文著作	期刊論文	0	0	100%	篇	
		研究報告/技術報告	1	1	100%		
		研討會論文	0	1	10%		
		專書	0	0	100%		
	專利	申請中件數	0	0	100%	件	
		已獲得件數	0	0	100%		
	技術移轉	件數	0	0	100%	件	
		權利金	0	0	100%	千元	
	參與計畫人力（本國籍）	碩士生	2	2	100%	人次	
		博士生	0	1	50%		
		博士後研究員	0	0	100%		
		專任助理	0	0	100%		
國外	論文著作	期刊論文	1	2	80%	篇	
		研究報告/技術報告	0	0	100%		
		研討會論文	0	1	10%		
		專書	0	0	100%	章/本	
	專利	申請中件數	0	0	100%	件	
		已獲得件數	0	0	100%		
	技術移轉	件數	0	0	100%	件	
		權利金	0	0	100%	千元	
	參與計畫人力（外國籍）	碩士生	0	0	100%	人次	
		博士生	0	0	100%		
		博士後研究員	0	0	100%		
		專任助理	0	0	100%		

其他成果 (無法以量化表達之成果如辦理學術活動、獲得獎項、重要國際合作、研究成果國際影響力及其他協助產業技術發展之具體效益事項等，請以文字敘述填列。)	本計畫研究成果分為兩部分：第一部份為探討在甲烷燃料中加入不同比例之一氧化碳，以瞭解一氧化碳含量對 CH4/CO/air 當量預混火焰之層流火焰速度、火焰形狀、火焰前端位置、火焰溫度、火焰結構及化學動力結構之影響，此部分之研究成果已發表在高等級之燃燒期刊(Combustion Flame, Vol. 156, pp. 362-373, 2009, SCI, IF: 2.923)。第二部份為探討在甲烷/一氧化碳燃料中加入不同比例之氫氣，以瞭解氫氣含量對 H2/CH4/CO/air 當量預混火焰之層流火焰速度、火焰形狀、火焰前端位置、火焰溫度、火焰結構及化學動力結構之影響，此部分之研究成果目前正在撰寫成論文，將先投稿至明年七月在美國 UC Irvine 舉行的第 23 屆國際爆炸與反應系統動力會議發表，之後再轉投至衝擊係數高於 3.0 以上之 International Journal of Hydrogen Energy 國際期刊。

	成果項目	量化	名稱或內容性質簡述
科教處計畫加填項目	測驗工具(含質性與量性)	0	
	課程/模組	0	
	電腦及網路系統或工具	0	
	教材	0	
	舉辦之活動/競賽	0	
	研討會/工作坊	0	
	電子報、網站	0	
	計畫成果推廣之參與（閱聽）人數	0	

國科會補助專題研究計畫成果報告自評表

請就研究內容與原計畫相符程度、達成預期目標情況、研究成果之學術或應用價值（簡要敘述成果所代表之意義、價值、影響或進一步發展之可能性）、是否適合在學術期刊發表或申請專利、主要發現或其他有關價值等，作一綜合評估。

1. 請就研究內容與原計畫相符程度、達成預期目標情況作一綜合評估

■達成目標

□未達成目標（請說明，以 100 字為限）

□實驗失敗

□因故實驗中斷

□其他原因

說明：

2. 研究成果在學術期刊發表或申請專利等情形：

論文：■已發表 □未發表之文稿 □撰寫中 □無

專利：□已獲得 □申請中 ■無

技轉：□已技轉 □洽談中 ■無

其他：(以 100 字為限)

本計畫第一部份之研究成果已發表在 Combustion Flame, Vol. 156, pp. 362-373, 2009, SCI, IF: 2.923。第二部份之研究成果目前正在撰寫成論文，將投稿至國際期刊。

3. 請依學術成就、技術創新、社會影響等方面，評估研究成果之學術或應用價值（簡要敘述成果所代表之意義、價值、影響或進一步發展之可能性）（以 500 字為限）

本研究主要在探討氫氣、甲烷及一氧化碳重組燃料之燃燒特性，由於氫氣、甲烷及一氧化碳各別的可燃極限、燃燒速度及化學特性不同，相互混合之後的燃燒特性亦不相同，因此本研究初期先進行甲烷及一氧化碳混合燃料的燃燒特性研究，之後再進行將氫氣加入甲烷及一氧化碳混合燃料中，以瞭解加氫對火焰結構及化學動力之影響。經由實驗量測與數值模擬之研究結果顯示，當 10%及 20%的氫氣加入 CH4/CO 燃料時，最大燃燒速度分別發生在 CH4/CO 燃料體積比為 1：9 及 1：15.67 時，此結果乃是因主宰之化學反應動力機制由甲烷轉換至氫氣及一氧化碳，並由 OH + CO ↔H + CO2、OH + H2 ↔H + H2O 及 HO2 + H ↔OH + OH 反應式主宰反應速率及熱釋放率。本研究第一部份成果已發表在國際知名燃燒期刊，顯見其學術價值相當高。第二部份之研究成果將先投稿至明年七月在美國 UC Irvine 舉行的第 23 屆國際爆炸與反應系統動力會議發表，之後再轉投至國際期刊。